

**Alma Mater Studiorum  
Università di Bologna**

**Scuola di Dottorato di Ricerca  
in Scienze Mediche e Chirurgiche**

**Dottorato di Ricerca in Scienze Biomediche  
Progetto formativo in Neurofisiologia**

XXV ciclo

Settore concorsuale di afferenza: 05/D1

Settore scientifico-disciplinare: BIO/09

Tesi di Dottorato

**Coding of reaching in 3-D space**

Dott. Federica Bertozzi

Coordinatore:  
Prof. Claudio Galletti

Tutor:  
Prof. Patrizia Fattori

Dipartimento di Fisiologia umana e generale  
Esame finale anno 2013

## CONTENTS

<b>1.</b>	<b>INTRODUCTION</b>	<b>4</b>
1.1.	Encoding of 3D space	4
1.2.	Neural substrate of reaching in monkeys	6
1.3.	The role of parietal area V6A in reaching	8
1.4.	Effect of target depth in reaching	10
1.5.	The role of frontal areas in reaching	14
1.6.	The representation of depth and direction signals: studies in humans	15
1.7.	Kinematic properties of reaching movements	17
1.8.	Aim of the work	20
<b>2.</b>	<b>MATERIALS AND METHODS</b>	<b>22</b>
2.1.	Experimental and surgical procedures	22
2.2.	Reaching task	25
2.3.	Kinematic recording	28
2.4.	Neural data Analysis	30
2.5.	Kinematic data analysis	32
<b>3.</b>	<b>RESULTS</b>	<b>35</b>
3.1.	Tuning for depth and direction in the different task phases	38
3.2.	Spatial tuning in different task phases	42
3.3.	Cell Categories	47
3.4.	Movement trajectories	53
3.5.	Movement time	58

<b>3.6.</b>	<b>Velocity Profiles</b>	<b>60</b>
<b>3.7.</b>	<b>Mean peak velocity</b>	<b>61</b>
<b>3.8.</b>	<b>Mean peak acceleration</b>	<b>63</b>
<b>3.9.</b>	<b>Mean peak deceleration</b>	<b>65</b>
<b>3.10.</b>	<b>Percentage of movement at the peak velocity</b>	<b>66</b>
<b>3.11.</b>	<b>Percentage of movement accelerating</b>	<b>69</b>
<b>3.12.</b>	<b>Percentage of movement decelerating</b>	<b>71</b>
<b>4.</b>	<b>DISCUSSION</b>	<b>75</b>
<b>4.1.</b>	<b>Depth and directional tuning</b>	<b>75</b>
<b>4.2.</b>	<b>Caveats</b>	<b>80</b>
<b>4.3.</b>	<b>Spatial tuning in the different task phases</b>	<b>81</b>
<b>4.4.</b>	<b>Kinematic of reaching movements</b>	<b>83</b>
<b>4.5.</b>	<b>Correlation between kinematic and neural data</b>	<b>85</b>
<b>5.</b>	<b>REFERENCES</b>	<b>87</b>

## 1. INTRODUCTION

In everyday life, we frequently execute reaching movements, for example to grasp a cup of tea or to reach the handle of the door. These actions are usually performed accurately, automatically and without thinking to the hand trajectory or to the muscles contraction. However, our brain performs complex computations integrating the visual and proprioceptive information to program appropriate reaching actions. To execute reaching movements, the information about the target location is necessary to process the hand trajectory and the corresponding motor command that guides the muscles. Multiple sensory systems generally provide spatial information, and the movement often involves the coordination of several body segments, as in orienting the eyes, head and arm together towards the target (Jeannerod, 1988; Lacquaniti, 1997). In the present thesis, I aimed to study the sensory-motor transformations in 3D space and in particular the neural encoding of arm movements when the reach targets are located at different depths and directions. I investigated the incidence and the temporal relationship of the effect of target spatial position on the neurons of macaque medial posterior parietal cortex.

### 1.1. Encoding of 3D space

The execution of goal-directed actions requires the accurate identification of target position in three-dimensional space. The localization of a visual target in 3D space depends on the combination of visual signals, as well as retinal disparity, binocular direction signals and fixation distance information (Pouget and Sejnowsky, 1994). The fixation distance signals are obtained from several information: the accommodation of the eyes, the vertical disparity and the binocular eye position, corresponding to the angle between the gaze projections during the binocular vision of a target, known as vergence angle. Vergence seems to be the most important one, in particular for the encoding of depth fixation. Most of the vergence range is used for fixation distance that are approximately equal to the arm length and to the peri-personal space (Viguiet *et al.*, 2001). Interestingly, in infants, reaching performance develops at the same time as

binocular control (von Hofsten, 1977). Another important variable is the version angle that measures the conjugated movements of the eyes towards a gaze target and it can represent the fixation direction. It is possible to represent the reach target location by processing the ocular vergence and version when the reach target corresponds to the gaze target, because in this case the target position coincides with the fixation position. This situation occurs very frequently, the goal-directed action is usually associated to an eye movement that ‘catches’ the reach target bringing its image on the fovea.

Depth and direction signals, represented with vergence and version parameters respectively, are significant variables in planning and execution of eye and reaching movements. It is generally assumed that target depth and direction are processed in functionally separated visuomotor circuits (Cumming and DeAngelis, 2001; Vindras *et al.*, 2005). But in more complex conditions, direction and distance cannot be considered as independent variables in the neural computation of spatial encoding (Crawford *et al.*, 2011). The distinct or common process of integration of the two different signals is still debated.

Another long-standing issue concerns the temporal evolution of direction and depth computation that has collected conflicting results. Many studies suggested that direction is processed before depth (Bhat and Sanes, 1998) in contrast with the hypothesis that the processing of direction happen after or at the same time of depth (Rosenbaum, 1980).

Another prominent issue in physiology regards the computation of several multisensory information used to encode the spatial goal-directed actions. To program and perform a reach movement, the brain has to discriminate and update the spatial position of the target and the hand. Different systems (e.g. visual, oculomotor and proprioceptive) provide distinct spatial information and the heterogeneity of these spatial representations needs to be integrated across different networks and to be transformed into commands suitable for reach action toward the target, merging the several signals in a unitary 3D map (Lacquaniti, 1997). How these multisensory afferences are integrated using the same reference frame remains still unclear.

## 1.2. Neural substrate of reaching in monkeys

The neural substrate of reach target location in monkeys is formed by the circuit that involves visual, parietal and frontal areas. Visual information are projected from the occipital pole following two main pathways: a dorsal one directed to posterior parietal cortex that resulted to be involved in the localization and the interaction with the objects and a ventral one that reaches the cortex of the inferior temporal lobe and that is dedicated for the recognizing of the objects features (Ungerleider and Mishkin, 1982). The dorsal visual stream includes at least two separate networks: a medial one passing mainly through the visual areas of the superior parietal lobule (SPL), and a lateral one passing mainly through the visual areas of the inferior parietal lobule (IPL). The dorsomedial visual stream has been supposed to process the visuomotor transformations necessary for guiding the reaching movements of the arm, while the dorsolateral visual stream is involved in the encoding of the visuomotor transformations necessary for grasping (Sakata and Taira, 1994; Tannè *et al.*, 1995). In contrast with this view, recent neurophysiological and anatomical data reported that the medial sector of the parieto-occipital cortex integrates and controls both reaching and grasping hand actions (Galletti *et al.*, 2003). This cortical region includes a retinotopically organized visual area, called V6 (Galletti *et al.*, 1999a) and, dorsally to V6, a not-retinotopically organized area, called V6A (Galletti *et al.*, 1999b), as shown in Figure 1. About half of the cortical connections of V6 is with visual areas of the occipital lobe (V1, V2, V3, V3A), and the other half with the areas of the dorsal visual stream: 30% with the visual areas of the dorso-lateral visual stream (V4T, MT/V5, MST, LIP) and 22% with bimodal (visual and somatosensory) areas of the dorso-medial visual stream (V6A, MIP, VIP). Area V6 is not directly connected with the ventral visual stream neither with the frontal areas (Galletti *et al.*, 2001). A different pattern of cortical connections was identified in the area V6A that contains neurons connected with area MIP, PEc, PG, PGm, F7 and F2 (Gamberini *et al.*, 2009). V6A receives its major input from area MIP, cortical region responsive to passive somatosensory and visual stimulation and to active arm-reaching movements. The strong connections found between V6A and MIP support the view that the two areas form part of a circuit involving reciprocal interaction, in which visual/somatic/motor information is processed before and during the act of reaching. Minor connections of V6A were found with area AIP, known to be involved in coding object features and hand movements for grasping objects, and with area F2, containing both reaching- and grasping-related

neurons. This supports the view that V6A is involved in the control of both reaching and grasping movements (Galletti and Fattori, 2003; Gamberini *et al.*, 2009).

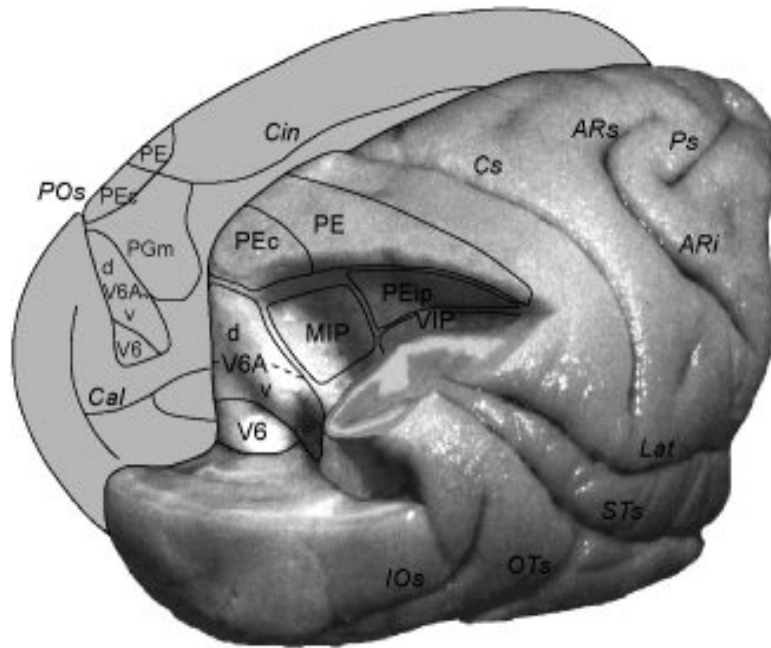


**Figure 1. Medial Posterior Parietal Cortex of macaque brain**

Posterolateral view of a partially dissected macaque brain (Gamberini *et al.*, 2009). The inferior parietal lobule of the right hemisphere has been cut away at the level of the fundus of the intraparietal sulcus to show the cortex of the medial bank of this sulcus. The occipital lobe of the same hemisphere has been cut away at the level of the fundus of the parieto-occipital and lunate sulci to show the cortex of the anterior bank of the parieto-occipital sulcus. The mesial surface of the left hemisphere is drawn, with the main sulci and the posterior parietal areas reported. POs, parieto-occipital sulcus; Cal, calcarine sulcus; Cin, cingulate sulcus; IOs, inferior-occipital sulcus; OTs, occipito-temporal sulcus; STs, superior temporal sulcus; Cs, central sulcus; Ars, superior arcuate sulcus; Ari inferior arcuate sulcus; Ps, principal sulcus; areas V6, V6Ad, V6Av, PEc, PE, MIP, PEip, VIP, PGm are also indicated.

### 1.3. The role of parietal area V6A in reaching

Many cells in area V6A are sensitive to reach movements towards targets located in the peri-personal space (Fattori *et al.*, 2001; Galletti *et al.*, 1997a). The V6A somatic representation supports the hypothesis that reaching responses could be related to the update of somatosensory input coming from the moving arm. The sensitivity for passive somatosensory stimuli in V6A (Breveglieri *et al.*, 2002) actually is in line with this view. However, the observation that reach-related activity in V6A is generally stronger during active than passive arm movements suggested that skeletomotor information could be partially responsible for the reach signals reported in literature. There are evidences demonstrating that visual and somatosensory signals cannot fully explain reaching responses. In Galletti *et al.* (1997), neurons modulated by reaching movements showed an increased firing rate 200 ms before the beginning of the motor action. This phenomenon must be due to other information that became available before the muscle activation. It is possible an involvement of a preparatory motor activity, as well as the computation of an efferent copy of motor signal delivered by the dorsal premotor areas F2 and F7, which are reciprocally connected with V6A (Matelli *et al.*, 1991; Matelli *et al.*, 1998; Gamberini *et al.*, 2009).

Neurons of area V6A were found to be very sensitive to reaching movements towards different directions: Fattori and collaborators (2005) studied neural activity while monkeys were involved in a body-out reaching task on foveated targets placed on a frontal plane. The presence of significant reach-related discharges when the targets were reached in darkness demonstrates that the sensitivity of V6A cells on the goal-directed actions was independent of visual feedback of the moving arm. It has also been reported that about 40% of neurons modulated by reaching movements showed strong direction tuning (Figure 2A-B). These data suggest that V6A reach-related neurons are able to encode the movement direction and the arm spatial position. These findings are in line with the results found in area V6A while the monkeys performed several reaching tasks towards different directions where retinal, eye and arm related signals were separated (Marzocchi *et al.*, 2008). This study focused on the early stage of movement direction programming and suggested the involvement of area V6A in the mechanisms underlying the early combination of eyes and arm signals for the composition of motor commands to perform reaching actions towards different directions.

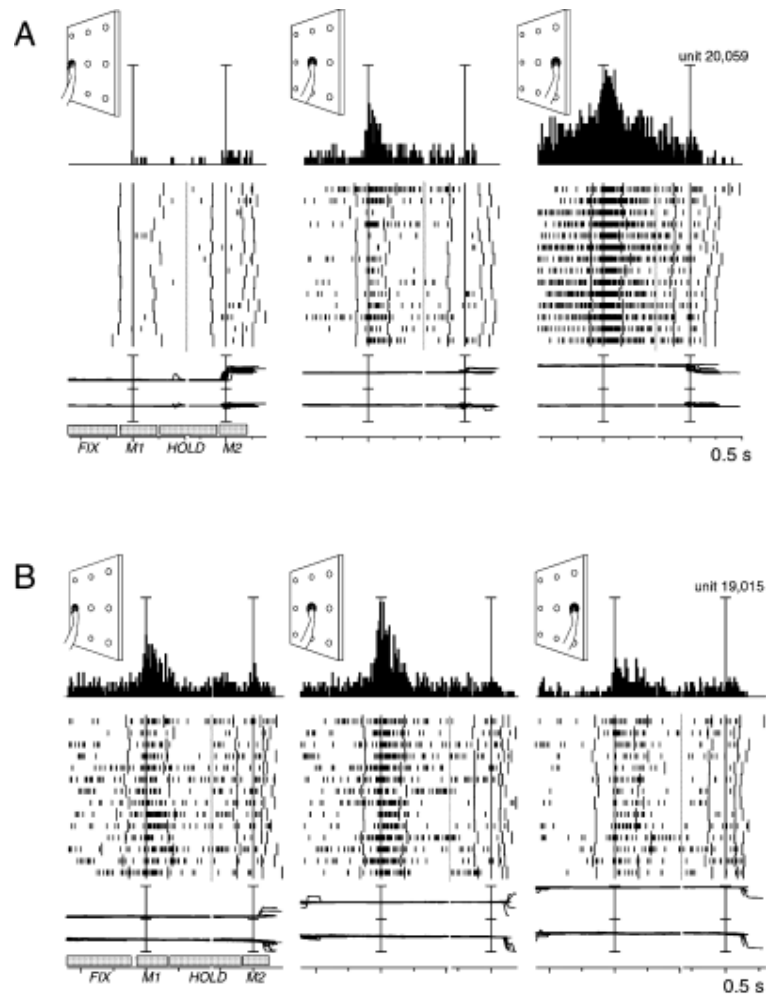


**Figure 2A-B. Examples of reach-related neurons modulated by movement direction (Fattori *et al.*, 2005)**

Each inset contains the peri-event time histogram, raster plots and eye position signals. It is positioned in the same relative position as the target on the panel, as sketched in the top left corner of each inset. Neural activity and eye traces show two alignments in each inset: the first one indicates the onset of outward movements and the second one the onset of inward movements. The mean duration of fixation (FIX), movement (M1), hold (HOLD) and return (M2) is showed in the bottom left inset. Scalebar in peri-event time histograms corresponds to 70 spikes/s in the first neuron and 100 spikes/s in the second neuron.

**A**, Neuron sensitive to the spatial position of the target during reaching movement preferring rightward goal-directed actions.

**B**, Neuron spatially modulated during reach movements with a preference for reaches directed to the central position.

#### **1.4. Effect of target depth in reaching**

Compared to direction tuning, fewer studies analyzed how the depth sensitivity, the other important variable to execute reaching movements, is represented in monkey brain. Genovesio and Ferraina (2004) reported that LIP neurons are involved in the processing of target distance integrating visual disparity signals with vergence signals in a manner that can be used to encode the distance of a target in 3D space. Gaze signals are transformed in egocentric reference frame to process the depth of the reach target. In another study, Ferraina *et al.* (2009) analyzed in area PE the vergence modulation of reach-related activities for target located at different distances. The authors reported that PE reach-related neurons combined binocular eye position signals about fixation depth with hand position signals to encode reach movement amplitude. The main goal of that work was to investigate the influence of hand position on reach distance tuning in order to clarify which coordinate system was used to encode target spatial location but the interaction and the temporal evolution of both depth and direction signals were not described.

A more recent study (Breveglieri *et al.*, 2012) investigated how vergence but also version signals are processed in area V6A while monkeys maintained steady fixation. These results revealed that the majority of V6A neurons were modulated by both variables suggesting that the integration of vergence and version signals is already present in this early node of the dorsal visual stream (Figure 3A-B). It is interesting to note that during fixation the version selectivity decayed more rapidly than the vergence one supporting the hypothesis that direction signals were processed before distance information.

## Vergence and version influence

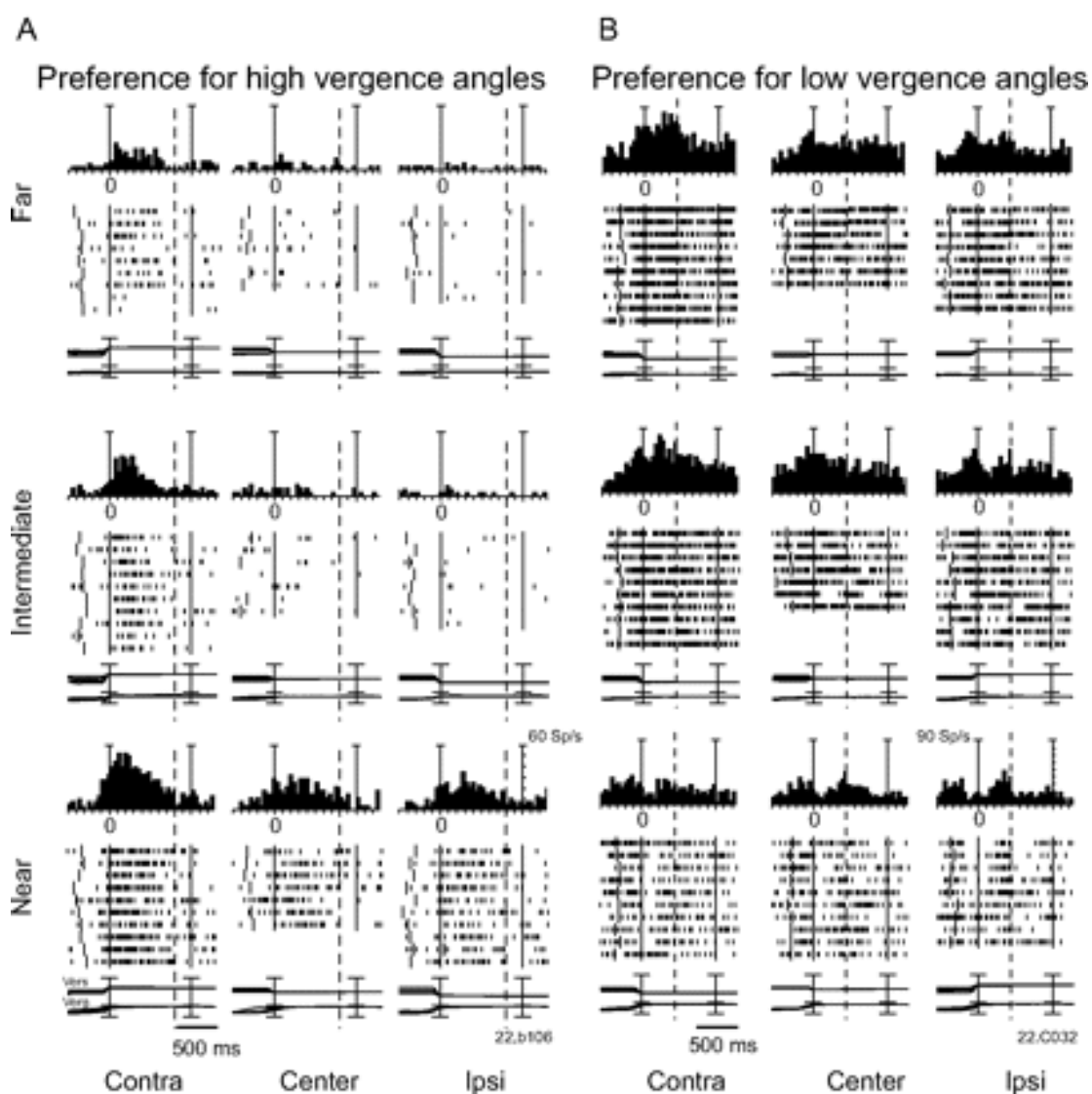


**Figure 3A-B. Example of two V6A neurons tuned for both vergence and version signals during fixation (Breveglieri *et al.*, 2012)**

Neural responses to the nine fixation targets located at three different depths (lines) and three different directions (columns). Rasters are arranged from near (bottom) to far (top) and from contralateral (left) to ipsilateral (right) and are aligned twice: at the fixation onset and at the stop signal for gaze fixation. Dashed lines indicate the point at which trials were cut for the double alignment.

**A**, Neuron showing a clear preference for the near contralateral space.

**B**, Neuron spatially tuned with a preference for the far contralateral space.

The data previously described regard only fixation targets and skip to investigate the effect of vergence and version signals during the execution of goal-directed movements. Only Lacquaniti *et al.* (1995) evaluated the effect of both direction and depth signals on the neural responses in area 5 during reaching actions. The monkeys were trained to perform goal-directed movements towards targets located at similar directions within 3 different workspaces, starting from 3 initial hand positions. Each starting location was located in the middle of an imaginary cube where at each corner of the cube a reach target was placed (Figure 4A-C).

This experimental setup allowed maintaining equal movement direction across space, varying the pattern of muscular and joint activity required for these reaching actions. The majority of area 5 neurons was influenced by the spatial location of the hand within a shoulder-centered spherical reference frame with neurons encoding azimuth or elevation or reach amplitude individually. The activity of another population of neurons was not related to the final hand position, but rather to the vectorial difference between initial and final hand position, defined as movement vector.

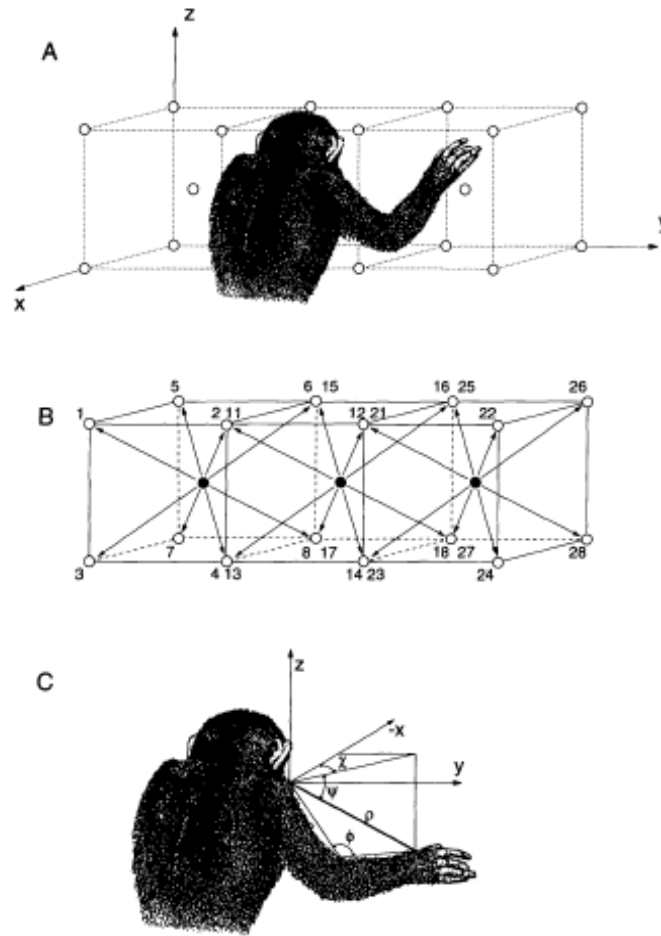


**Figure 4A-C. Experimental apparatus used to study reaches occurring at different depths and directions (Lacquaniti *et al.*, 1995)**

**A**, Experimental setup with the empty circles representing the reach targets and  $x$ ,  $y$ ,  $z$  representing the spatial Cartesian coordinates.

**B**, Black filled circles represent the initial positions of the hand. The monkeys perform movement starting from one of the three possible initial positions towards one of eight reach directions (arrows).

**C**, Shoulder-centered reference frame. Wrist coordinates are elevation  $\Psi$ , azimuth  $\chi$  and distance  $\rho$ .

### **1.5. The role of frontal areas in reaching**

Electrophysiological recordings in primary motor cortex (M1) and in dorsal premotor cortex (PMd) revealed the presence of neurons involved in the process of encoding reach target location, integrating direction and depth signals. Fu *et al.* (1993) described neurons modulated by movement direction, distance and by the interaction of the two parameters in both M1 and PMd. Successive analysis of the reported data indicated a temporal separation: movement direction was encoded first, followed by target position and then by movement depth (Fu *et al.*, 1995). According to these studies, Messier and Kalaska (2000) found a strong and prevalent modulation for the interaction of depth and direction signals in reach-related activities of PMd neurons and an increased tuning to movement amplitude during the motor execution. Another important finding revealed by the studies previously described was that most of PMd cells were found to be sensitive to both movement direction and distance but only very few neurons were tuned only for target distance signal. These results are in contrast with the data found in PPC (Lacquaniti *et al.*, 1995) and with the hypothesis that depth and direction information are processed independently (Bagesteiro *et al.*, 2006; Gordon *et al.*, 1994; Sainburg *et al.*, 2003; Vindras *et al.*, 2005; Van Pelt and Medendorp, 2008; Crawford *et al.*, 2011) but suggest that these reach movement variables converge at single-cell level in PMd.

The mentioned studies demonstrate that the process of goal-directed actions involved many areas in the integration of depth and direction information. Movement depth and direction signals are both critical and strictly correlated, even if their computation seems to be temporally separated.

## 1.6. The representation of depth and direction signals: studies in humans

In humans, the involvement of posterior parietal areas encoding reach target position in 3D space is supported by data collected on patients suffering from optic ataxia. After lesions in the superior parietal lobule and parieto-occipital junction, ataxic patients misreached the target showing error of trajectory, finger pre-shaping and movement end-point. These difficulties occurred more frequently in the peripheral vision but happened also towards foveated targets when the visual feedback was absent (Perenin and Vighetto, 1988; see Battaglia-Mayer *et al.*, 2006 for review). These findings were in accordance with the data reported by Prado *et al.* (2005) about the critical role of medial intra-parietal sulcus (IPS), PMd and medial occipito-parietal junction (mPOJ) in the execution of visually-guided actions. These results were also confirmed analyzing the effects of a reversible inhibition of posterior parietal cortex (PPC) activity using transcranial magnetic stimulation (TMS): after this manipulation the subjects showed deficits in the accuracy of hand movement trajectory (Desmuget *et al.*, 1999). The aforementioned studies confirmed the role of parietal cortex processing goal-directed action towards targets located in a certain spatial location. Parietal and frontal areas were also found to be sensitive to the laterality of reaching movements and the magnitude of these direction responses increased moving from posterior to anterior areas (Fabbri *et al.*, 2010). However, less is known about the sensitivity of these human regions to movement extent. Fabbri *et al.* (2012) investigated the role of directionally tuned neuronal population encoding movement amplitude in frontal and parietal regions and found differences between the two areas in the integration of movement depth and direction. These results revealed that parietal areas encode combinations of movement depth and direction and that in the frontal pole the neural responses could be correlated to reach depth where the cerebral activity grew with the increase of movement extent. The role of parietal areas encoding reach depth variable was found initially by Baylis and Baylis (2001) that described deficits in visually-guided reaching movements towards targets located at different depth, as effect of disease involving posterior parietal regions. In agreement with these data, Danckert *et al.* (2009) demonstrated that patients with lesions in parietal cortex show more deficits in pointing to objects placed at different depth than at different directions (Figure 5) and this findings support the important role of PPC encoding the location of reach targets especially in the depth dimension.

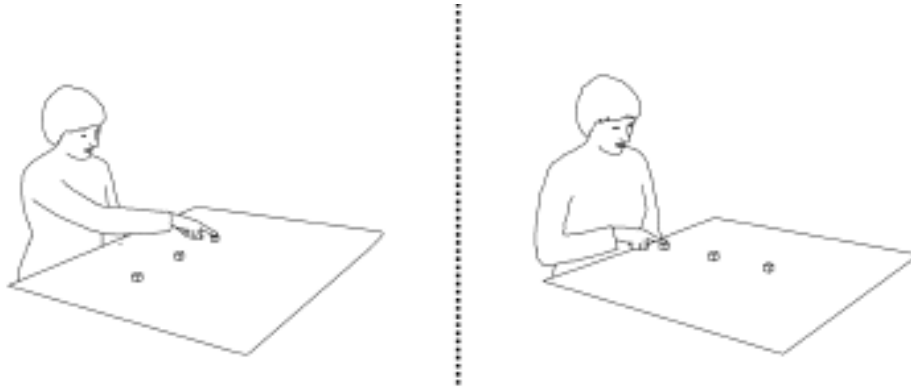


**Figure 5. Experimental setup for movement towards different directions (left) and for movement in depth (right) (Dankert *et al.*, 2009)**

The subjects and the patient perform pointing movements towards one of the three targets for each trial. The patient had more deficits in movements in the sagittal axis than in the frontoparallel plane, as a consequence of a lesion in the right superior parietal cortex.

## 1.7. Kinematic properties of reaching movements

Reach movement in three-dimensional space can be studied analyzing different motor properties: dynamic, kinematic or other aspects of motor behavior. It is possible that cortical areas involved in the process of one or more movement kinematic parameters exist and that this encoding occurs following an extrinsic Cartesian coordinates system within the peri-personal space. The kinematic motor parameters used to describe the movement vectors are velocity and acceleration. It is possible to calculate the relative averages (mean velocity, mean acceleration), the maximum (peak velocity, peak acceleration), the minimum values (peak deceleration) and the percentage of motion that occurs when the peaks are reached (time of peak velocity, time of peak acceleration, time of peak deceleration). Kinematic properties characterizing reaching actions have been widely studied in humans. It has been described that velocity profiles are single-peaked and bell-shaped (Morasso, 1981), peak velocity and peak acceleration are correlated with movement amplitude (Gordon *et al.*, 1994b) and an increase in the target distance relative to the hand causes an increase of both movement duration and wrist peak velocity (Gentilucci *et al.*, 1991; Kudoh *et al.*, 1997). Furthermore, there is also a wide literature that focused on movement trajectory features and shapes. Different hypotheses in the execution of goal-directed actions have been formulated: a simple view is that the human movement trajectories are roughly straight in the workspace (Morasso, 1981; Georgopoulos and Massey, 1988; Gordon *et al.*, 1994b) and an alternative strategy provides straight trajectories in joint space which may result a curved hand path in workspace (Atkeson and Hollerbach, 1985). Atkeson and Hollerbach (1985) found curved paths for movements in the sagittal plane. Cruse and Brüwer (1987) suggested that the shapes of human reaching trajectories reflect a compromise between the subject trend to reproduce simultaneously a straight line in both workspace and joint space. Another explanation of the movement curvature found by Atkeson and Hollerbach (1985) was related to the unconstrained nature of the selected tasks, as monkeys also have been reported to use more curved paths during unconstrained similar reaches (Wenger *et al.*, 1999; Jindrich *et al.*, 2011). In addition, monkeys also showed curvature during more constrained center-out tasks (Scott *et al.*, 1997).

Messier and Kalaska (1999) had also demonstrated that, in humans, the kinematic parameters describing the beginning of the movement are not completely predetermined and cannot predict depth and distance of a reaching target in a simple ballistic manner.

Compensatory adjustments are necessary during the execution of the movement to correct the initial variability of movement direction and to scale velocity and acceleration relative to action amplitude. This study revealed some differences between depth and direction dimensions (i.e. variability in movement amplitude was higher than in direction), supporting the hypothesis that the two components were processed independently (see also Gordon *et al.*, 1994a-b). The finding that the variability of peak velocity, peak acceleration and end-point distribution in movement direction and amplitude were differently influenced during the execution of the goal-directed action suggested that depth and direction are not specified and controlled simultaneously but in different moments. In contrast to these results, this study also reported evidences for the correlation of movement velocity, acceleration and duration with target distance. Subjects varied movement duration as well as velocity and acceleration as a function of reaching extent.

In contrast with psychophysical data in humans, as the work previously described, less is known about the kinematic properties of monkey reaching movements towards targets located at different depths and directions. Some comparative kinematic studies on reaching and grasping behavior in humans and monkeys have been carried out to investigate the similarities and differences existing across the two species (Fogassi *et al.*, 1991; Christel and Billard, 2002; Roy *et al.*, 2000, 2002, 2006; Jindrich *et al.*, 2011; Sartori *et al.*, 2012). Although these studies seem to support the hypothesis that monkeys and humans share a number of kinematic features, important differences have been reported and the debate continues to unfold.

Roy *et al.* (2000) investigated kinematic characteristics of macaque hand movement involved in pointing, reaching and grasping under unperturbed and perturbed conditions. The main finding reported by this study was that monkey kinematics showed a high similarity with human kinematics, in particular for the pointing towards different directions, the perturbation effect and the reaching and grasping temporal pattern. Indeed, in accordance with human evidences, monkeys reaching movements showed a bell-shaped wrist velocity profile. These similarities suggested that the macaque monkey could be a suitable model for studying human motor system. The only disagreement between monkey and human data was that monkeys pointing movement displayed a double, instead a single velocity peak, as Georgopoulos *et al* (1981) found for re-directed movements. This observation probably reflected the variation of experimental conditions rather than a real difference between human and monkey (Roy *et al.*, 2000).

Another relevant similarity between the two species involved the comparison of ipsilateral and contralateral movements. Human and monkey studies investigating reaching movements revealed asymmetry comparing different directions respect to the hand used: reaching durations towards contralateral target were significantly longer than towards ipsilateral or central ones and this effect is truly due to movement direction and not to different wrist distances (Roy *et al.*, 2002). All these kinematic results revealed that the study of monkey's reaching movements is a useful step to the understanding of visuo-motor control in human but few studies investigated kinematic motor properties of monkey's reaching actions. Furthermore, most studies mentioned above involved planar, i.e. two-dimensional, reaching movements but the depth component of the three-dimensional reaching movements was less considered with the exception of few psychophysical works in humans.

## 1.8. Aim of the work

As previously reported, in humans, the role of the superior parietal lobule (SPL) in encoding depth and direction signals was demonstrated by studies describing patients with lesions in SPL that showed larger visuomotor deficits in depth than in direction (Baylis and Baylis, 2001; Danckert *et al.*, 2009). The direction component has also been studied through electrophysiological analysis of macaque monkey parietal neurons, but the depth dimension and the interaction of the two variables were less considered. Most single-unit studies used center-out reaching tasks, with initial hand and target positions located on the same frontal plane (Andersen and Cui, 2009; Batista *et al.*, 1999; Battaglia-Mayer *et al.*, 2001; Buneo *et al.*, 2002; Chang *et al.*, 2009; Snyder *et al.*, 1997). Fewer works employed body-out reaching movements, with the arm moving from a position near the trunk to targets located on a single plane (Fattori *et al.*, 2001, 2005; Bosco *et al.*, 2010), or at different depths (Bhattacharyya *et al.*, 2009; Ferraina *et al.*, 2009). However, these studies did not compare the effect of direction and depth signals on neural responses. This has been only reported by Lacquaniti *et al.* (1995) in area PE, where separate populations of neurons were found to encode the depth and the direction of reaching targets, as described in the previous paragraph. These results were in accordance with several psychophysical studies (Bagesteiro *et al.*, 2006; Gordon *et al.*, 1994; Sainburg *et al.*, 2003; Vindras *et al.*, 2005; Van Pelt and Medendorp, 2008), supporting that these two spatial variables are processed in separate networks (Crawford *et al.*, 2011). To clarify how these variables are integrated, we want to investigate whether there is an encoding of both depth and direction information in single parietal neurons, and to compare depth and direction tuning during fixation, planning and reaching epochs.

We studied the above issues in the medial posterior parietal area V6A of macaques (Galletti, *et al.*, 1999), where several types of neurons are involved in various phases of visually guided reaches (Fattori *et al.*, 2005; Fattori *et al.*, 2001). V6A contains neurons that encode the spatial location of visual targets (Galletti *et al.*, 1993, 1995), neurons sensitive to the version and vergence angle of the eyes during fixation and saccades (Breveglieri *et al.*, 2012; Galletti *et al.*, 1995; Hadjidimitrakis *et al.*, 2011), and cells whose activity is modulated by the arm reaching movement (Fattori *et al.*, 2004; Fattori *et al.*, 2001; Fattori *et al.*, 2005) and arm spatial position (Breveglieri *et al.*, 2002; Fattori *et al.*, 2005).

Single cells were recorded while two *Macaca fascicularis* monkeys performed a fixation-to-reach task to foveated targets located at different depths and directions in three-dimensional (3D) space. We found that in a substantial percentage of V6A neurons depth and direction signals jointly influenced fixation, planning and arm movement-related activity in 3D space. While target depth and direction were equally encoded during fixation, depth tuning became stronger during arm movement planning, execution and target holding. The spatial tuning of fixation activity was often maintained across epochs, and the depth tuning was more maintained across the epochs. These findings support for the first time the existence of a common neural substrate for the encoding of target depth and direction during reaching movements in the posterior parietal cortex. Present results also highlight the presence in V6A of several subpopulations of cells that are recruited during the progress of a fixate-to-reach task in 3D space and process independently or jointly eye position and arm movement planning and execution signals in order to control reaches in 3D space.

To further investigate whether target depth and direction are processed commonly or independently and to study the spatial and temporal properties of monkey's reaches, we collected and analyze the kinematic recordings of monkey arm movements.

The task employed in this study was aimed at moving the hand towards visual target located at different depths and directions but at the same elevation (at eye level). For the neural data, it has been demonstrated that depth and direction influence V6A neural responses during movement execution. It is possible that depth and direction influence also the metrics of the reach action and that this effect on the reach kinematic variables can account for the spatial tuning we found in V6A neural activity. For this reason, we recorded and analyzed behavioral data when the monkey performed reaching movements in 3-D space. We evaluated how the target spatial position, in particular target depth and target direction, affected the kinematic parameters and trajectories describing the motor action properties.

## 2. MATERIALS AND METHODS

The electrophysiological recordings and the neural data reported in this thesis have been the subject of a recent publication in which I am coauthor: Hadjidimitrakis *et al.*, 2013.

Experiments were performed following the national laws on care and use of laboratory animals and with the European Communities Council Directive of November 24, 1986 (86/609/EEC) and that of 22th September 2010 (2010/63/EU). All the experimental protocols were approved by the Bioethical Committee of the University of Bologna. During training and recording sessions, particular care was taken to avoid any behavioral and clinical sign of pain or distress.

### 2.1. Experimental and surgical procedures

The experiment was performed on two male macaque monkeys (*Macaca fascicularis*) weighing 4.4 Kg (Monkey A) and 3.8 Kg (Monkey B). Before recordings, monkeys were habituated to sit in a primate chair and to interact with the experimenters. Then, they were trained to perform the motor task described below using either hand (recordings were performed while the monkey used the hand contralateral to the recorded hemisphere). When the training was completed, a head-restraint system and the recording chamber were surgically implanted under general anesthesia (sodium thiopental, 8mg/kg\*h, i.v.) following the procedures reported by Galletti *et al.* (1995). A full program of postoperative analgesia (ketorolac trometazyn, 1mg/kg i.m. immediately after surgery, and 1,6 mg/kg i.m. on the following days) and antibiotic care (Ritardomicina, benzatinic benzylpenicillin + dihydrostreptomycin + streptomycin, 1-1.4 ml/10kg every 5-6 days) followed surgery.

Extracellular recording techniques and procedures to reconstruct microelectrode penetrations were similar to those described in other reports (e.g. Galletti *et al.*, 1996). Single cell activity was extracellularly recorded from the anterior bank of the parieto-occipital sulcus. Area V6A was initially recognized on functional grounds following the criteria described in Galletti *et al.* (1999), and later confirmed following the cytoarchitectonic criteria according to Luppino *et al.* (2005). We performed multiple electrode penetrations using a five-channel multielectrode recording system (5-channel MiniMatrix, Thomas Recording). The electrode signals were amplified (at a gain of

10,000) and filtered (bandpass between 0.5 and 5 kHz). Action potentials in each channel were isolated with a waveform discriminator (Multi Spike Detector; Alpha Omega Engineering) and were sampled at 100 kHz. The behavioural task and the stimulus presentation were controlled by custom-made software implemented in a Labview Realtime environment. Eye position was monitored through an infrared oculometer system (ISCAN) and was recorded at 500 Hz. Gaze direction was controlled by an electronic window (5 x 5 degrees) centred on the fixation target: this value conforms to other reaching studies (Batista and Andresen, 2001; Battaglia-Mayer *et al.*, 2001, 2005; Marzocchi *et al.*, 2008; Scherberger *et al.*, 2003; Snyder *et al.*, 2006). If the monkey fixated outside this window, the trial was aborted immediately.

Histological reconstructions have been performed following the procedures detailed in a recent publication from our lab (Gamberini *et al.*, 2011). Briefly, electrode tracks and the approximate location of each recording site were reconstructed on histological sections of the brain on the basis of electrolytic lesions and several other cues, such as the coordinates of penetrations within recording chamber, the kind of cortical areas passed through before reaching the region of interest, the depths of passage points between grey and white matter. All neurons of the present work were assigned to area V6A (Figure 6).

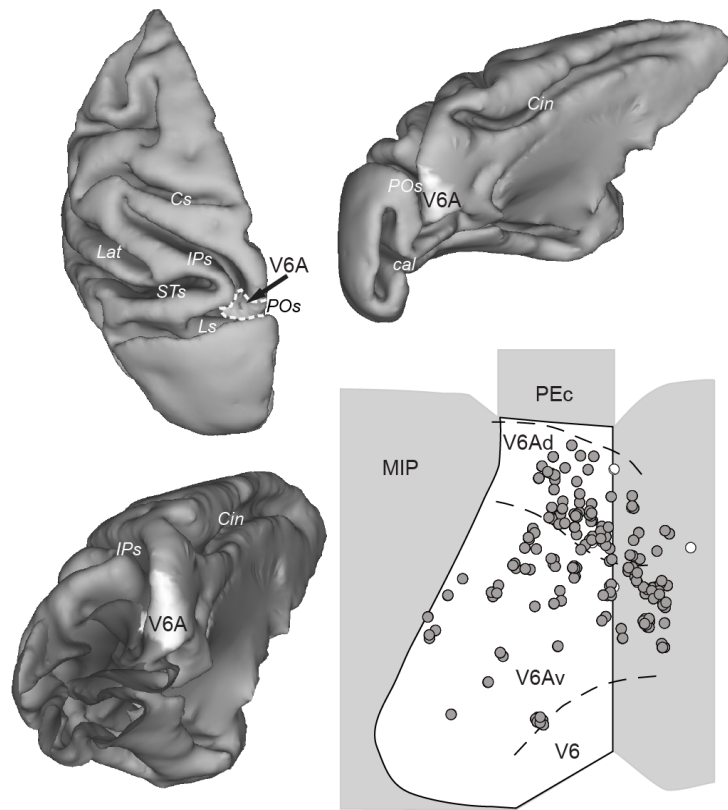


**Figure 6. Anatomical location of V6A and of recording sites.**

Top: The location of area V6A in the parieto-occipital sulcus (POs) is shown in dorsal (left) and medial (right) view of a hemisphere reconstructed in 3D using Caret software. Dashed contours (left) and white area (right) represent the borders and mesial extent, respectively, of V6A. Bottom-left: Posterior view of a reconstructed hemisphere with the occipital lobe removed to show the extent of V6A (white area). Bottom-right: Flattened map of area V6A showing the recording sites. Each circle represents a single site. White and grey circles represent sites where no modulated and at least one modulated neuron, respectively, was found. Cs, central sulcus; Cin, cingulate sulcus; Lat, lateral sulcus; STs, superior temporal sulcus; IPs, intraparietal sulcus; Ls, lunate sulcus; POs, parieto-occipital sulcus; Cal, calcarine sulcus; V6: area V6; V6Ad: dorsal V6A; V6Av:ventral V6A; MIP:medial intraparietal area; PEc: caudal area PE .

## 2.2. Reaching task

Electrophysiological signals were collected while monkeys were performing a body-out fixation-to-reach task specifically designed to study reach-related neural responses. The animals performed arm movement with the contralateral limb, with the head restrained, in darkness, while maintaining steady fixation of the target. Before starting the movement, the monkey had their arm on a button (home-button (HB), 2.5 cm in diameter) located outside the monkey's visual field and next to its trunk (Figure 7A). Reaches were performed to one of nine Light Emitting Diodes (LED, 6 mm in diameter) positioned at eye level. The LEDs, mounted on the panel at different distances and directions with respect to the eyes always at eye level, were used as fixation targets and they were also mounted on microswitches embedded in the panel, so to be used as reaching buttons. As shown in the Figure 7B, target LEDs were arranged in three rows: one central, along the sagittal midline and two lateral, at version angles of  $-15^\circ$  and  $+15^\circ$ , respectively. Along each row, three LEDs were located at vergence angles of  $17.1^\circ$ ,  $11.4^\circ$  and  $6.9^\circ$ . Given that the interocular distance for both animals was 30 mm, the nearest targets were located at 10 cm from the eyes, whereas the LEDs placed at intermediate and far positions were at a distance of 15 cm and 25 cm, respectively. The range of vergence angles was selected in order to include most of the peripersonal space in front of the animal, from the very near space (10 cm) up to the farthest distances reachable by the monkeys (25 cm). The monkeys were easily able to reach all the LEDs of the panel. The vectors between the starting position of the hand and the targets measure 24 centimeters for the nearest, 26 centimeters for the intermediate and 32 centimeters for the farthest positions.

The time sequence of the task with LED and arm status and the vergence and version angles of the eyes are shown in Figure 7C. A trial began when the monkey pressed the button near its chest (HB press). After pressing the button, the animal was waiting for instructions in complete darkness. It was free to look around and was not required to perform any eye or arm movement. After 1000 ms, one of the nine LEDs was switched on (LEDon). The monkey had to fixate the LED while keeping the HB button pressed. Then, the monkey had to wait for 1000–1500 ms for a change in the color of the LED (green to red) without performing any eye or arm movement. The color change was the go signal (GO) for the animal to release the HB and start an arm movement towards the target (M). Then, the monkey reached the target (H) and held its hand on the target for 800-1200 ms. The switching off of the target (Redoff) cued the monkey to release the LED and to return

to the HB (HB press), which ended the trial and allowed the monkey to receive its reward. Fixation had to remain stable on the target throughout the trial till the LED switched off, otherwise the trial was aborted and a new trial began without any reward. The correctness of reaching performance was evaluated by a software supervisor system (see Kutz *et al.*, 2005), which checked the status of microswitches (monopolar microswitches, RS components, UK) mounted under the home-button and the LEDs-button presses/releases were checked with 1 ms resolution. The retinotopic coordinates of reaching targets remained constant throughout the task, whereas the direction of movement changed trial by trial according to target position. The task was performed in darkness, in blocks of ninety randomized trials, ten for each LED target. The luminance of LEDs was adjusted in order to compensate for difference in retinal size between LEDs located at different distances. The background light was switched on briefly between blocks to avoid dark adaptation.

At the beginning of each recording session, the monkeys were required to perform a calibration task where they fixated ten LEDs mounted on a frontal panel at a distance of 15 cm from the eyes. For each eye, signals to be used for calibration were extracted during fixation of five LEDs, one central aligned with the eye's straight ahead position and four peripheral placed at an angle of +/- 15° (distance: 4 cm) both in the horizontal and vertical axes. From the two individual calibrated eye position signals we derived the mean of the two eyes (the conjugate or version signal), and the difference between the two eyes (the disconjugate or vergence signal) using the equations: version =  $(R+L)/2$  and vergence =  $R-L$ , where R and L was the position of the right and left eye, respectively.

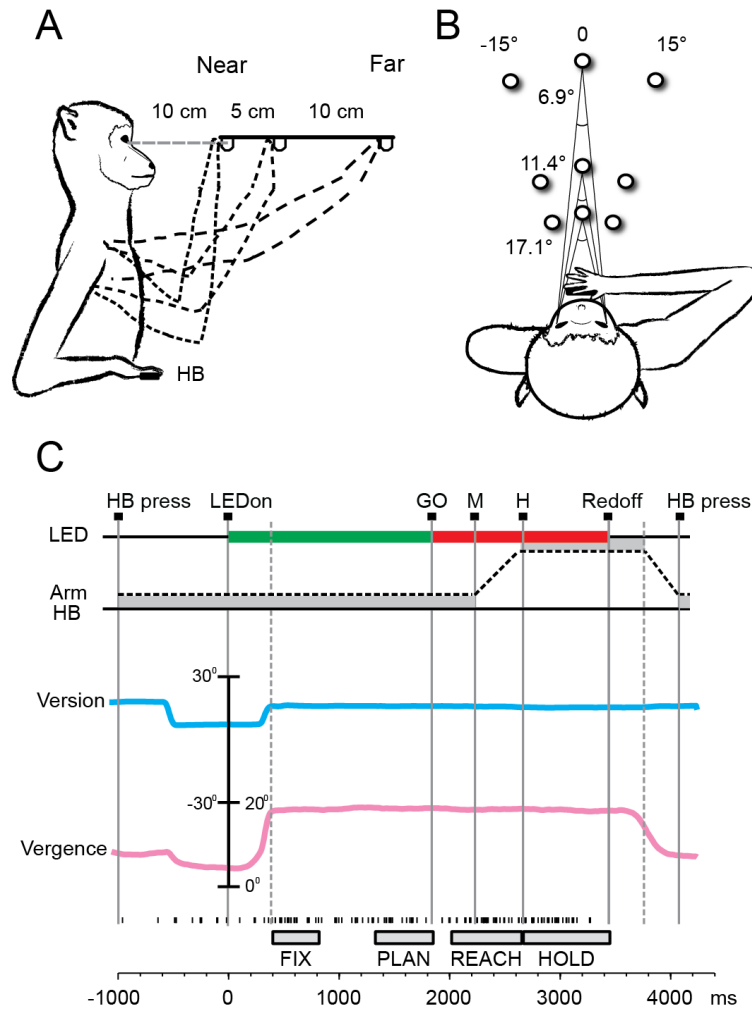


**Figure 7. Experimental setup and task sequence**

**A**, Scheme of the set up used for the reaching in depth task. Eye and hand movements were performed in darkness towards one of the 9 LEDs located at eye level at different depths and directions.

**B**, Top view of the reaching in depth set up task indicating the vergence and version angle of the targets with respect to the eyes.

**C**, Time sequence of task events with LED and arm status, the eye's vergence and version traces and the spike train of neural activity during a single trial. From left to right vertical continuous lines indicate: trial start (HB press), target appearance (LEDon), go signal (GO), start of the arm movement period (M), beginning of the holding the target period (H), switching off of the LED (Redoff), and trial end (HB press). Long vertical dashed line indicates the end of the saccade (left) and the start of the inward arm movement (right).

### 2.3. Kinematic recording

One monkey was employed in this study. The monkey performed the same task previously described. Arm movements were recorded with a Vicon three-dimensional motion analysis system with six infrared high-resolution cameras (Vicon Motion System Ltd., Oxford, UK) at a frequency of 60 Hz. Twelve infrared reflective markers were applied on several marker on the monkey's limb: 4 in the upper part of the arm (UPPA 1-4), 4 in the forearm (FORA 1-4), 2 on the wrist (WIR 1 and 2), one in the back of the hand (HAND) and the last one in the thumb (THU), as shown in Figure 8. We recorded instantaneous 3-D spatial location in Cartesian coordinates  $x$ ,  $y$ ,  $z$  of each marker during the reaching movements toward the nine target positions. The orientations of the axes with respect to the animal are shown in Figure 9. The monkey used the right arm for half of the recordings and the left arm for the other half of recordings. Recording of movement trajectories and neural recordings were performed in separate sessions.

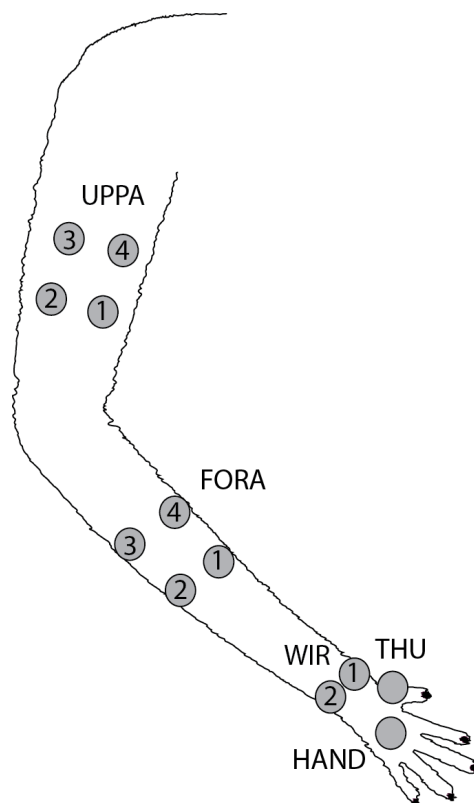


**Figure 8. Schematic representation of the monkey's right arm with the relative infrared reflective markers applied on the skin.**

In this schematic view we indicated the marker code and numeration. The marker code is arbitrary defined and it is useful for the analysis that followed the recording sessions.

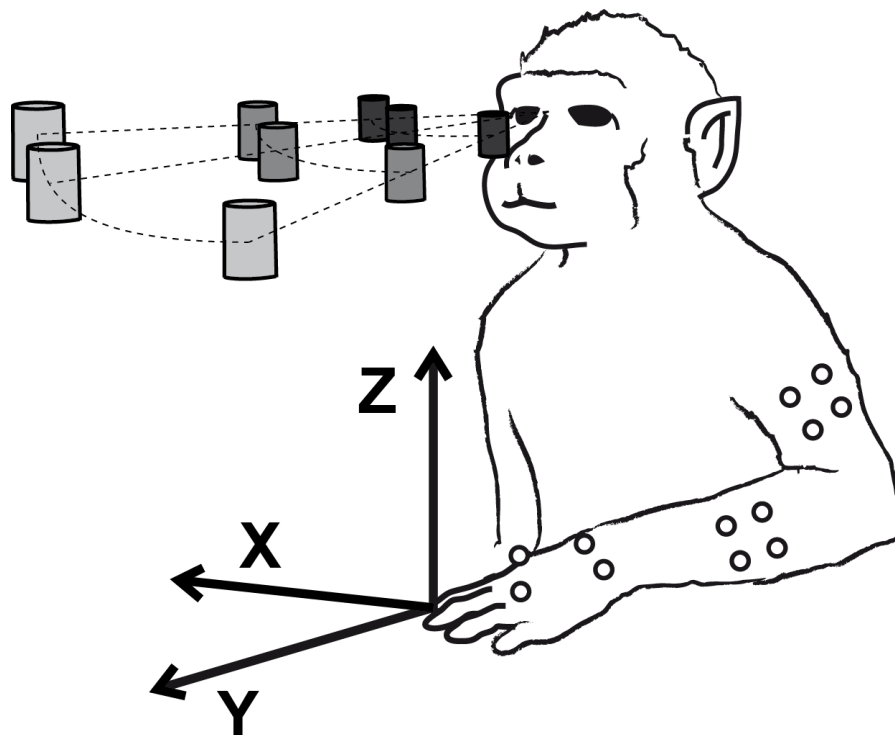


**Figure 9. Cartesian coordinates x, y and z**

X, y, z spatial coordinates relative to animal's body indicating kinematic workspace. The origin of the three dimensions corresponds to the home button that the animal had to press.

## 2.4. Neural data analysis

The effect of different target positions on neural activity was analysed in different time periods during the task. The task epochs taken into account for the analysis are indicated in the bottom part of Figure 7C. They were: a) the early fixation epoch (FIX) from 50 ms after the end of the fixation-saccade till 450 ms after it, b) the preparation epoch (PLAN) was the last 500 ms of fixation before the GO signal, c) the reach epoch (REACH) from 200 ms before the start of the arm movement (M) till the end of it signalled by the pressing of the LED target (H) and d) the hold epoch (HOLD), from the pressing of the LED target (H) till the switching off of the target (Redoff) that was the Go signal for the monkey to start a return movement to press the HB. The HOLD epoch lasted either 800 or 1200 ms, depending on the trial. Rasters of spiking activity were aligned on specific events of the task sequence, depending on the epoch analyzed. Because the monkey was not required to gaze at the fixation point after the LED switch-off, the eye position was not necessary maintained still during backward reaching movement from the panel to the home-button. Therefore, we decided not to investigate the vergence and the version effect on the reaching activity during backward arm movements. The effect of target depth and direction on activity was analyzed only in those units with a mean firing rate higher than 3 spikes/s and in those neurons that were tested in at least seven trials for each spatial position. The reasons for this conservative choice are connected to the implicit high variability of biological responses and are explained in detail in Kutz *et al.* (2003).

Significant modulation of neural activity relative to different target locations was studied using a two-way Analysis of Variance (ANOVA) test performed separately for each epoch with factors being target's depth and direction. The neural modulation relative to ANOVA's factors was assessed when factor 1 and/or factor 2 and/or the interaction factor 1 x 2 were significant ( $p < 0.05$ ). Target depth was defined as the distance of the target from the animal (near, intermediate, far) and target direction was its position with respect to the recording hemisphere (contralateral, central, ipsilateral). To find whether the incidence of each of the main effects differed significantly between two epochs a two-proportion z test (Zar, 1999) was applied, as detailed in Fluet *et al.* (2010). To quantify the selectivity of neuronal activity in each epoch for depth and/or direction signals, we calculated an index termed eta squared ( $\eta^2$ , (Zar, 1999)) using values obtained from the ANOVA test, and by applying the following formula:  $\eta^2 = SS_{\text{effect}}/SS_{\text{total}}$ , where  $SS_{\text{effect}}$  is the deviance of the main effect, and  $SS_{\text{total}}$  the total deviance. We calculated this index for

each of the two main effects (i.e., depth and direction) and for each of the four epochs of interest. To compare the index of the same cell in different epochs, confidence intervals on the  $\eta^2$  indices were estimated using a bootstrap test. Synthetic response profiles were created by drawing  $N$  firing rates (with replacement) from the  $N$  repetitions of experimentally determined firing rates. The  $\eta^2$  was recomputed using these  $N$  firing rates. Ten thousand iterations were performed, and confidence intervals were estimated as the range that delimited 95% of the computed indices (Batista *et al.*, 2007).

To analyze the spatial tuning of activity, a stepwise multilinear regression model was applied in each epoch considered. Regression methods quantify relationship between dependent (neural activity) and independent (target depth and direction) variables. Given that the target was foveated in all epochs of interest, its depth and direction in space were represented in head-centered coordinates and were equal to the vergence and version angles of the eyes, respectively. We are aware that our experimental configuration cannot distinguish between eye- and head/body-centered frames of reference of target encoding. That being said, in the rest of the thesis, when we refer to spatial tuning analysis and data the terms depth and vergence, as well as direction and version are interchangeable.

In the multiple linear regression model relating the neural activity in the epochs of interest to the different target positions we used this equation for the firing rate:

$$A(X_i, Y_i) = b_0 + b_1 X_i + b_2 Y_i$$

where  $A$  was the neural activity in spikes per second for the  $i$ th trials;  $X_i$  and  $Y_i$  the positions of the target defined as vergence and version angles, respectively, of the eyes during target fixation;  $b_1$  and  $b_2$  were regression coefficients and  $b_0$  the intercept. After being tested for their significance, the vergence and version coefficients were normalized with the standard deviation of vergence and version, correspondingly. The standardized coefficients allow a comparison among the independent variables and provide information about its relative influence in the regression equation. In our study this allowed to compare the vergence and version coefficients and to account for the fact that angle range was different for vergence and version. The regression coefficients were selected using a backward stepwise algorithm (Matlab function *stepwise*) that determined whether the coefficients were significantly different from zero. At the conclusion of the stepwise algorithm, only the coefficients that were statistically significant from zero to  $p < 0.05$

remained. These coefficients were then used to determine the spatial preference only in the cells with a significant main effect (ANOVA  $p < 0.05$ ) in a certain epoch. In modulated neurons without significant linear coefficients a Bonferroni post-hoc test ( $p < 0.05$ ) was applied to define the preferred position.

Population averaged spike density functions (SDF) were generated for the cells modulated by target depth/direction in the epochs of interest. In every cell, a SDF was calculated for each trial (Gaussian kernel, half width at half maximum 40 ms) and averaged across all the trials of the preferred and the opposite depths and directions as defined by the linear regression analysis. The peak discharge of the preferred condition was used to normalize the SDF. Population SDF curves representing the activity of the preferred and opposite condition were constructed by averaging the individual SDFs of the cells, aligned at the behavioral event of interest. In the cells with linear spatial tuning of movement activity (REACH) we calculated the response latency to movement execution for the preferred condition. The cell's response latency was defined as the mean latency of the three target positions of the preferred condition (near/far, ipsi/contra). For each position, we quantified the firing activity in the epoch PLAN. To find the onset of the reach-related response, a sliding window (width=20 ms, shifted of 2 ms) was used to measure the activity starting from 200 ms before the movement start. The distributions of activities in the two windows across trials were compared with a Student's t-test ( $p < 0.05$ ). The onset of the response was determined as the time of the first of five consecutive bins (10 ms) where comparisons were statistically significant ( $p < 0.05$ ). The above procedure, also used in a recent paper on V6A (Breveglieri *et al.*, 2012), was adapted from an earlier work (Nakamura and Colby, 2000).

All analyses were performed using custom scripts written in MATLAB (Mathworks, Natick, MA, USA).

## 2.5. Kinematic data analysis

Data were analyzed off-line with a second-order Butterworth dual pass filter (low-pass cut-off frequency of 15Hz). In all the photographs of the recording video, each marker was classified with the relative label to allow the trajectory reconstruction and the calculation of the kinematic variables. Off-line analyses have been run by a Matlab program developed in our laboratory. For each marker, instantaneous velocity has been determined using a five-point central finite difference algorithm. Movement velocity has been used to determine the beginning (velocity above 30 mm/s) and the end (velocity below 30 mm/s) of each trial (Figure 10). The path curvature was calculated as the percentage increment of the length of the real trajectory traced by the wrist, between the onset and the termination times, with respect to the ideal straight path (Casadio *et al.*, 2007). The ideal trajectory was represented by the distance between the initial and the final points of the real trajectory. We compared the movement curvatures performed with the right limb with those performed with the left limb using a t-test ( $p < 0.05$ ).

The kinematic parameters taken into account were: movement time (MT), mean velocity (MV), mean acceleration (MA), peak velocity (PV), peak acceleration (PA), peak deceleration (PD), mean percentage of the movement at the peak velocity (TPV), mean percentage of movement accelerating (TPA), mean percentage of the movement decelerating (TPD) (Figure 10). To highlight the similar and different timing modulation of proximal and distal arm segments, we grouped the markers in categories based on the temporal trend they showed reaching velocity, acceleration and deceleration peaks and their proximity to the body. All these variables were assessed for each individual movement, for each marker, as well as for each target position. In fewer cases, however, one or more markers were imperfect or not visible for a portion of movement (e.g. for light reflection) and the corresponding parameters were excluded from the following statistical analysis. Mean values for each dependent measure were calculated for the trial blocks and were analyzed performing two separate analysis of variance (one way ANOVA,  $p < 0.05$ ) using as independent variables the movement depth (near, intermediate or far) for the first ANOVA and the movement direction relative to the arm used (ipsilateral, central or contralateral) for the second ANOVA.

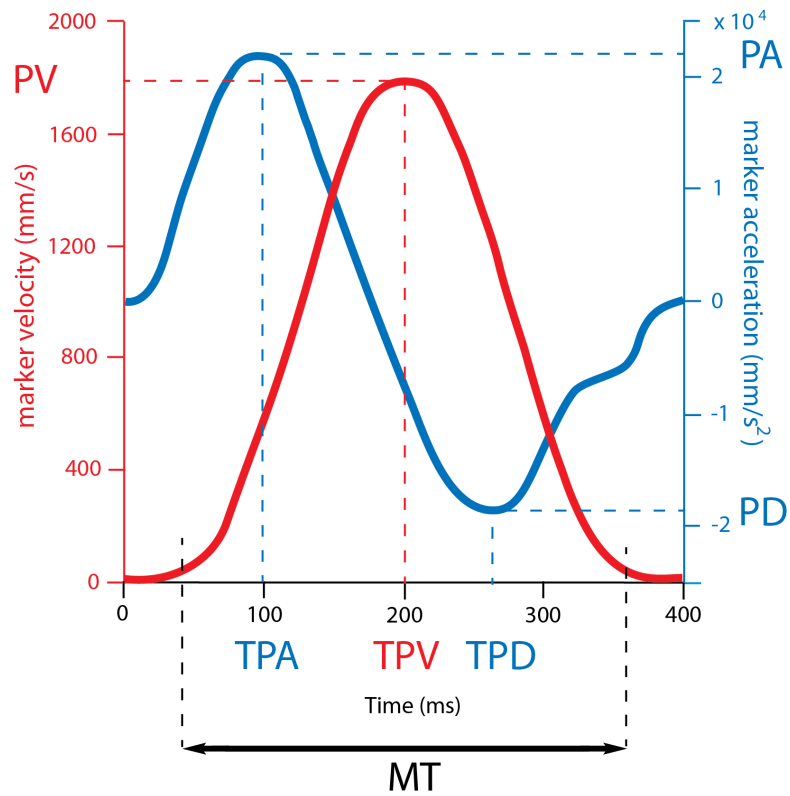


**Figure 10. Kinematic parameters profiles**

For each marker, velocity (red line) and acceleration (blue line) were calculated in order to determine the peak of velocity (PV), acceleration (PA) and deceleration (PD), as well as the relative times (TPV, TPA, TPD). Movement time (MT) corresponds to the time from movement onset (velocity above 30 mm/s) until the velocity dropped below 30 mm/s.

### 3. RESULTS

We recorded neuronal activity in V6A and identified 288 well isolated and stable cells in two monkeys (Monkey A: 192, Monkey B: 96). Animals were required to execute reaches to foveated targets located at different directions and depths. Targets' elevation was kept constant at eye level. Figure 11 illustrates four examples of modulated neurons. All cells were tuned in several time epochs, both in depth and direction. The first neuron (Figure 11A) was modulated by target depth in all epochs and preferred intermediate to far positions. The cell was also tuned for target direction during both fixation and arm-movement planning, showing higher activity for contralateral positions. The second neuron (Figure 11B) responded strongly during all the epochs for targets located in the near space. In PLAN and REACH epochs, an additional preference for targets located in the contralateral space emerged. The third neuron (Figure 11C) was modulated by target direction in all epochs and preferred ipsilateral positions. In addition, it showed a preference for near space only during PLAN and REACH. Finally, the fourth cell (Figure 11D) was modulated by both depth and direction in the first two epochs, before arm movement execution, responding strongly for far positions and showed a small -though significant- preference for contralateral space. In REACH and HOLD epochs the effect of direction disappeared, while a strong depth tuning with a preference for targets located in near space emerged.

The examples in Figure 11 highlight the main characteristics of V6A cells during reaches in 3D space, i.e. the coexistence in single cells of modulations by both target direction and depth, and the fact that direction and depth can affect all epochs or be present only early or late in the task.

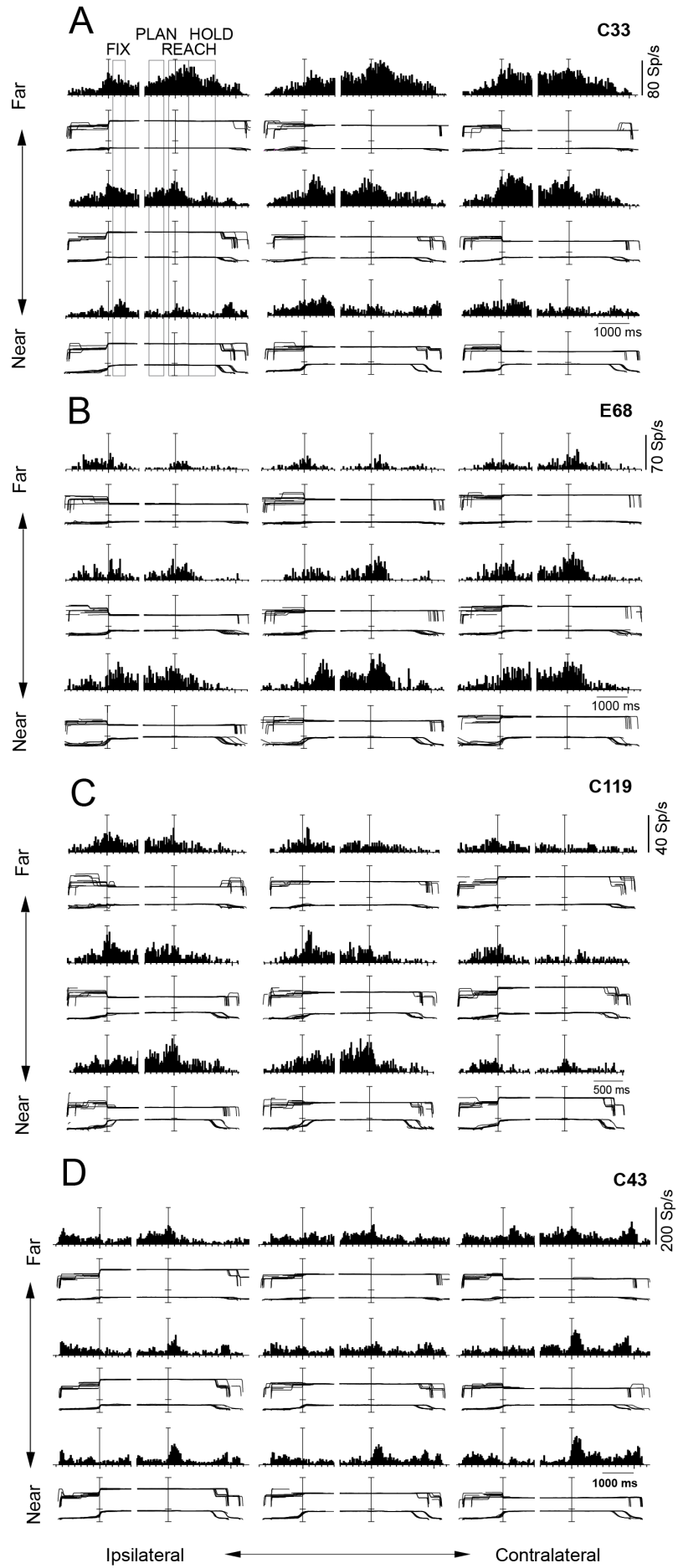


**Figure 11. Example neurons with depth and direction tuning in several epochs.**

**A-D**, Spike histograms and version and vergence eye traces for the nine target positions, arranged at three directions (columns) and three depths (rows). Vertical bars indicate the alignment of activity and eye traces at the start of fixation and at the start of arm movement. Realignment is evidenced with a gap in histograms and eye traces.

**A,B,D**, Neurons showing depth tuning starting from fixation till the holding the target period. Modulations by direction in A and D occurred quite early before- and disappeared during arm movement, whereas in B it occurred shortly before and was preserved during arm movement.

**C**, Neuron modulated by target direction from fixation till the holding of the target period and by depth shortly before and during the arm movement: in both A and B, the neurons showed the same depth preference before and after the arm movement, whereas in D the preference was inverted.

### 3.1. Tuning for depth and direction in the different task phases

To quantify the effect of depth and direction a two way ANOVA was performed in each epoch. In total, 98% of the cells were modulated ( $p < 0.05$ ) by at least one of the two factors in at least one epoch (94% for depth and 86% for direction). As shown in Figure 12, during FIX similar numbers of cells were modulated by depth only, direction only and both signals. In the subsequent epochs, the percentage of cells modulated by depth only and by both signals slightly increased, whereas the incidence of tuning by direction only significantly decreased (two-proportion z-test,  $p < 0.05$ ). As shown in Table 1, in epochs PLAN, REACH, and HOLD the overall effect of target depth and direction were not equally represented, with the effect of depth being 10-20% more frequent than the effect of direction. In all epochs, a good percentage of neurons were jointly sensitive to both depth and direction signals, with more and more cells of this kind as the task progressed.

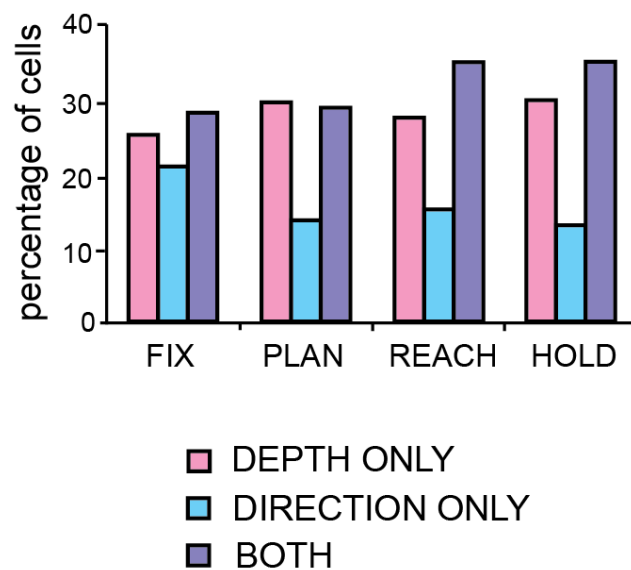


**Figure 12. Incidence of depth and direction tuning in the population (N=288) of V6A neurons.**

Percentage of neurons with tuning for depth only (pink), direction only (light blue), or both signals (violet) during several task epochs (fixation, planning, movement and holding, ANOVA,  $p < 0.05$ ).

EPOCH	DEPTH		DIRECTION	
	ANOVA	Regression	ANOVA	Regression
FIX	155/288 (53,8%)	133/155 (85,8%)	143/288 (49,6%)	110/143 (76,9%)
PLAN	170/288 (59%)	141/170 (82,9%)	124/288 (43%)	100/124 (80,6%)
REACH	182/288 (63,2%)	154/182 (84,6%)	146/288(50,7%)	115/146%(78,8%)
HOLD	189/288 (65,6%)	159/189 (84,1%)	140/288(48,6%)	101/140 (72,1%)

**Table 1.** Number of neurons modulated for depth and direction in each epoch.

To evaluate the time course of depth/direction selectivity in the different task epochs, we calculated the eta square index ( $\eta^2$ ) as detailed in the METHODS. The  $\eta^2$  index was used to measure the strength of the effect of the two factors on the firing rate. Figure 13A plots the average values of  $\eta^2$  for depth and direction in the neurons with a significant main effect of these variables in each epoch. The depth and direction selectivity were not significantly different during FIX (Student's t-test  $p>0.05$ ), whereas depth selectivity was significantly higher than direction selectivity in all the other epochs (Student's t-test  $p<0.05$ ).

Figure 13B illustrates the selectivity of depth and direction factors in single cells modulated in pairs of temporally adjacent epochs (FIX-PLAN, PLAN-REACH, REACH-HOLD). The  $\eta^2$  indices found in each epoch for depth (Figure 13B, top) and direction (Figure 13B, bottom) were used to plot single points, which represent single cells. Filled circles represent neurons with a significantly different index between two adjacent epochs (bootstrap test, 10.000 iterations,  $p<0.05$ ); empty circles indicate cells with similar selectivity (bootstrap test, 10.000 iterations,  $p>0.05$ ). Figure 13B confirmed, at the single cell level, the results shown for the population of V6A neurons in Figure 13A, in that neurons were significantly more affected by depth as the task progressed, i.e. in PLAN versus FIX, in REACH versus PLAN, and in REACH versus HOLD, while direction selectivity did not significantly change in the different epochs.

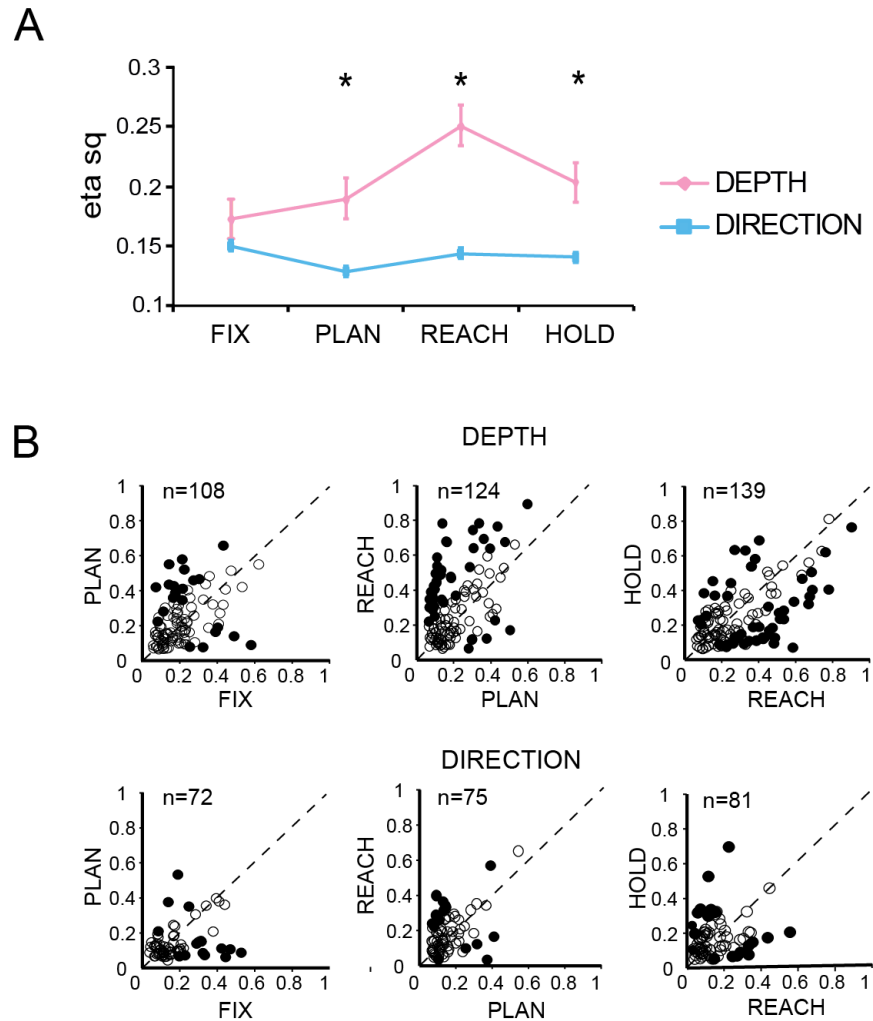


**Figure 13. Comparison of depth and direction selectivity across epochs in the population (N=288) of V6A neurons.**

**A**, Time course of depth (pink) and direction (light blue) selectivity calculated as mean±S.E. of the eta squared ( $\eta^2$ ) index for the population of neurons modulated in each epoch. Depth selectivity increased after the fixation epoch and reached a maximum at the movement epoch. Direction selectivity remained constant during task progress. Asterisks indicate a significant (Student's t- test,  $p < 0.05$ ) difference between the average values of indices.

**B**, Scatter plots of  $\eta^2$  index in neurons modulated by depth (upper panels) and direction (lower panels) in pairs of adjacent epochs. Each point represents one neuron. Filled and empty circles indicate cells with  $\eta^2$  index that was significantly different (bootstrap test, 10.000 iterations,  $p < 0.05$ ) or not, respectively, between two adjacent epochs. In single neurons depth selectivity was enhanced during the REACH epoch.

### 3.2. Spatial tuning in different task phases

To quantify the spatial tuning of the neurons a linear regression analysis was performed with target depth and direction as independent variables. Since the target to be reached out was always foveated, the depth and direction in space of the target could be defined in head/body-centered coordinates, i.e. with the vergence and version angles, respectively, of the eyes. The linear regression model was used because we observed that few neurons displayed their maximal firing rates for intermediate and central positions and these positions were the least preferred in our population (10% of cells, Bonferroni post-hoc). As shown in Table 1, most of the neurons that were significantly modulated by target depth and direction (ANOVA,  $p < 0.05$ ) had discharges that were linearly correlated ( $p < 0.05$ ) with vergence and version angles, respectively. In each neuron, the sign of the linear correlation coefficients (standardized) were used to determine the spatial preference in a certain epoch. Neurons with significant linear vergence tuning were classified as near or far, whereas cells linearly tuned by version angle were classified as contralateral or ipsilateral, depending on the sign of the linear version coefficient and the recording hemisphere.

The percentage of cells falling into the above groups in each epoch is illustrated in Figure 14. Neurons tuned for “far” reachable space were found to be more than those tuned for “near” reachable space (Figure 14, top). The difference was statistically significant in all epochs apart from REACH ( $\chi^2$ ,  $p < 0.05$  in FIX, PLAN and HOLD). Regarding the directional tuning (Figure 14, middle), contralateral neurons were more numerous than ipsilateral ones in all epochs, but the difference was never statistically significant ( $\chi^2$ ,  $p > 0.05$ ). The bottom part of Figure 14 shows that near and far cells were similarly tuned for contralateral and ipsilateral space (two-way  $\chi^2$ ,  $p > 0.05$ ). In summary, the analysis of the spatial tuning showed that the distributions of spatial preference within the reachable space tested were quite similar across epochs.

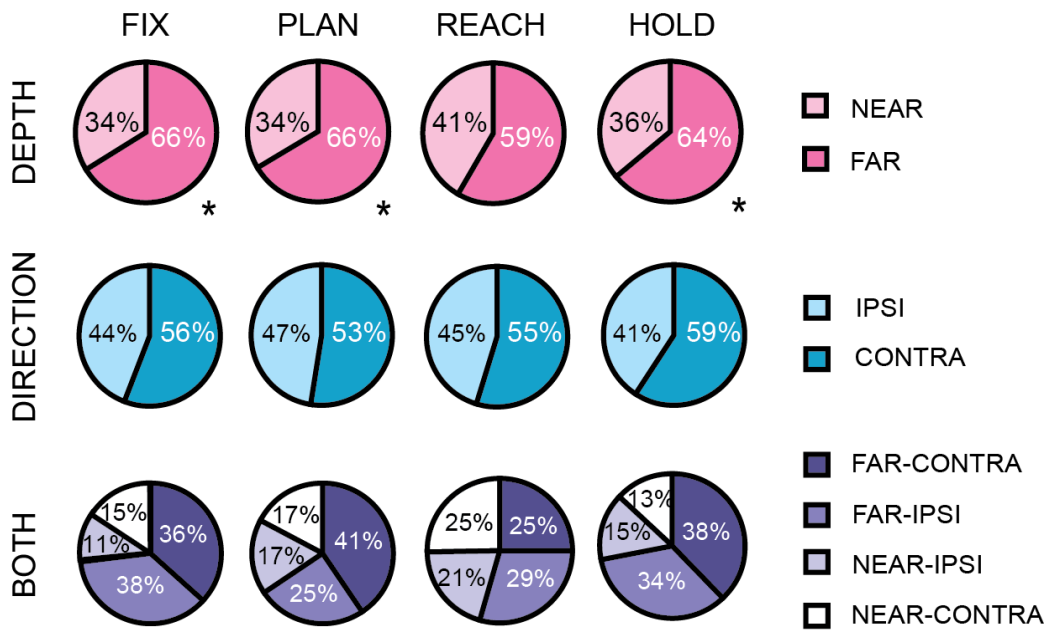


**Figure 14. Spatial tuning in single epochs**

Top: Percentage of neurons linearly modulated by depth that preferred far (dark pink) and near (light pink) space in each epoch. Middle: Percentage of the neurons linearly modulated by direction that preferred contralateral (medium blue) and ipsilateral (light blue) space in each epoch. Bottom: Percentage of the neurons belonging to combination of classes in cells linearly modulated by both depth and direction. Asterisks indicate a statistically significant ( $\chi^2$ ,  $p < 0.05$ ) spatial preference.

We then addressed the question of whether the constancy in the distribution of preferred depths and directions across the task was the result of a single group of neurons being active, or whether different subpopulations of cells were spatially tuned in each epoch. For this purpose we defined and quantified cells that preserved, changed, lost or acquired their spatial tuning from one epoch to the next. The results of this analysis are shown in Figure 15. The spatial tuning of depth modulations (Figure 15, left) was remarkably consistent across epochs (40-50% of the cases), and the consistency of spatial tuning increased as the task progressed through the epochs. In only 3% of neurons the spatial tuning changed as the task progressed. The coefficients of determination ( $R_{sq}$ ) were calculated to measure how well the coefficients of one epoch can predict the value of the coefficients in the next one. The depth coefficients were strongly correlated with highly significant  $R_{sq}$  values (range 0.73-0.77,  $p < 0.0001$ ). It is interesting to note that these values were quite constant across the epoch comparisons, thus demonstrating an equal strength of depth tuning consistency as the task progressed.

As illustrated in the right part of Figure 15, the direction tuning was less consistent across epochs than depth tuning (less than 30% of the cases), without significant changes as the task progressed. In about 35% of cases the directional tuning was lost, and in another 35% of cases it emerged only at the later epoch of each pair. As a result, the subpopulation of cells tuned in direction in a certain epoch was in large part different from that recruited in the next one. The version coefficients of adjacent epochs were strongly correlated, as for vergence, with highly significant  $R_{sq}$  values (range: 0.56-0.86,  $p < 0.0001$ ). In contrast to what observed in depth tuning, these values were more variable across epoch comparisons, with the PLAN/REACH pair showing the highest and the FIX/PLAN the lowest  $R_{sq}$  value, respectively. In other words, the spatial tuning that appeared early in the task exerted a strong influence on the spatial tuning of the activity in the latter epochs. However, a considerable number of neurons lost their spatial tuning, and different subpopulations of spatially tuned cells became active during planning, arm movement execution and holding of the static arm position. This latter finding, together with the similar one relative to the depth tuning, suggests that additional spatial information -other than eye position- became available for the tuning of activity in PLAN, REACH and HOLD epochs.

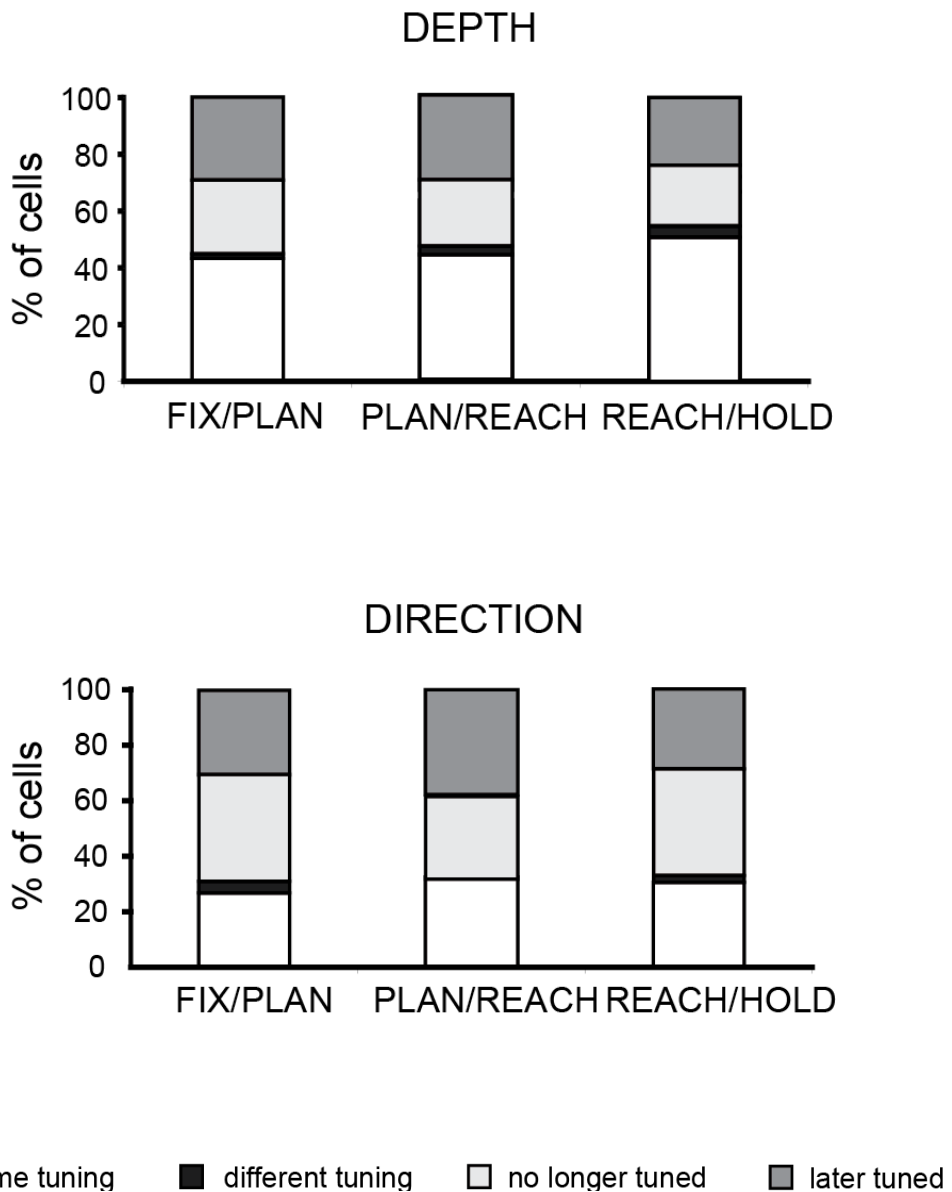


**Figure 15. Tuning consistency across epochs.**

Percentages of cells that showed the same (white), different (black) tuning, and those that lost (light gray) or acquired later (medium gray) the tuning in depth (top) and direction (bottom) in pairs of consecutive epochs during the task progress.

To characterize the sources of additional spatial input during movement execution, we determined the latency of response in the neurons linearly modulated in REACH. Latency was measured as the time at which REACH activity became significantly higher than PLAN activity (see Methods). The mean latency of reaching responses (n=143) was  $41.6 \pm 155$  (S.D.) ms after the movement onset (Figure 16). In 74 cells (52%) the response started before the movement onset, whereas in 69 neurons (48%) the response started after the movement onset. The first group of cells are likely activated by a corollary discharge from the premotor cortex (Gamberini *et al.*, 2009; Matelli *et al.*, 1998; Shipp *et al.*, 1998), whereas the second one could reflect proprioceptive and tactile signals from the arm that are known to affect an important fraction of V6A neurons (Breveglieri *et al.*, 2002). To test whether there was a difference in the onset of depth reaching responses compared to the direction ones, mean latencies were calculated separately for the preferred depth and direction. Neurons with depth modulations (n=113) had a mean latency of  $+24.6 \pm 148.8$  ms; directionally tuned cells (n=78) a mean latency of  $61.6 \pm 163.6$  ms. The two latency distributions were not statistically different (Kolmogorov-Smirnov test,  $p > 0.05$ , Wilcoxon signed rank test,  $p > 0.05$ ). This suggests that depth and direction signals affect the reaching-related activity with a similar time course.

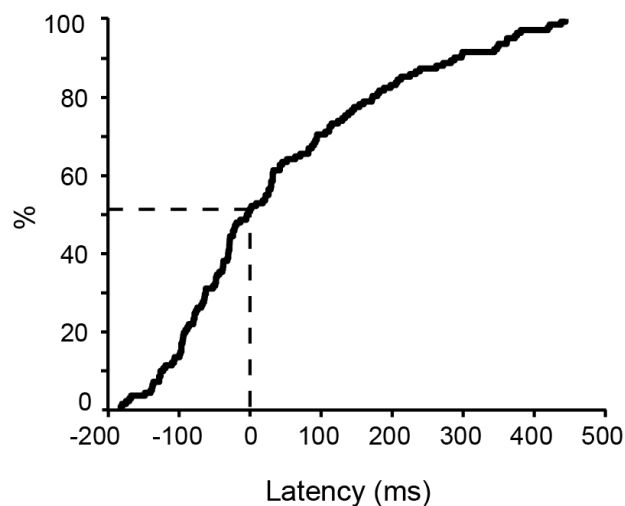


**Figure 16. Time course of reach-related responses**

Cumulative frequency distribution plot of the latencies of reach-related responses in cells with a significantly higher REACH activity compared to PLAN. The horizontal axis shows time with respect to the beginning of the movement (movement onset). The vertical axis indicate the percentage of cells tested (n=143).

### 3.3. Cell Categories

We divided the V6A cells reported in this study into three main categories based on the presence of modulation in epochs FIX and REACH. Neurons were classified as ‘FIX cells’ when they showed spatial tuning in FIX, but not in REACH, ‘REACH cells’ when the opposite condition occurred, and ‘FIX-REACH cells’ when the neurons were modulated in both epochs. The percentage of cells ascribed to each category are reported in Figure 17. Cells modulated by depth (Figure 17, top), were more frequently represented in the category of ‘FIX-REACH cells’ ( $\chi^2$ ,  $p < 0.05$ ), whereas neurons modulated by direction were evenly distributed between the three categories (Figure 17, bottom). We then calculated the percentage of cells modulated in PLAN or HOLD that fell into each of these categories (Figure 17, middle and right panels). Exact numbers are reported in the Figure legend. PLAN cells and HOLD cells belonged mostly to the ‘FIX-REACH cells’ category, whereas a minority of them did not fall to any of the three main categories (~15% for depth, ~20% for direction). Overall, the above analysis confirmed the coincidence of modulations between the epochs and revealed the existence of distinct categories of cells.

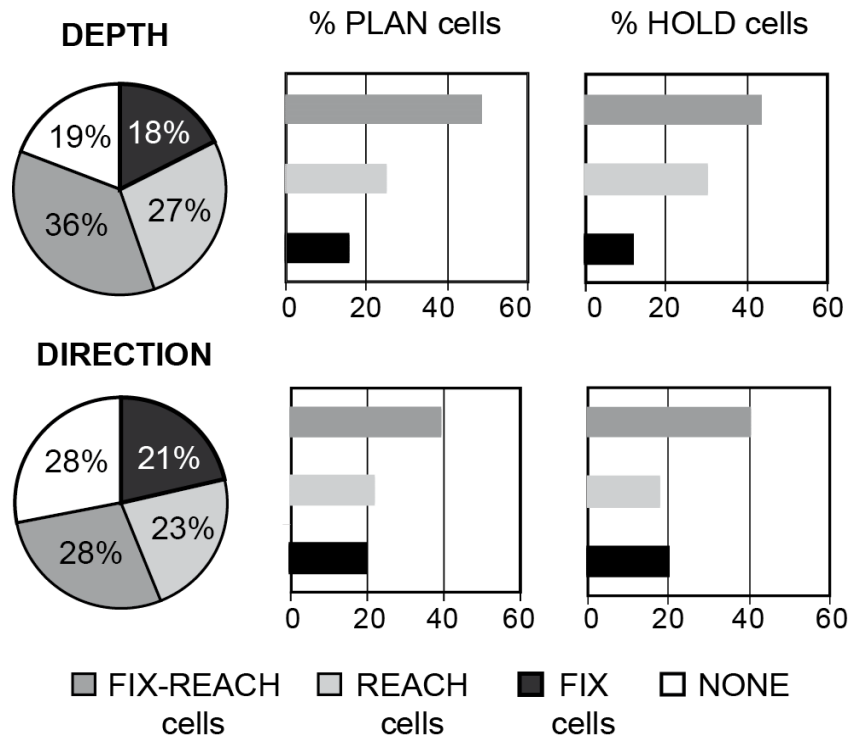


**Figure 17. Depth and direction tuning in subpopulations of V6A cells**

Left: Percentage of neurons with modulations by depth (upper left panel) and direction (lower left panel) present in FIX and REACH epochs ('FIX-REACH cells', dark gray), in FIX but not in REACH ('FIX cells', black), and vice versa ('REACH cells', light gray), or in none of them (white). Middle and right: Percentage of neurons modulated by depth (upper panels) and direction (lower panels) in PLAN (central panels) and HOLD (right panels) epochs that fell into the coincident (dark gray) or mutually exclusive (black, light gray) FIX-REACH modulations. For depth tuning (top, middle and right panels), both PLAN and HOLD cells were more likely defined as 'FIX-REACH cells' (82 cells in both PLAN and HOLD, 48% and 43 %, respectively,  $\chi^2$ ,  $P < 0.05$ ), whereas the 'FIX cells' category had the fewer number of neurons (PLAN: 26 cells/15% ; HOLD 22 cells/12% ). For the cells modulated by direction (bottom, middle and right panels), a similar clustering of PLAN and HOLD cells into the three categories was found, with a clear prevalence of the 'FIX-REACH cells' type ( $\chi^2$ ,  $P < 0.05$ ).

Population spike density functions (SDFs) allowed us to investigate the temporal pattern of activity in the three main categories of cells. The population SDFs were constructed by averaging the single neuron SDFs for the preferred and opposite condition. Figure 18 illustrates the average population activity of each category of cells for depth (left panels) and direction (right panels) modulations. In FIX cells the activity in the preferred and opposite conditions started to diverge about 200 ms before fixation onset, at around the time of fixation saccade. The activity of non preferred depths and directions then decreased rapidly at or below the baseline level, while that of the preferred depths and directions remained high during the first part of fixation (FIX), decreasing with different speeds with time: more slowly the depth tuning and more rapidly the direction tuning (Figure 18, top left and right panels, respectively). At the population level, both depth and directionally tuned ‘FIX cells’ showed arm movement related responses that were not significantly different in the preferred and opposite conditions.

It is worth noting that the activity in the preferred depth, but not in the preferred direction, was higher than that in non-preferred condition during the whole fixation period, including the PLAN epoch before the reaching movement. The difference in temporal evolution of activity between the ‘FIX cells’ modulated in depth and those directionally tuned is in line with a recent study from our lab that showed a more tonic effect of vergence with respect to version (Breveglieri *et al.*, 2012). It also agrees with the increased consistency in spatial tuning between FIX and PLAN in the depth dimension that we observed in the present study (Figure 15).

In ‘REACH cells’ the time course of modulation was very similar for depth and direction tuning (Figure 18, middle panels). The population activity for the preferred and opposite conditions diverged well after the fixation onset. In the preferred condition the population activity remained stable during fixation, whereas in the non-preferred one it progressively decreased till the go signal for reaching. After the go signal, the activity increased (much more in preferred condition), reaching its peak at movement onset. The difference in activity between the preferred and opposite conditions was evident during the whole movement period and during most of the HOLD period.

FIX-REACH neurons (Figure 18, bottom panels) showed a temporal pattern of activity that combined those of FIX and REACH cell categories. In this category of cells, the preferred condition was defined based on the activity in REACH epoch, which was

congruent in the vast majority of cases (>90%) with the preferred condition in FIX. ‘FIX-REACH cells’ displayed two peaks of activity, one around fixation onset and another around arm-movement onset. Between these two events, the curves representing the preferred and opposite conditions were well separated. The time course of population activities was similar in depth (Figure 18, bottom left panel) and direction (Figure 18, bottom right panel) modulations. Interestingly, the activity in preferred conditions (both for depth and direction) decreased during fixation as in FIX neurons, but then increased in the last part of fixation (PLAN), just before the movement onset, as it occurred in REACH neurons. In summary, V6A neurons were found to encode different types of signals during a reach-in-depth task: eye-position and arm movement related information influenced independently (‘FIX cells’, ‘REACH cells’), or jointly (‘FIX-REACH cells’) the activity of V6A neurons. Regarding the anatomical distribution in V6A of the above types of cells, the histological reconstruction of the recording sites did not show any segregation of the main cell categories, as shown in Figure 19.

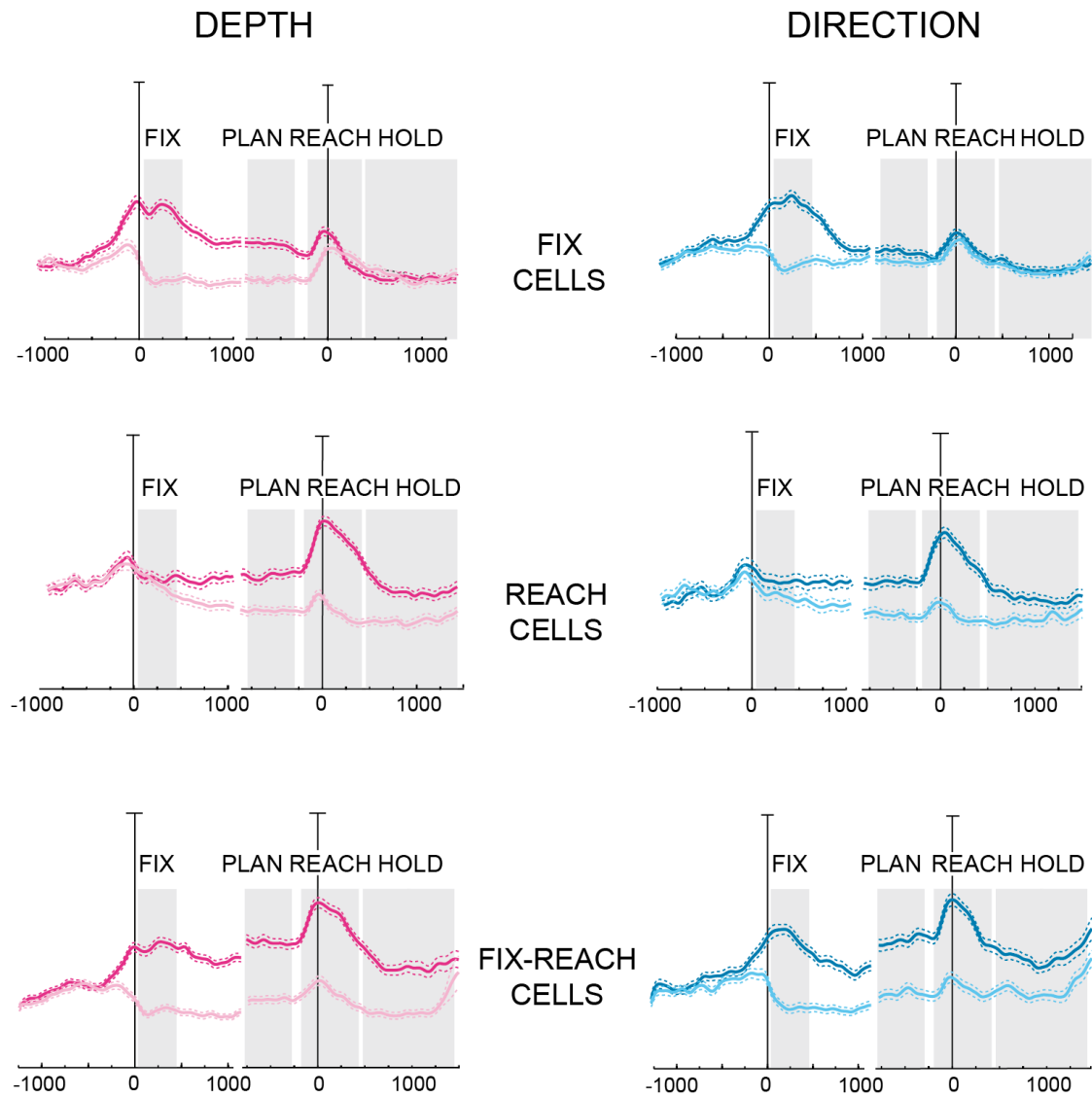


**Figure 18. Population average activity in the main categories of V6A cells.**

Average normalized spike density functions (SDF) for each defined subpopulation. Top/ Middle/ Bottom: Population activity represented as SDF of ‘FIX cells’/ ‘REACH cells’/ ‘FIX-REACH cells’ modulated by depth (left) and direction (right) doubly aligned at the beginning of fixation and at movement onset. For each cell category and type of modulation the average SDF for the preferred (dark color) and opposite (light color) condition are plotted. Solid and dashed curves represent the population average and standard errors, respectively. Scale bar in all SDF plots: 100% of normalized activity. Gray shaded areas indicate the time span of the four task epochs.

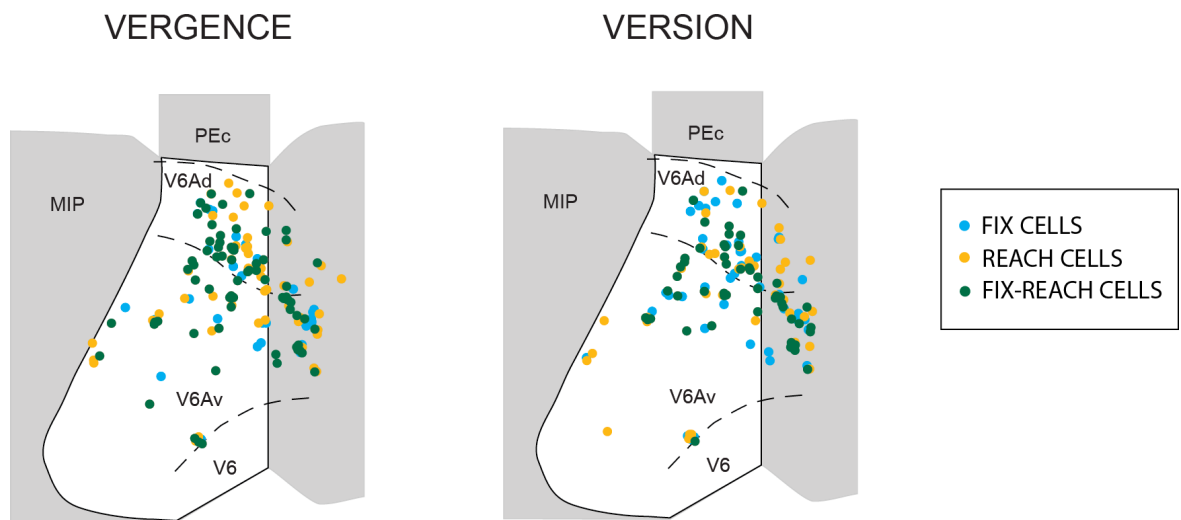


**Figure 19. Anatomical reconstructions of the recording sites.**

Flattened maps of area V6A showing the neurons modulated by vergence signals (left map) and by version signals (right map). Each circles represents a single cell. Light-blue circles represent ‘FIX cells’, yellow circles represent ‘REACH cells’ and green circles represent ‘FIX-REACH cells’. V6: area V6; V6Ad: dorsalV6A; V6Av: ventral V6A; MIP: medial intraparietal area; PEc: caudal area PE .

### 3.4. Movement trajectories

In one monkey, we reconstructed the trajectory of each reaching movement to each target. We did this for each of the twelve markers. Here, the movement paths of the marker WIR2 is described because the wrist represents the most significant marker for the study of the arm transport component. The position of the marker WIR2 is shown in Figure 8. Figure 20 shows 90 examples of wrist trajectories (10 for each target position) for each limb employed during the performance of the task. The similarity of the paths demonstrates that trajectories of different replications of the same movement were highly stereotyped and highly overlapping in a trained monkey. The differences in elevation between wrist trajectories towards distinct spatial depths (evident in the Figure 20A) were provided by an horizontal arm posture necessary to touch the farthest targets (black lines) and a vertical forearm posture employed to touch the nearest targets (red lines). The paths followed by the hands described curved trajectories in workspace, in particular the right wrist paths. For the right wrist (Figure 20B), the trajectories showed a curvature towards the right workspace and for the left wrist (Figure 20A) we observed a quite symmetrical trend. There are also other differences between the left and the right trajectory patterns and they are probably due to a not completely symmetrical posture of the two arms in the execution of the reaching task. The same features were observed in Figure 21A-B where WIR2 trajectories relative to each target position were averaged and plotted in three dimensions. This figure reveals that the shapes of movements towards different spatial positions but performed with the same hand were similar and stereotyped. Considering that the reach targets were located at the same elevation (at the same level in z dimension) it is important to compare the behavioral data of the two arms in the other two dimensions (x and y). In Figure 22 the mean left and right wrist (Figure 22A-B) and thumb (Figure 22C-D) trajectories were plotted in x and y dimensions, representing respectively the direction and the depth domain. As described in the other figures, the left and the right wrist followed curved paths, but the left was more linear with respect to the right. To measure the different path curvatures, we quantified the percentage of increase of each trajectory extent relative to the ideal straight line. The curvature of the movements performed with the right arm is significantly higher (t-test,  $p < 0,05$ ) with respect to the movements performed with the left arm, as shown in Figure 23. The difference between the two limbs probably reflects the different strategies that the animal uses to perform reaching task or the different level of training.

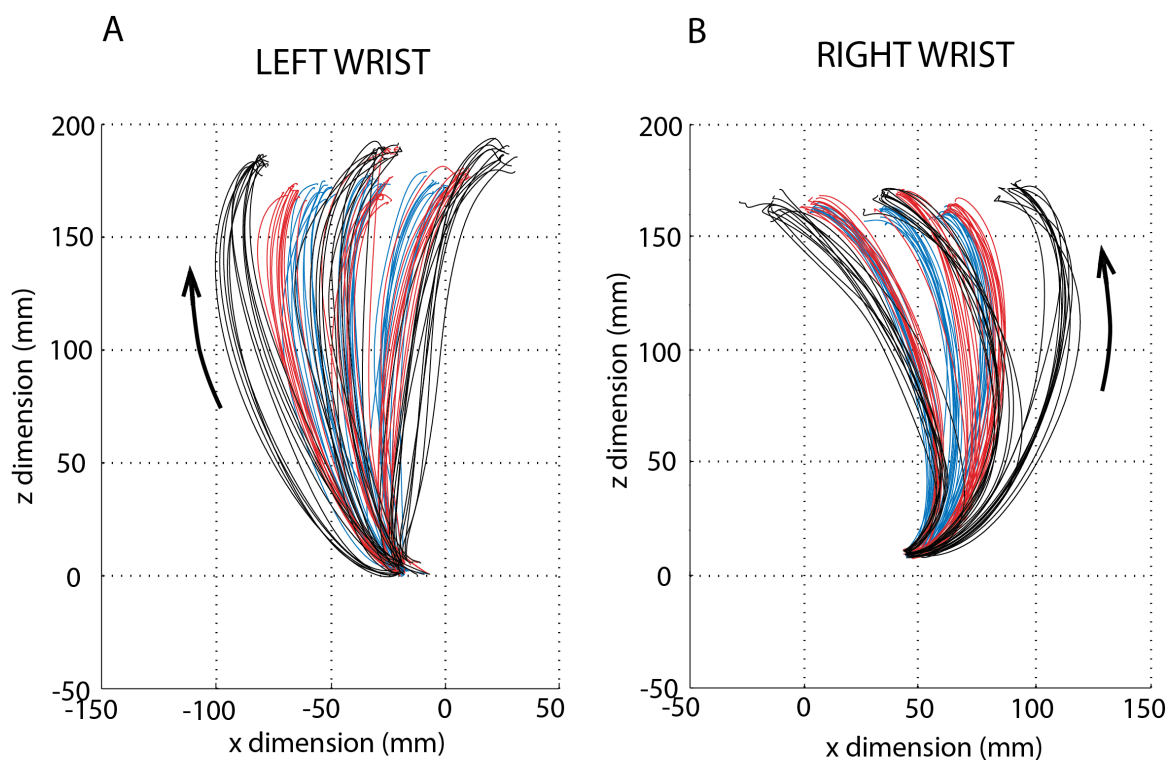


**Figure 20. Examples of wrist trajectories**

Two dimensional plots of representative examples of WIR2 trajectories during the execution of the reaching task employing the left arm (A) and the right arm (B). 10 replications were plotted for each spatial position the animal reached with the same limb: the black lines represented the trajectories towards the farther targets, the blue lines towards the intermediate and the red lines towards the nearest. Arrows indicate the direction of the movement vectors. X and z axes correspond to those shown in Figure 9.

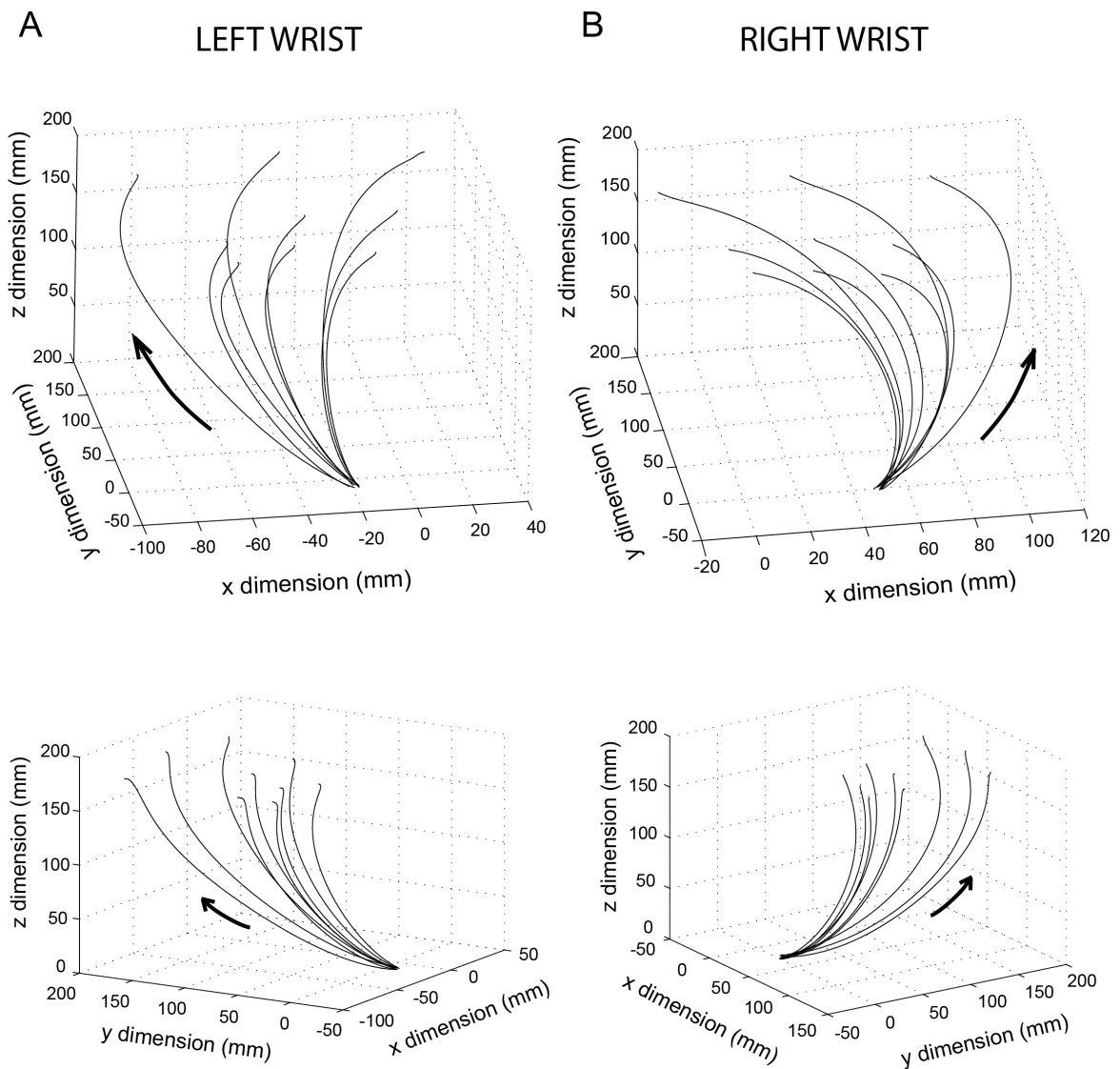


**Figure 21. Mean wrist trajectories in 3D**

WIR2 trajectories obtained averaging all the trajectories recorded using the same hand and reaching the same targets. Arrows indicate the direction of the movement vectors. X, y and z axes correspond to those shown in Figure 9.

- A. Top (upper panel) and lateral view (lower panel) of the nine mean wrist trajectories that represent the nine movements required by the tasks and performed with the left arm.
- B. Top (upper panel) and lateral view (lower panel) of the nine mean trajectories of the right wrist during the execution of goal-directed actions towards the nine spatial positions.

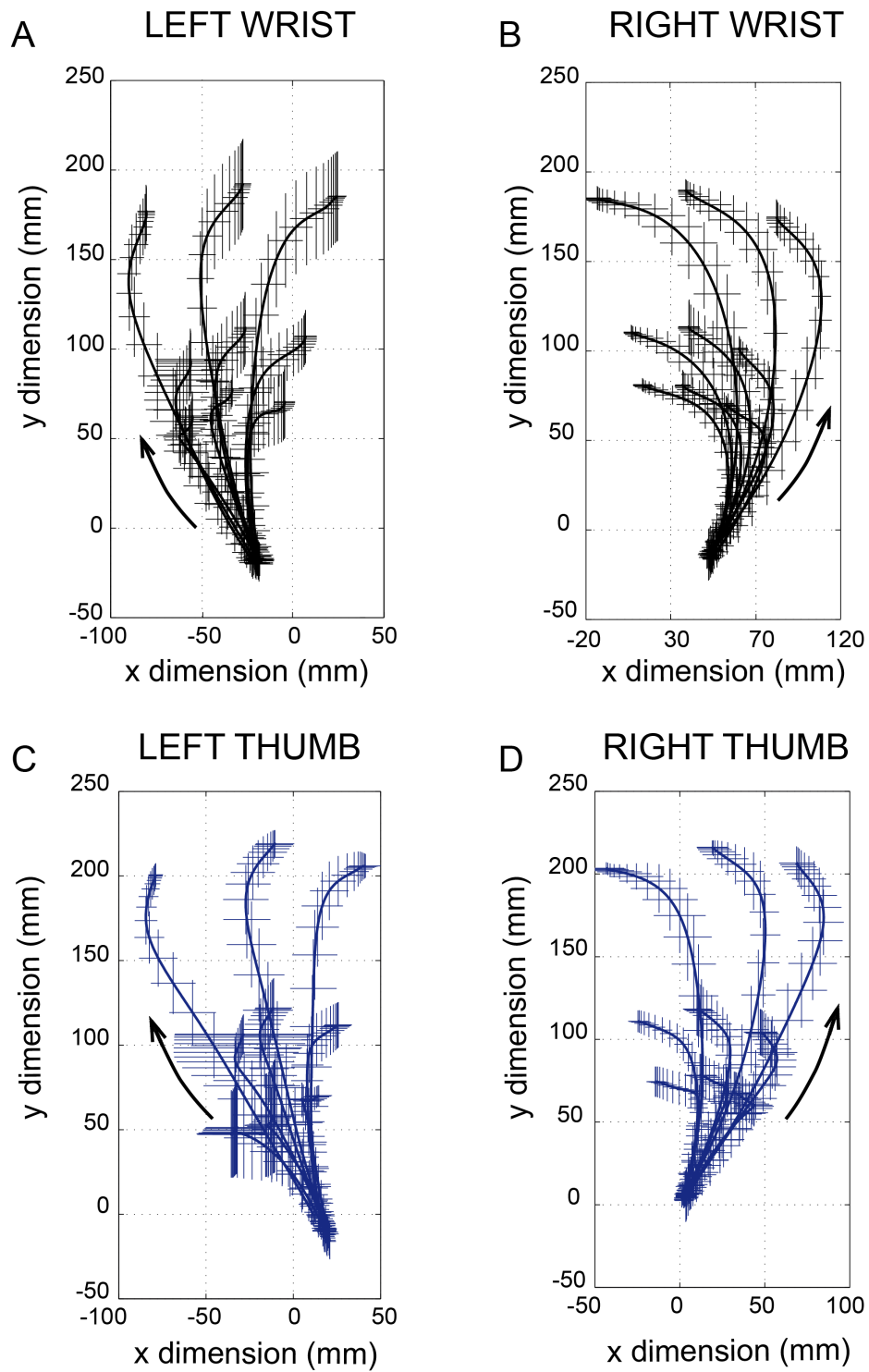


**Figure 22. Mean wrist and thumb trajectories and their variability**

Top view of the mean movement trajectories of the left (A) and of the right wrist (B) and of the left (C) and of the right thumb (D) in x and y dimension. Vertical and orizontal tick markers represent standard deviation. Arrows indicate the direction of the movement vectors.

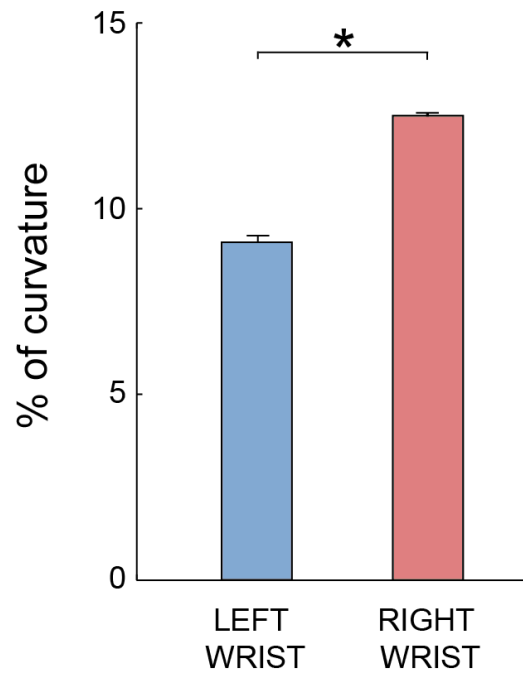


**Figure 23. Percentage of movement curvature comparing the trajectories performed with the left and the right limb.**

Mean path curvature (%) of the wrist trajectories during the execution of the reaching movements performed using the left (blue column) and the right arm (red column). Error bars represent the standard errors of the means. Asterisk denote the statistical difference ( $p < 0,05$ ) of the trajectory curvature when the movements are performed with the right limb instead of the left limb.

### **3.5. Movement time**

Movement durations of each marker were calculated for near, intermediate and far reaches and compared with a one way ANOVA ( $p < 0,05$ ) (Figure 24A). The same procedure was performed for the different spatial directions relative to the arm used (Figure 24B). In the figures we reported the data of only one marker for each arm segment because markers included in the same body part have the same displacement and show equal values. In Figure 24A the mean durations of the farther movements were statistically longer than the others. Only few markers displayed differences between movement times towards intermediate targets and those towards near targets. For the direction dimension, all the markers considered showed significant differences in movement direction in all the possible comparisons and longer movements when the arm was directed towards the contralateral space (Figure 24B).

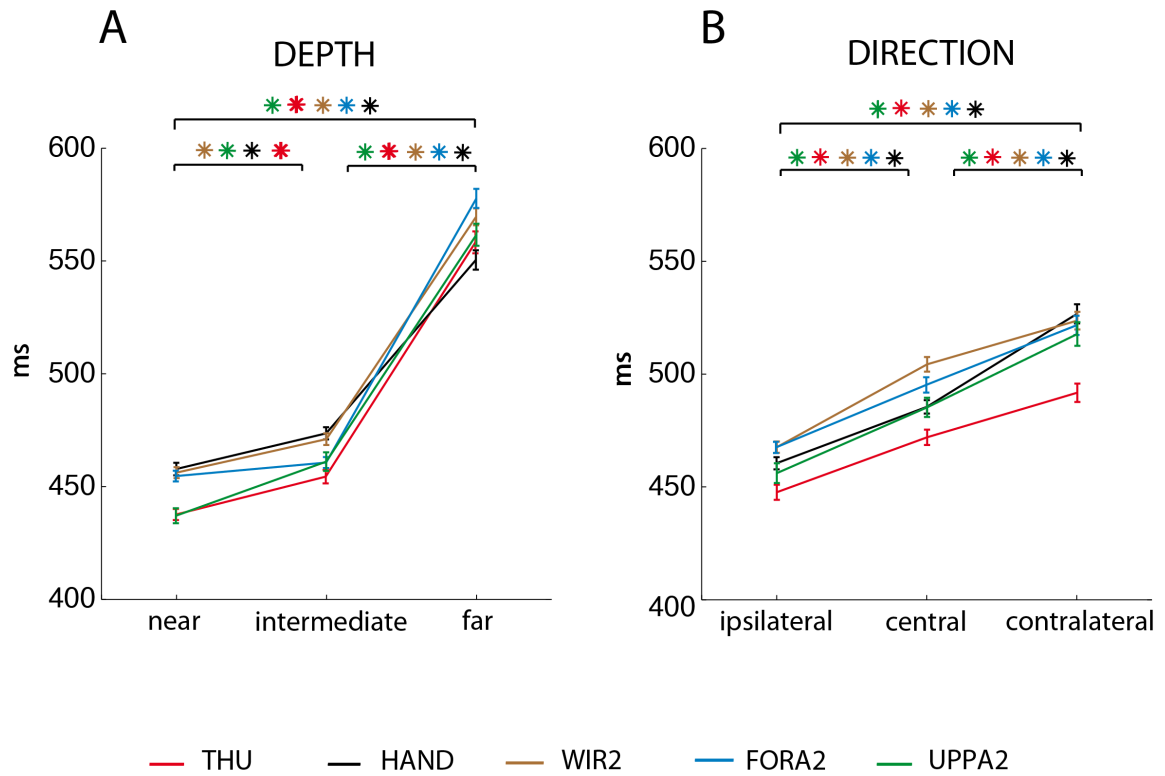


**Figure 24. Movement time**

Mean movement durations (ms) of thumb, hand, wrist, forearm and arm during the execution of the reaching movements. Error bars represent the standard errors of the means. Asterisks denote the markers with movement durations significantly ( $p < 0,05$ ) different in two task conditions.

**A.** Mean movement durations as a function of target depth

**B.** Mean movement durations as a function of target direction

### 3.6. Velocity Profiles

For each marker, velocity profiles describing the movements towards the different spatial positions showed single bell-shaped peaks, in agreement with human studies (Morasso, 1981). Figure 25 reports examples of the velocity curves of the left wrist relative to each target direction and target depth. The maximum velocity was reached by the ipsilateral movement directed towards the farther target, as shown in the Figure 25.

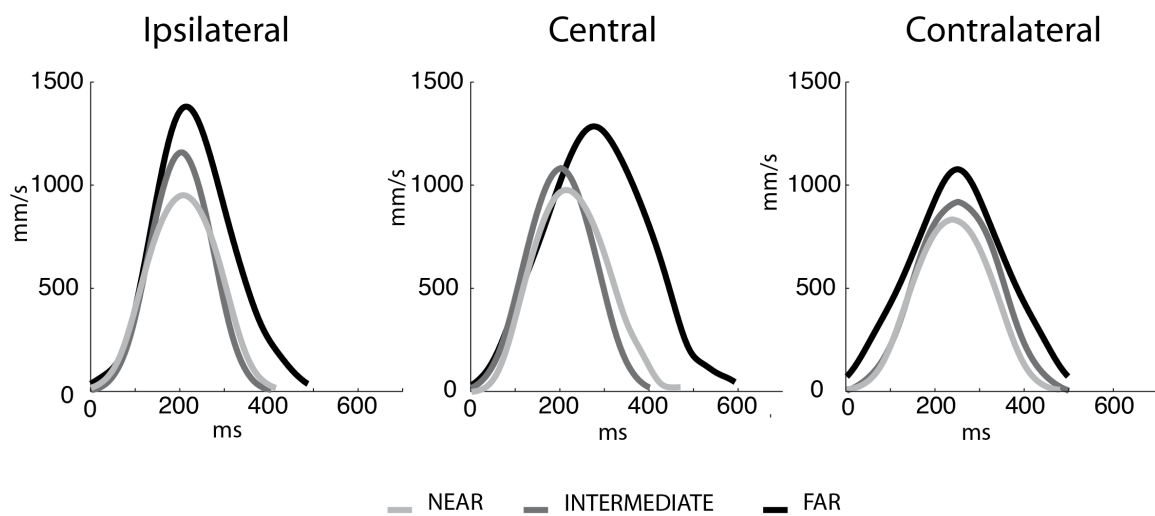


**Figure 25. Wrist velocity profile**

Examples of velocity profiles of movements of the left wrist aimed at each of 9 targets located in three different directions and three different depths, are indicated with the grey scale.

### **3.7. Mean peak velocity**

Figure 26 reports the mean peak velocities of each arm portion during goal-directed movements towards targets located at different depth (Figure 26A) and direction (Figure 26B). Peak velocities of each marker were statistically different in all the component of the depth dimension with a clear trend towards the far space. The monkey increased the velocity moving the hand towards the farthest targets in order to compensate for the longest movement duration necessary to reach them. This allowed to decrease the difference between the time spent to touch the farthest targets with respect to the time spent to reach the nearest targets. Comparing different spatial direction, the distal markers reached a significantly higher velocity when the movement was directed towards ipsilateral targets than the contralateral ones. This phenomenon was absent for the proximal markers: the forearm and the superior part of the limb. In both dimensions, the peak velocities corresponding to distal markers were higher with respect to the peak velocities of the proximal ones because the velocities were directly correlated to the trajectory extent.

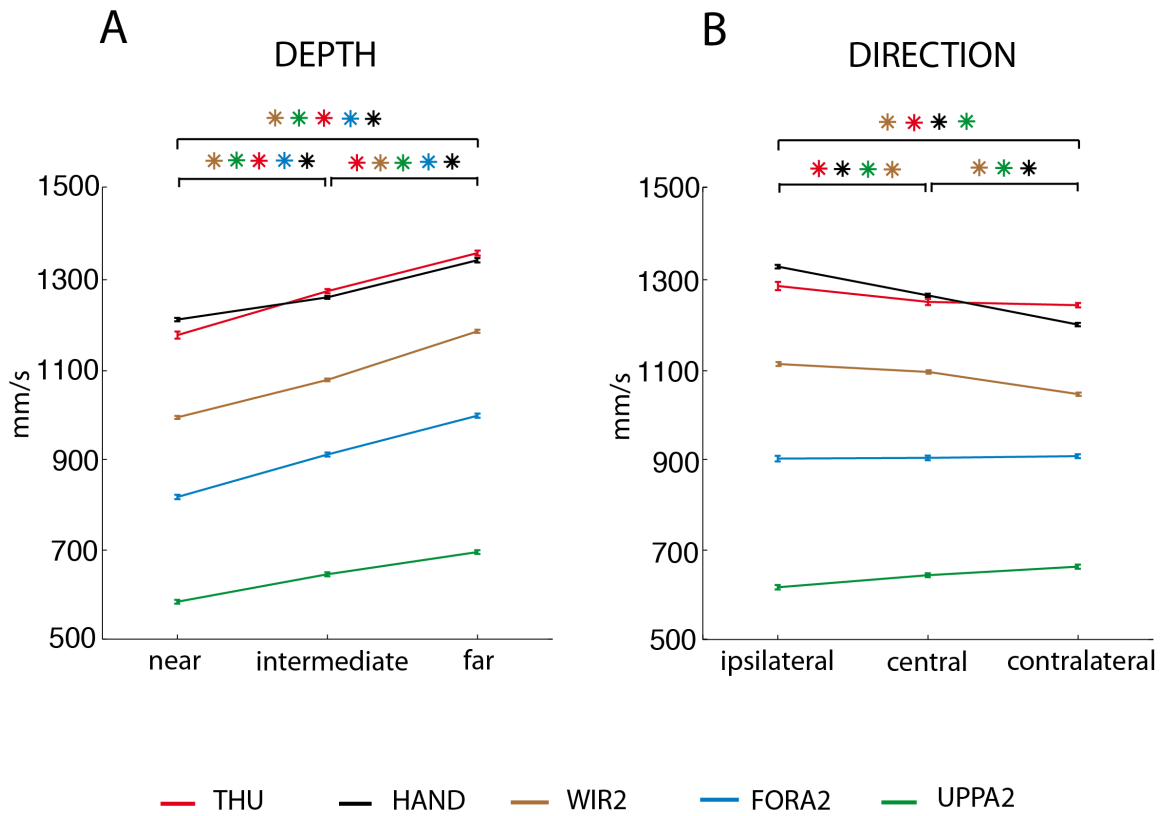


**Figure 26. Peak velocity**

Peak movement velocities (mm/s) of thumb, hand, wrist, forearm and arm during the execution of the reaching movements. Error bars represent the standard errors of the means. Asterisks denote the markers that had movement velocities significantly ( $p < 0,05$ ) different in two task conditions.

**A.** Peak movement velocities as a function of target depth

**B.** Peak movement velocities as a function of target direction

### **3.8. Mean peak acceleration**

Peak accelerations of thumb, hand, wrist, forearm and arm movements were calculated for each dimension. The values measured from the most proximal parts of the arm were significantly higher for the movement with the greater amplitude. The markers relative to the others limb portions showed variable results comparing to movement towards different depths (Figure 27A). For the direction dimension, all the markers considered, with the exception of the superior part of the arm, showed significant differences in all the possible comparisons, displaying higher acceleration for the movements directed towards the ipsilateral space (Figure 27B). In both dimensions, it is interesting to observe that the peaks of the distal markers were higher with respect to peaks of the proximal ones.

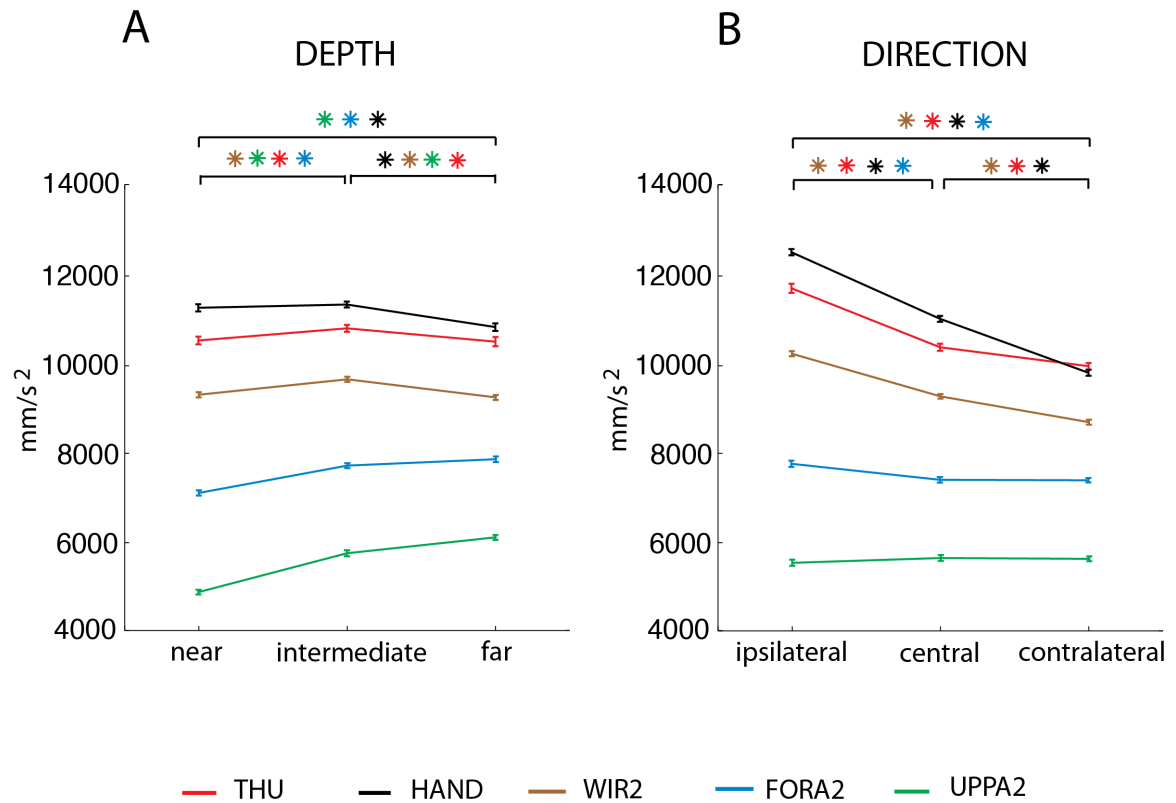


**Figure 27. Peak acceleration**

Peak movement accelerations (mm/s<sup>2</sup>) of thumb, hand, wrist, forearm and arm during the execution of the reaching movements. Error bars represent the standard errors of the means. Asterisks denote the markers that had movement accelerations significantly (p < 0,05) different in two task conditions.

**A.** Peak movement accelerations as a function of target depth

**B.** Peak movement accelerations as a function of target direction

### 3.9. Mean peak deceleration

For the depth dimension, multiple comparisons revealed variable significant differences in all the markers considered. For the majority of the markers, the deceleration was statistically stronger during the movements performed towards intermediate targets, as shown in Figure 28A. For the direction dimension, the distal arm portions showed the maximum deceleration corresponding with the movements directed towards the ipsilateral space while forearm and arm did not reveal the same trend in direction (Figure 28B). In both dimensions, relevant observation is referred to the peaks of distal markers that were higher respect to the peaks of the proximal ones.

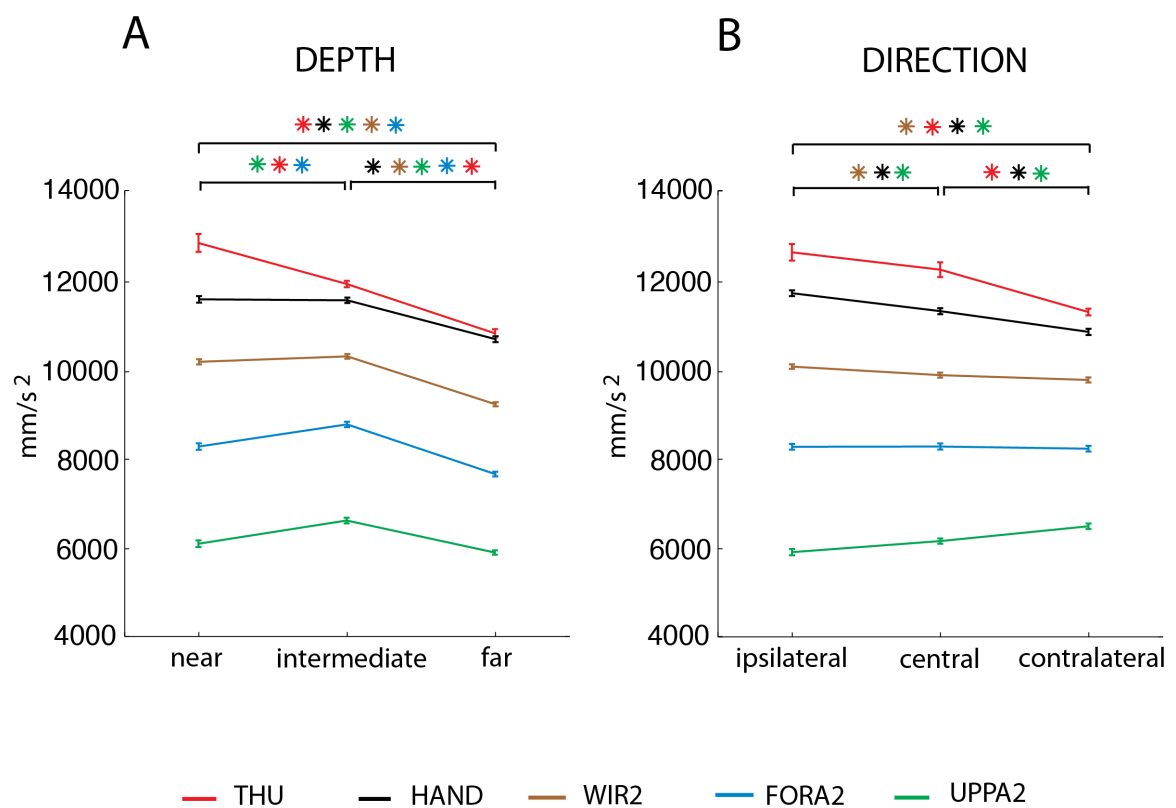


**Figure 28. Peak deceleration**

Mean peak deceleration, measured from the thumb, the back of the hand, the wrist, the forearm and the arm during the execution of reaches in depth and in direction. Error bars represent the standard errors of the means. Asterisks denote the markers that had movement decelerations significantly ( $p < 0,05$ ) different in two task conditions.

**A.** Peak movement decelerations as a function of target depth

**B.** Peak movement decelerations as a function of target direction

### **3.10. Percentage of movement at the peak velocity**

A significant target depth effect was observed in the majority of the markers taken into account, as shown in Figure 29A. The maximum velocity was reached earlier in the movements with a large extent with respect to the movements with a short extent. Comparing movements characterized by different directions, we found that the proximal arm portions showed a common trend, reaching the peak velocity earlier in the contralateral actions than in the other ones but this phenomenon was absent or inverted in the distal part of the arm (Figure 29B). In contrast with the depth dimension, in the direction dimension the velocity control of the movements showed different temporal patterns for distal and proximal markers. In both dimensions, velocity peaks of the upper part of arm were reached later respect to the peaks of the other markers.

Considering only the markers that showed a significant difference in the velocity timing, we compared movements directed towards near and far targets and movements towards ipsilateral and contralateral ones. We divided them in categories depending on their temporal pattern and their proximity to the shoulder (Figure 30). The markers located in the upper arm and in the forearm represented the proximal markers, while the markers located on the wrist, hand and thumb were considered as distal ones. Figure 30 (upper part) shows that both proximal and distal markers maintained the same trend in the depth domain, reaching the peak velocity earlier when the movements were directed towards the far targets with respect to the near ones. In the direction dimension, the proximal markers reached the maximum velocity earlier in the contralateral actions than in the ipsilateral ones, while the distal markers showed the opposite temporal trend (Figure 30, bottom).

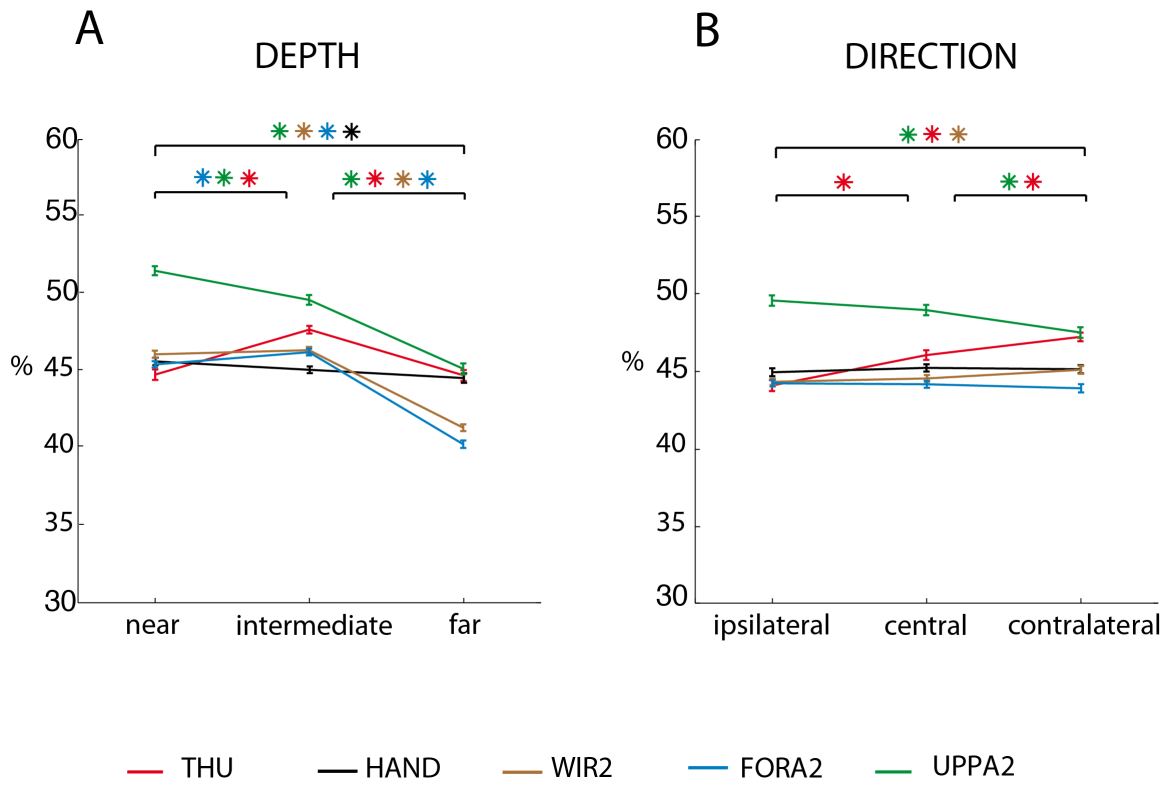


**Figure 29. Percentage of movement at the peak velocity**

Mean percentage of movements when the velocity of each marker reached the maximum. Error bars represent the standard errors of the means. Asterisks denote the markers that were significantly ( $p < 0,05$ ) different in two task conditions.

**A.** Percentage of movement at the peak velocity as a function of target depth

**B.** Percentage of movement at the peak velocity as a function of target direction

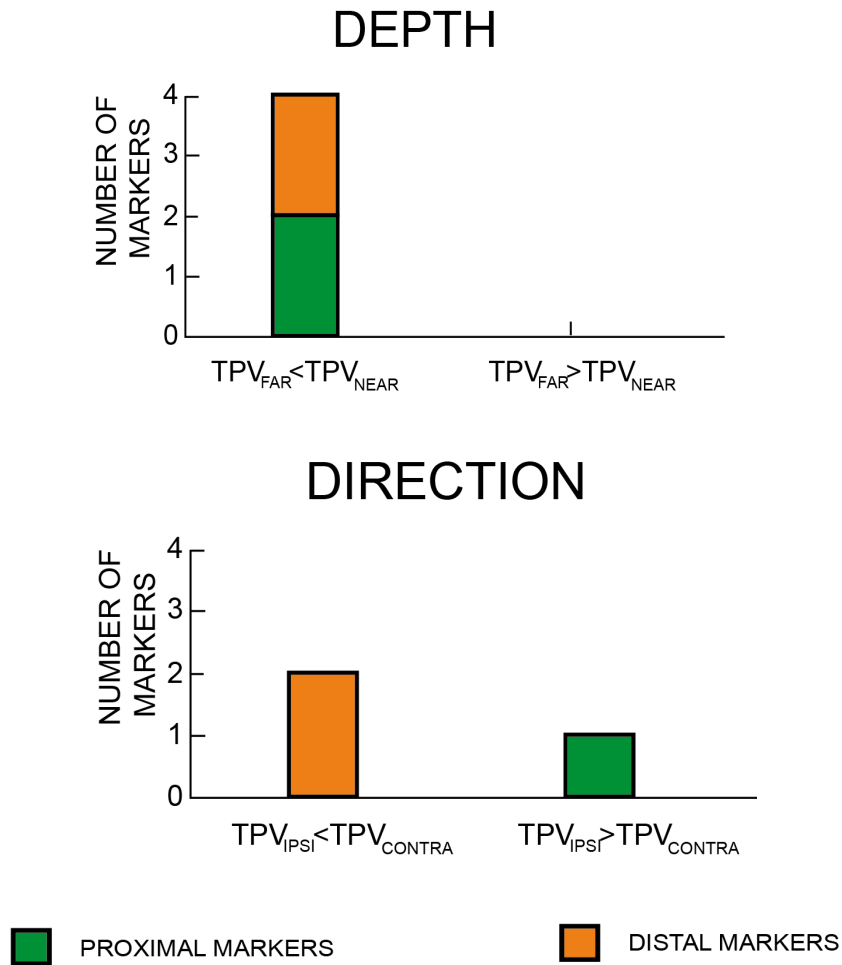


**Figure 30. Number of proximal and distal markers following different temporal velocity patterns in depth (upper histogram) and in direction (lower histogram)**

Top: Number of proximal (green) and distal markers (orange) reaching the peak velocity earlier (left column) and later (right column) when movements were directed towards the far targets with respect to the near ones.

Bottom: Number of proximal (green) and distal markers (orange) reaching the peak velocity earlier (left column) and later (right column) when movements were directed to ipsilateral targets with respect to contralateral ones.

### **3.11. Percentage of movement accelerating**

A significant depth effect was observed for all the markers considered, the peak acceleration was reached earlier for the movements towards the far space and later for the movements towards the near space (Figure 31A). For the direction dimension, we did not find a common trend for all the markers. The proximal arm portion showed a later peak acceleration in the ipsilateral movements, but for the distal markers this phenomenon was absent, as shown in Figure 31B. In the direction dimension, the acceleration control of the movements showed different temporal patterns for distal and proximal markers. In both dimensions, acceleration peaks of the upper part of arm were reached later respect to the peaks reached by the other markers.

The upper part of Figure 32 shows that, in the depth domain, both proximal and distal markers modulated acceleration similarly. In fact they increased velocity earlier when the movements were directed towards the far targets with respect to the near ones. In the direction dimension, the proximal markers accelerated earlier when monkey performed contralateral actions, while distal markers showed an opposite temporal trend. Wrist presented similar behavior of proximal markers (Figure 32, bottom).

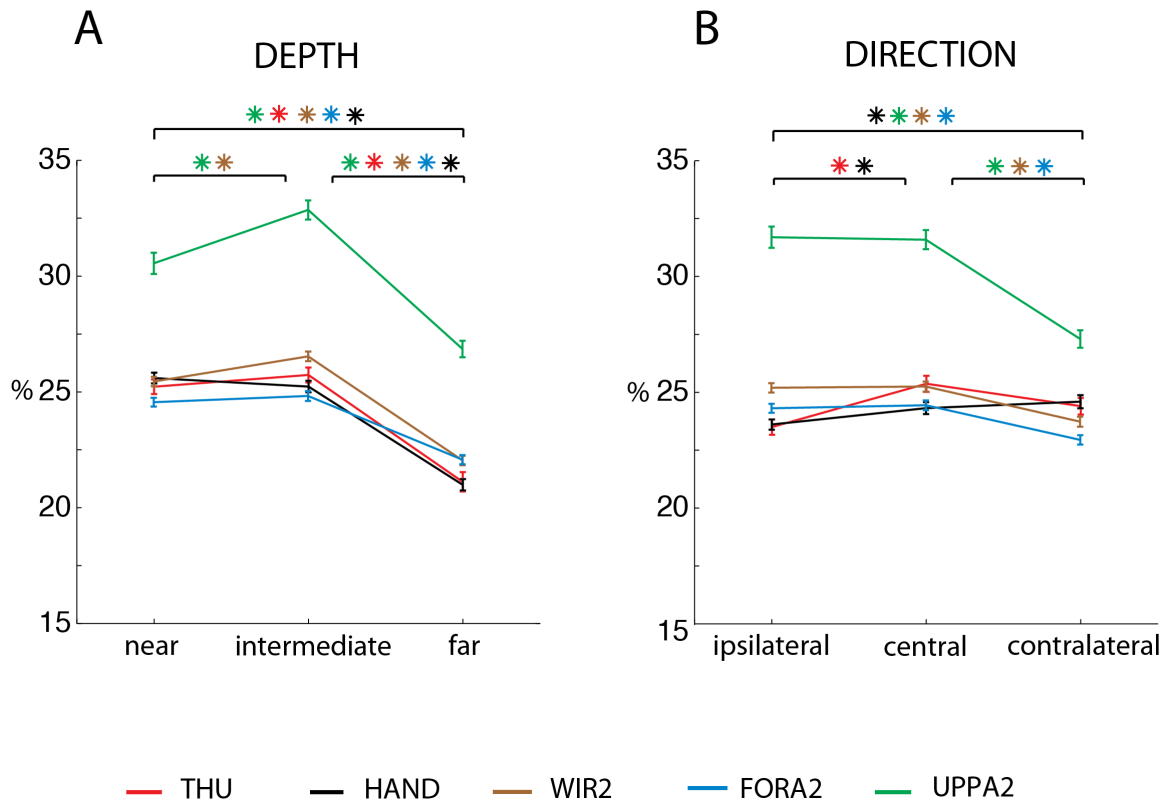


**Figure 31. Percentage of movement accelerating**

Mean percentage of movements when the acceleration of each marker reached the maximum. Error bars represent the standard errors of the means. Asterisks denote the markers that were significantly ( $p < 0,05$ ) different in two task conditions.

**A.** Percentage of movement at the peak acceleration as a function of target depth

**B.** Percentage of movement at the peak acceleration as a function of target direction

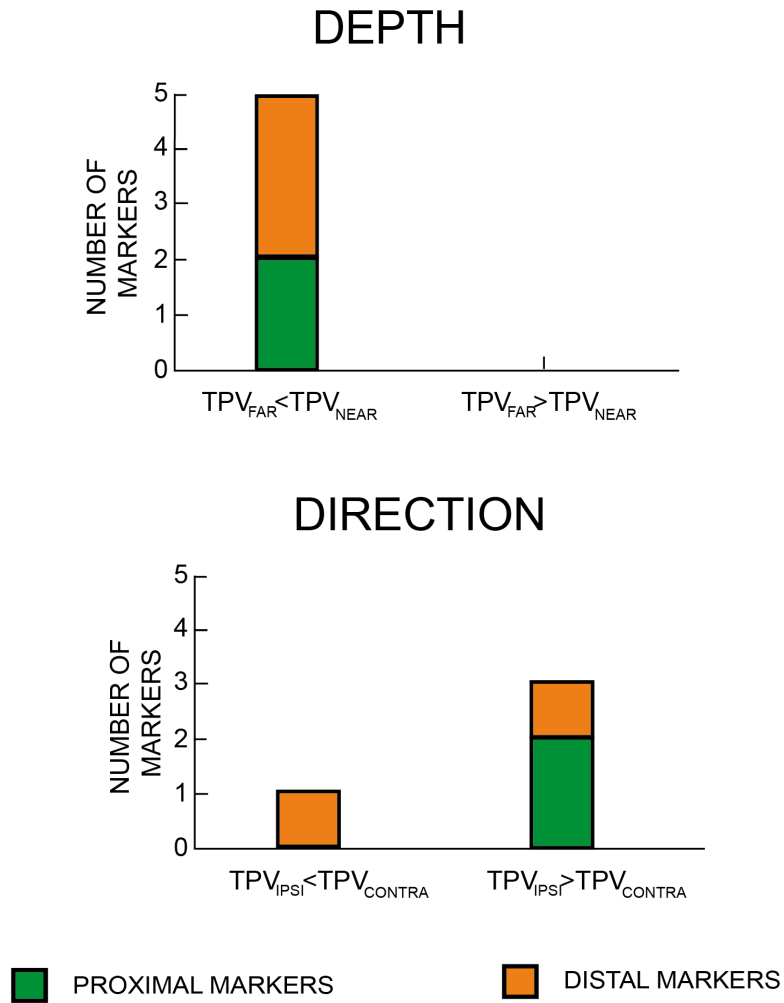


**Figure 32. Number of proximal and distal markers following different accelerating temporal patterns in depth (upper histogram) and in direction (lower histogram)**

Top: Number of proximal (green) and distal markers (orange) accelerating earlier (left column) or later (right column) when movements were directed towards far targets with respect to near ones.

Bottom: Number of proximal (green) and distal markers (orange) accelerating earlier during ipsilateral actions than during contralateral ones (left column) and earlier during contralateral movements than during ipsilateral ones (right column).

### **3.12. Percentage of movement decelerating**

In Figure 33A, the deceleration peak occurred statistically earlier during the movements with a large amplitude than in the others, for all markers considered. For the direction dimension, the deceleration peaks measured from the distal markers were reached earlier for the ipsilateral movements and later for the contralateral ones, as shown in Figure 33B. In the direction dimension, the deceleration control of movements showed different temporal patterns for distal and proximal markers. In both dimensions, deceleration peaks of the proximal markers were reached later with respect to the peaks of the distal ones.

Figure 34 (upper part) shows that, in the depth domain, both proximal and distal markers decelerated earlier when the movements were directed towards the far targets and later when directed towards the near ones. In the direction dimension, the proximal markers decelerated earlier during contralateral actions with respect to ipsilateral ones, while the distal markers showed opposite temporal trend (Figure 34, bottom).

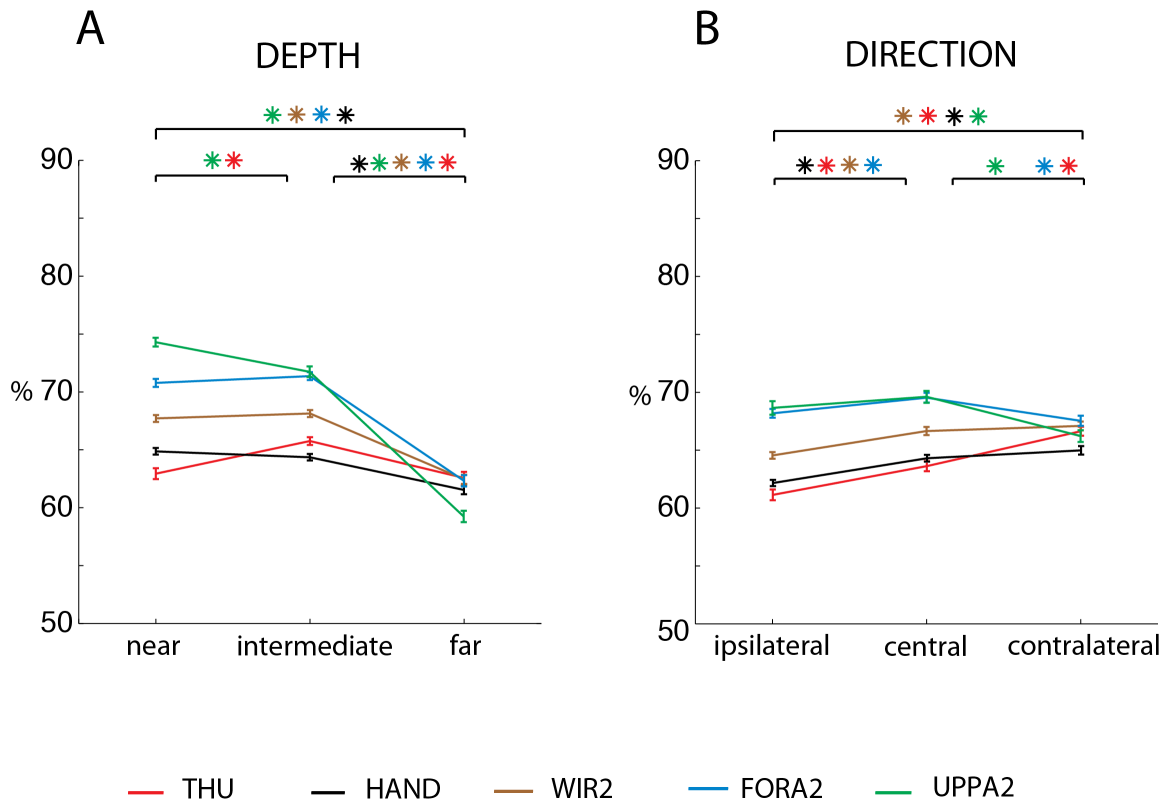


**Figure 33. Percentage of movement decelerating**

Mean percentage of movements when the deceleration of each marker reached the maximum. Error bars represent the standard errors of the means. Asterisks denote the markers that were significantly ( $p < 0,05$ ) different in two task conditions.

**A.** Percentage of movement at the peak deceleration as a function of target depth

**B.** Percentage of movement at the peak deceleration as a function of target direction

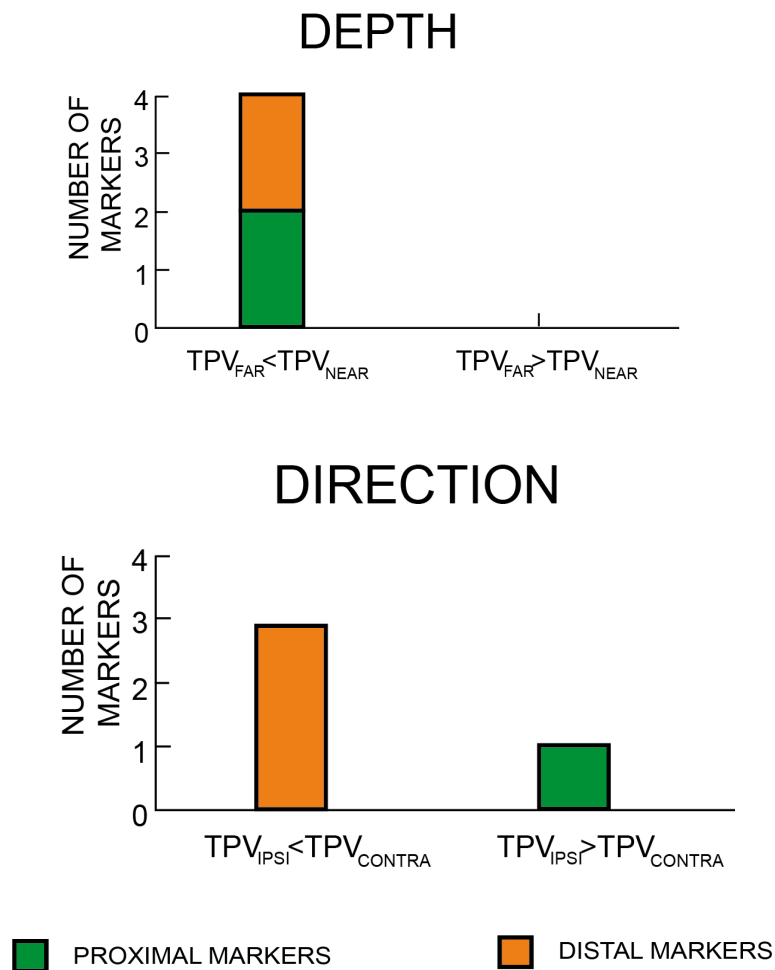


**Figure 34. Number of proximal and distal markers following different decelerating temporal patterns in depth (upper histogram) and in direction (lower histogram)**

Top: Number of proximal (green) and distal markers (orange) decelerating earlier (left column) and later (right column) when the movements were directed towards far targets with respect to near ones.

Bottom: Number of proximal (green) and distal markers (orange) decelerating earlier during ipsilateral actions than during contralateral ones (left column) and earlier during contralateral movements than during ipsilateral ones (right column).

## 4. DISCUSSION

The major goals of the present study were to investigate the coexistence in the same cells, as well as the incidence and temporal evolution, of depth and direction tuning of V6A activity during eye-hand coordinated movements in 3D space. We found in V6A an extensive convergence of target depth and direction signals on single neurons during reaches. In addition, the influence of depth signals was somewhat stronger than direction during planning and execution of reaches, and during holding of the targets. In many cells spatial modulations of activity occurred in multiple epochs, from fixation through reach planning and execution, till holding period. An important fraction of V6A neurons maintained their spatial preference over the time course of the task, whereas a few cells changed it. The depth tuning was more maintained across epochs than the direction tuning. In addition, we aimed at describing the kinematics of arm movements in 3-D space (including also depth) in the monkey. By doing that, we wanted to check whether the monkey could be a useful model to study reaching in depth. Lastly, we investigate whether and how these new findings provide the basis for novel predictions regarding the kinematic control of the limb and we found that the cortical V6A firing rates did not reflect the arm's mechanical properties. Below, we discuss the implications of our major findings for the V6A encoding of arm reaching in 3D space, the transformations of sensory-to-motor signals underlying eye-hand coordinated movements and the correlation with the kinematic parameters.

### 4.1. Depth and directional tuning

Our results show that a significant number of neurons are modulated by both target depth and direction. This finding is in contrast with the general view that depth and direction of reaching targets are processed independently (Crawford *et al.*, 2011; Flanders *et al.*, 1992). The view of separate pathways for depth and direction is based on several behavioral studies (Bagesteiro *et al.*, 2006; Gordon *et al.*, 1994; Sainburg *et al.*, 2003; Vindras *et al.*, 2005; Van Pelt and Medendorp, 2008), but the neurophysiological support to it is relatively weak. To our knowledge, only Lacquaniti *et al.* (1995) studied this issue in the parietal cortex of macaques and they reported that in area PE distinct subpopulations of neurons represented the distance, azimuth, and elevation of the target

location and/or final arm position during movement and posture, respectively. In contrast, in the premotor cortex most studies found a convergence on single neurons of distance and directional information (Fu *et al.*, 1995; Fu *et al.*, 1993; Kurata, 1993; Messier and Kalaska, 2000). A conceptual framework of how the parietal and frontal networks might code direction and distance is presented below.

The encoding of reach depth and direction occurs within a network of parieto-frontal areas shown in Figure 35. In the several nodes of this network, visual signals and eye position information interact with arm position somatosensory signals to generate the motor output. Visual input from striate and extrastriate areas enters the network primarily via area V6 of the parietoccipital cortex (Galletti *et al.*, 1999; Galletti *et al.*, 2003; Shipp *et al.*, 1998). The direction of a reaching target is precisely calculated from its retinal location, whereas to define its distance, the brain must in addition use signals related to the vergence angle of the eyes, binocular disparity and monocular depth cues. Vergence angle information has been shown to influence the activity of many neurons in V6A, in the ventral intraparietal area (VIP) and in the parietal reach region (PRR) that comprises parts of V6A, of the medial intraparietal area (MIP) and PEc/PGm (Bhattacharyya *et al.*, 2009; Breveglieri *et al.*, 2012; Colby *et al.*, 1993). In addition to their tuning by vergence, a substantial fraction of PPR neurons were found to be modulated also by retinal disparity (Bhattacharyya *et al.*, 2009). This integration of vergence and disparity signals that has been also reported in the lateral bank of the intraparietal sulcus (Genovesio and Ferraina, 2004; Gnadt and Mays, 1995) is sufficient to encode the egocentric distance of visual targets. For foveated targets, vergence angle is the most important signal that the reach-related areas could use to calculate the reach amplitude (Foley, 1980; Melmoth *et al.*, 2007). Moreover, as it is shown in the present study (FIX cells) and in Breveglieri *et al.* (2012), many V6A cells are modulated by both the vergence and version angles, so they are able to encode the 3D spatial coordinates of a reaching target. Similar convergence of version and vergence signals –though not tested yet- could also occur in areas MIP, PEc/PGm and VIP that receive visual and eye position input (Battaglia-Mayer *et al.*, 2001; Breveglieri *et al.*, 2008; Colby *et al.*, 1993; Eskandar and Assad, 1999; Ferraina *et al.*, 1997; Johnson *et al.*, 1996). All the cited areas could send the 3D spatial information about target location to the dorsal premotor cortex (PMd), with which they are strongly connected (Gamberini *et al.*, 2009; Matelli *et al.*, 1998; Shipp *et al.*, 1998) and then from PMd this information is transmitted to the primary motor cortex.

The other major contribution to the reach circuit regards the proprioceptive information about hand position. This input arises from the primary and secondary somatosensory cortex and enters the circuit mainly at the level of area PE. In the primary somatosensory area (S1) more neurons were found to be sensitive to movement amplitude than direction (Tillery *et al.*, 1996), while in PE Lacquaniti and colleagues (1995) reported that the number of neurons modulated by target/movement distance to be twice as much compared to the azimuth and elevation. These findings provide neurophysiological support to behavioral data arguing that proprioception is more reliable in depth than vision (Flanders *et al.*, 1992; Monaco *et al.*, 2010; Sainburg *et al.*, 2003; van Beers *et al.*, 2002). Furthermore, PE is strongly and reciprocally connected with the primary motor cortex (Johnson *et al.*, 1996; Jones *et al.*, 1978; Strick and Kim, 1978), where during the execution of arm movements in 3D space the preferred direction in the majority of neurons was aligned with the depth axis, thus showing a representation bias for reaches in depth (Naselaris *et al.*, 2006). The above data strongly suggest that the reach-related areas that receive mainly proprioceptive information are more specialized for the control of reaches in depth.

Target (movement) distance and direction information are likely to be encoded in two main schemes in the reach network (Figure 35). Areas like V6A or MIP, that are involved in the initial processing stages, rely more on visual input and integrate this input with version and vergence eye signals to encode distance and direction jointly in extrinsic, visual (target) coordinates. On the other hand, areas like PE that are implicated in the final stages of reach processing use almost exclusively proprioceptive information and represent the target in the intrinsic coordinates of the shoulder and elbow angles. Within this encoding scheme, the 3D spatial coordinates of the target are more likely to be represented by separate neuronal populations with depth having a stronger effect, as Lacquaniti *et al.* (1995) demonstrated. In agreement with the above scheme, there are several lines of evidence. Area PE, unlike V6A and MIP does not receive visual information (Johnson *et al.*, 1996; Bakola *et al.*, 2012) and vergence angle influences the reaching activity of a small fraction of cells (Ferraina *et al.*, 2009). In addition, reach targets are represented in a hand-centered reference frame in PE (Buneo *et al.*, 2002; Bremner and Andersen, 2012), whereas V6A and MIP cells use predominantly eye-centered or intermediate reference frames (Marzocchi *et al.*, 2008; Chang and Snyder, 2010).

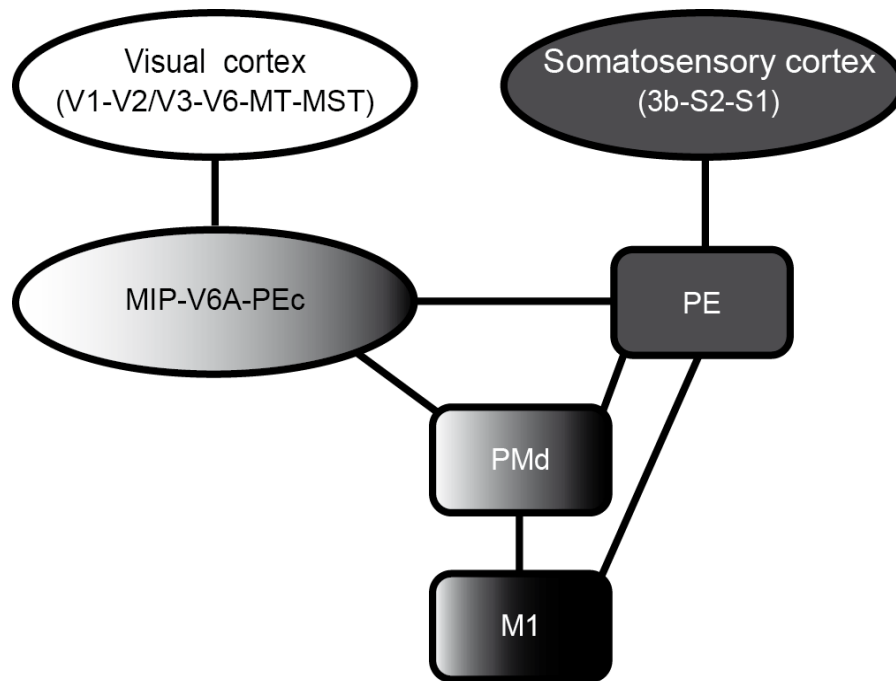


**Figure 35. Distance and direction coding in the cortical reach-related areas.**

Areas are depicted in different grayscale gradients according to the relative proportion of visual (white) and proprioceptive (black) information they receive. Areas closer to visual input process jointly target distance and direction, whereas those that receive mainly somatosensory input represent spatial parameters separately and are more specialized for depth encoding.

The dorsal premotor cortex receives a more balanced input from the two streams of information (Matelli *et al.*, 1998). In line with this evidence, both target localization and movement-related activities have been reported for this cortical area (Alexander and Crutcher, 1990; Johnson *et al.*, 1996; Shen and Alexander, 1997). Fu *et al.* (1993) demonstrated that in PMd there are neural populations encoding both movement direction and movement distance, as well as, target location. Similarly, Messier and Kalaska (2000) found that the majority of PMd cells encoded both the movement distance and direction. Interestingly, both these studies reported that directional information tended to be specified earlier in the task, i.e. during the target cue or movement planning periods, whereas movement distance exerted its effect mostly during movement execution. Our study also revealed an increase in the number of V6A neurons with depth modulations and an enhanced depth sensitivity as the task progressed. However, we found that the direction and depth effects were comparable in the early stages of the task. The discrepancy between our results and those reported in PMd could be due to differences in the experimental setup used. Alternatively, signals about the retinotopic target location could be transmitted directly to some PMd cells without interacting with vergence signals in order to specify the movement direction that is more crucial in the initial stages of movement preparation and execution. Overall, neurophysiological studies from PMd suggest that the processing distance and direction information is more independent in this cortical sector than in the parietal cortex. Data from a recent fMRI study in humans are in line with this view (Fabbri *et al.*, 2012).

The increase in the number of neurons modulated by target depth/movement distance from target appearance to movement execution seems to be common among the parietofrontal reach-related areas. Apart from V6A and PMd, it has been also observed in area PE during a reaching task where only the depth was varied (Ferraina *et al.*, 2009). Localizing and moving towards targets in depth is much more demanding computationally and requires a better degree of control (Danckert *et al.*, 2009). In several studies, where arm movements in 3D were performed, the variability of endpoints was found to be larger along the depth axis where visual uncertainty is higher (Apker *et al.*, 2010; Gordon *et al.*, 1994; McIntyre *et al.*, 1997). A way to achieve a better motor control in depth could be to recruit more neurons receiving inputs other than visual (i.e. proprioceptive, efference copy). SPL neurons presumably are well suited for controlling reaching, especially in depth, as suggested by data from neurological patients. A larger

impairment of depth processing after damage in SPL was reported almost 100 years ago in a human case study (Holmes and Horrax, 1919), and it was recently confirmed that patients with lesions in SPL showed a stronger deficit in depth than in direction during reaching (Baylis and Baylis, 2001) and pointing (Danckert *et al.*, 2009) movements.

#### **4.2. Caveats**

The present work did not test whether target location and arm position were defined in a frame of reference centered to the eyes, body midline or shoulder. Reaches were always performed towards foveated targets. Our choice was dictated by a number of reasons. Firstly, moving the hand to reach a target whose image lies on the fovea is a very common natural behavior of primates (Land and Hayhoe, 2001). Secondly, the issue of the reference frames was beyond the scope of our study. It has been addressed in many parietal areas, including V6A (Marzocchi *et al.*, 2008), and the current state of knowledge is that single neurons use idiosyncratically eye-, hand/body-centered or mixed reference frame (Chang and Snyder, 2010; McGuire and Sabes, 2011).

In our study, depth was more represented than direction by 12-17%, depending on the epoch. This difference could be attributed to the fact that in our experimental setup the depth range explored was much larger than the range of directions. Although we cannot completely exclude this explanation, there are several lines of evidence that argue against it. Firstly, we did not find a stronger depth influence during the fixation epoch. Secondly, although the 30-degree range of visual angles is much smaller than the entire direction range ( $180^\circ$ ) or the oculomotor range ( $\sim 110^\circ$ ), we believe that it comprises most of the central space where the eyes and hands interact with objects in everyday life. Regarding the eyes's space, it has been shown that shifts of gaze larger than 15-20 degrees are always accompanied by head movements (Freedman and Sparks, 1997). Another factor that could explain the stronger depth effect is the difference in retinal size between targets located at different depths. Although the luminance of the targets was adjusted, it was not possible to fully compensate for this effect. However, several observations argue that the prevalence of depth modulations is not an artifact. If the stronger depth effect was due to the difference in the retinal stimulation between the near and far LEDs, we would expect it to be more pronounced in the early phases of the task, especially shortly after the target was fixated (FIX epoch), but this was not proven to be

the case. In addition, as reported in Galletti *et al.* (1999), a substantial fraction of V6A cells are not visually responsive. Overall, our view is that the limitations of our study listed above and do not bear on our major finding that depth and direction of reach targets are jointly processed in V6A.

### **4.3. Spatial tuning in the different task phases**

In the present study we reproduced the naturalistic conditions of eye-hand coordination in reaching, where the eyes fixate the target before the arm movement begins (Hayhoe *et al.*, 2003; Neggers and Bekkering, 2001). Shortly after target fixation, about 70% of V6A neurons were modulated by target depth and/or direction in space. These modulations likely reflect gaze-related activity, and well agree with the previously demonstrated sensitivity of many V6A neurons to eye position, both in a frontoparallel plane (Galletti *et al.*, 1995; Nakamura *et al.*, 1999) and in depth (Breveglieri *et al.*, 2012; Hadjidimitrakis *et al.*, 2011). The spatial tuning of neural activity during target fixation could represent the target location in 3D space, an essential information to control the reaching action.

During the planning epoch, the monkey continued to fixate the target waiting for the go signal to start arm movement. Activity during this time period is likely affected by both eye position and attentional signals, both reported to be present in V6A (Galletti *et al.*, 1995; Galletti *et al.*, 2010). In addition, PLAN activity could be related to the programming of the arm movement, one of the key functions of the posterior parietal cortex (Andersen and Buneo, 2002; Snyder *et al.*, 1997). The increase in selectivity of depth encoding that we found in this time epoch probably reflects the motor preparation processing, but more studies are needed at this regard.

The neural activity during REACH epoch is expected to have many different contributions. During movement execution, V6A neurons could receive visual information about target position, proprioceptive and somatosensory input about hand and arm position, and efferent copy of the arm motor command (Bosco *et al.*, 2010; Breveglieri *et al.*, 2002; Fattori *et al.*, 2005; Gamberini *et al.*, 2009; Matelli *et al.*, 1998). Furthermore, the latency analysis revealed that the responses of the neurons modulated in REACH could depend on hand sensory signals and certainly depend on motor signals. Behavioral evidence suggests that target and hand somatomotor information is

continuously compared during movement execution (Pélisson *et al.*, 1986). In our body-out reaching task the monkeys performed the arm movement in darkness, i.e. without seeing the arm, so they relied on somatomotor information, but not on visual feedback. As mentioned in a previous section of Discussion, movement in depth depends more on proprioception and this agrees well with the fact that V6A cells showed the maximum of depth selectivity during the movement period. The tuning of neural activity in the holding phase (HOLD) could be mainly attributed to proprioceptive and somatosensory inputs related to the static arm position in 3D space (Breveglieri *et al.*, 2002; Fattori *et al.*, 2001). It is interesting to note that HOLD period was characterized by the highest incidence of modulation in depth.

It has been suggested that neurons in the posterior parietal cortex integrate spatially consistent retinal, eye and hand information into ‘global tuning fields’ and that this type of neural processing could be the substrate for the eye-hand coordination (Battaglia-Mayer *et al.*, 2001). Evidence of neurons with consistent spatial tuning between eye position, arm movement and arm position related activities were reported in the superior parietal lobule, in particular in area PEc (Battaglia-Mayer *et al.*, 2001). In that area about 60% of neurons were found to have global tuning in direction across several epochs and tasks, whereas in the inferior parietal lobule area 7a a smaller incidence (~25%) of such cells was reported (Battaglia-Mayer *et al.*, 2005). A recent study employing a body-out reaching task reported that ~60% of 7a neurons changed or lost their directional tuning from fixation to preparation and movement execution (Heider *et al.*, 2010). In the present work, we found a similar incidence (~30%) of directional tuning consistency in area V6A, but we also found that tuning consistency was more frequent in depth than in direction, occurring in depth in about 50% of V6A neurons. This reflects, we believe, the higher difficulty in reaching objects located along the same line of sight, but at different depth, with respect to objects located along different lines of sight.

Based on the coincidence of modulations during the fixation and reaching epochs, we identified three main categories of V6A neurons that are activated during foveated reaches in 3D space i.e. the ‘FIX’, ‘REACH’ and ‘FIX-REACH’ cells. This classification scheme might seem arbitrary, since our population of cells was characterized by a continuum of multiple modulations in the epochs studied. However, our intention was to study the trend of tuning in the subpopulations of cells that lost modulation (‘FIX’ cells), acquire modulation (‘REACH’ cells) and maintain modulation (‘FIX-REACH’ cells) and we

choose the more representative epochs to create the categories. ‘FIX’ cells process target position through gaze signals, whereas ‘REACH’ cells could encode the parameters of the arm movement regardless of the spatial location of the target. ‘FIX-REACH’ cells integrate multiple signals on target location and arm movement. The ability to process independently (‘FIX cells’, ‘REACH cells’), or in combination (‘FIX-REACH cells’) eye- and arm-related signals highlights the key role of area V6A in transforming, also in the depth domain, the spatial information about target into a motor command to reach it.

#### **4.4. Kinematic of reaching movements**

The analysis of kinematic data of reaching movement in 3D space has revealed some features, typical of human behavior: stereotyped trajectories approximately curved in the workspace, velocity profiles with bell-shaped single peaks, movement durations towards contralateral targets significantly longer than towards ipsilateral ones and movement duration and velocity scaled with movement vector extent. These findings suggest that the metrics of monkey’s reaches are similar with human’s kinematics and that monkey can be a suitable model for studying human motor behavior also in depth.

This view was also supported by Roy *et al.* (2000) that found a lot of similarities between the two species, although their studies did not imply the depth dimension. Roy and colleagues (2000) reported only one exception in the similarities between monkey and human kinematic data: the presence of a double velocity peak, instead of the single peak observed in psychophysical human studies. This finding probably reflected the variation of experimental conditions and not a real difference between human and monkey. Indeed, our results reveal a clear single peak in the velocity profiles of all the movements the monkey performed and in all the markers taken into account (see Figure 25), in accordance with human data.

In agreement with Roy *et al.* (2002) and with human evidences (Marzi *et al.*, 1991; Hoptman and Davidson, 1994), we observed ‘advantages’ for movements made towards targets located at the same side of the body (ipsilateral) relative to the reaching arm when compared with movements directed towards targets placed on the opposite side (contralateral) of the body midline. These advantages for ipsilateral actions include shorter movement duration (see Figure 24B), higher peak velocity (see Figure 26B),

higher peak acceleration and deceleration, especially for the most distal segments of the arm (see Figure 27B and 28B, respectively). It has been commonly hypothesized that such advantages are related to efficiency of intrahemispheric processing: if a visual stimulus is presented in the hemispace on the same side of the arm involved in the movement (uncrossed condition), the information about the target does not have to cross the corpus callosum in order to reach motor areas controlling the responding arm, as it happens when the stimulus appears in the contralateral visual field (crossed condition). In contrast to this hypothesis, Carey *et al.* (1996) demonstrated that the advantages were related to the side to which the motor response was directed and not to the side where the target was presented. These results were explained in terms of models of biomechanical constraints on contralateral movements that are independent of the hemispace of target presentation. Gordon *et al.* (1994a), hypothesized that the differences in duration, velocity and acceleration reflected a failure to take into account the difference in total limb inertia in the two directions. The inertial loads at the hand are higher when hand path (in the horizontal plane) is perpendicular to the long axis of the upper arm (i.e. horizontal flexion of the upper arm, with some flexion of the forearm) than movements with hand path that are parallel to the long axis of the upper arm (horizontal extension of the forearm). As our targets were always foveated, we can suggest that the differences between ipsilateral and contralateral reaches maybe be due to biomechanical factors, in particular to the differences in inertial resistance of the limb to movement of the hand in different direction.

Gordon *et al.*, (1994a-b) also found that peak velocities, peak accelerations and movement durations were scaled to target distance, as our kinematic results revealed (see Figure 26A, 27A, 24A). They proposed that planning the direction of a hand movement might correspond to the selection of a particular spatiotemporal pattern of muscle activation. This would specify the relative amounts by which different muscles must be activated in order to project the hand in a given direction. Planning the amplitude of hand movement involved the specification of the magnitude of activation applied to the muscles in the synergy and this magnitude is planned without regard to the inertial resistance related to movement direction. For these reasons, the authors suggested that these two dimensions represented distinct features of reaching movements and could be, at least in part, independently specified by the brain. But in general, at the level of joint angles and torques, direction and depth of arm movement are not mechanically independent. This view is partially in contrast with neurophysiological data reported in this thesis because

we observed neural populations encoding both movement direction and movement depth. Area V6A probably represents a convergence point of both the signals.

In the present thesis, we highlight an interesting difference between depth and direction dimensions in the coherency of temporal patterns for distal and proximal markers (see Figures 30, 32 and 34). In the direction dimension, the motion of distal and proximal arm segments was more variable in timing than in depth dimension, where the trend was coherent for all the markers. For movements at different directions, the motion of the distal segments is controlled separately from that of the proximal segments because probably there are not advantages in having distal displacement developing synchronously with the proximal one. A similar phenomenon was found by Lacquaniti and Soechting (1982) that observed differences in timing in the motion of the wrist compared with that of the elbow and the shoulder during the arm transport towards objects presented along different orientation in space. The authors suggested that the moment of inertia for forearm rotation was different with respect to the moment of inertia for elbow and shoulder motion. It is possible that the different inertia exerted on the proximal and the distal segments of the arm can explain the different temporal patterns that we observed for movements performed in different directions. Feasible speculation to explain the synchronic temporal pattern for distal and proximal markers in depth dimension can be a similar magnitude of inertial load exerted on single arm segments, moving the arm towards different depths.

#### **4.5. Correlation between kinematic and neural data**

Our behavioral results discard the possibility that the motor parameters measured during the reaching movements can completely explain the spatial tuning found in V6A neural responses because, contrary to the kinematic variables, we did not find unitary preferences for actions directed towards contralateral and far targets in the neurophysiological recordings. In other words, we didn't find a significant number of cells that showed higher neural activity when the arm movements are directed far rather than near and contralateral rather than ipsilateral during the reach epoch (Figure 14). On the contrary, the movement times calculated for contralateral and far reaches were significantly higher with respect to those calculated for ipsilateral and near ones (Figure 24B, 26B), but this was not reflected in the neuronal preferences.

The only possible correlation between the kinematic data and the neural modulations found in V6A could be in the depth dimension. The movement times and the peak velocities for the far actions was statistically higher with respect to the near ones in all the markers considered (Figure 24B). However, if on one side we found relevant amount of V6A neurons with the same spatial preference for the far movements, during the fixation, the preparation and the holding periods (Figure 14), a similar number of cells showed preference for near and far targets during the execution of the reaching movements. This again does not fit with the kinematic parameters (movement times and peak velocities) significantly different for far targets.

Another important finding regards the proximal and the distal markers that, in the depth dimension, showed the same temporal pattern reaching peak velocity, peak acceleration and peak deceleration earlier during far movements than during near ones (Figure 30, 32, 34). For this reasons, it could be possible to hypothesize that area V6A could be involved in some phases of the motor regulation among different segments of the arm movements towards targets located at different distances. Nevertheless, V6A neural discharges do not seem to directly control the kinematic variables characterizing the reaching movements.

This area is involved in the sensorimotor transformation encoding the spatial information at a high hierarchical and cognitive level. An area directly involved in the control of arm muscles and in the integration of the motor information at a more mechanical level than V6A is area M1. Indeed, Scott and colleagues (2001) found a strong relation between joint power and distribution of preferred directions in neurons recorded in area M1 of non-human primates performing reaching movements.

In summary, present data support the role of V6A in integrating the spatial information for the localization of reaching targets in 3D space and in transforming visual and gaze signals in the required motor command. In particular, the reported studies suggested an involvement of this area in the integration of direction and depth, during arm reaching movements, independently from the kinematic parameters describing these actions.

## 5. REFERENCES

- Alexander GE, Crutcher MD (1990) Neural representations of the target (goal) of visually guided movements in three motor areas of the monkey. *J Neurophysiol* 64: 164-178.
- Andersen RA, Cui H (2009) Intention, action planning, and decision making in parietal-frontal circuits. *Neuron* 63: 568-583.
- Apker GA, Darling TK, Buneo CA (2010) Interacting Noise Sources Shape Patterns of Arm Movement Variability in Three-Dimensional Space. *J Neurophysiol* 104: 2654-2666.
- Atkeson CG, Hollerbach JM (1985) Kinematic features of unrestrained vertical arm movements. *Journal of Neuroscience* 5, 2318-2330.
- Bagesteiro L, Sarlegna F, Sainburg R (2006) Differential influence of vision and proprioception on control of movement distance. *Experimental Brain Research* 171: 358-370.
- Bakola S, Gamberini M, Passarelli L, Fattori P, Galletti C (2012) Cortical input to posterior parietal area PE in the macaque monkey. In: Australian Neuroscience Society Meeting. Gold Coast, Queensland, Australia.
- Bhat RB and Sanes JN (1998) Cognitive channels computing action distance and direction. *J Neurosci* 18:7566-7580.
- Batista AP, Buneo CA, Snyder LH, Andersen RA (1999) Reach plans in eye-centered coordinates. *Science* 285: 257-260.
- Batista AP, Santhanam G, Yu BM, Ryu SI, Afshar A, Shenoy KV (2007) Reference frames for reach planning in macaque dorsal premotor cortex. *J Neurophysiol* 98: 966-983.
- Battaglia-Mayer A, Ferraina S, Mitsuda T, Marconi B, Genovesio A, Onorati P, Lacquaniti F, Caminiti R (2000) Early coding of reaching in the parietooccipital cortex. *Journal of Neurophysiology* 83:2374-2391.
- Battaglia-Mayer A, Ferraina S, Genovesio A, Marconi B, Squatrito S, Molinari M, Lacquaniti F, Caminiti R (2001) Eye-hand coordination during reaching. II. An analysis of the relationships between visuomanual signals in parietal cortex and parieto-frontal association projections. *Cereb Cortex* 11: 528-544.

- Battaglia-Mayer A, Mascaro M, Brunamonti E, Caminiti R (2005) The Over-representation of Contralateral Space in Parietal Cortex: A Positive Image of Directional Motor Components of Neglect? *Cerebral Cortex* 15: 514-525.
- Battaglia-Mayer A, Archambault PS, Caminiti R (2006) The cortical network for eye-hand coordination and its relevance to understanding motor disorders of parietal patients. *Neuropsychologia* 44:2607-2620.
- Baylis GC, Baylis LL (2001) Visually misguided reaching in Balint's syndrome. *Neuropsychologia* 39: 865-875.
- Bhattacharyya R, Musallam S, Andersen RA (2009) Parietal Reach Region Encodes Reach Depth Using Retinal Disparity and Vergence Angle Signals. *J Neurophysiol*: 90359.92008.
- Bosco A, Breveglieri R, Chinellato E, Galletti C, Fattori P (2010) Reaching Activity in the Medial Posterior Parietal Cortex of Monkeys Is Modulated by Visual Feedback. *J Neurosci* 30: 14773-14785.
- Bremner Lindsay R, Andersen Richard A (2012) Coding of the Reach Vector in Parietal Area 5d. *Neuron* 75: 342-351.
- Breviglieri R, Galletti C, Monaco S, Fattori P (2008) Visual, somatosensory, and bimodal activities in the macaque parietal area PEc. *Cereb Cortex* 18: 806-816.
- Breviglieri R, Hadjidimitrakis K, Bosco A, Sabatini SP, Galletti C, Fattori P (2012) Eye Position Encoding in Three-Dimensional Space: Integration of Version and Vergence Signals in the Medial Posterior Parietal Cortex. *The Journal of Neuroscience* 32: 159-169.
- Breviglieri R, Kutz DF, Fattori P, Gamberini M, Galletti C (2002) Somatosensory cells in the parieto-occipital area V6A of the macaque. *Neuroreport* 13: 2113-2116.
- Buneo CA, Jarvis MR, Batista AP, Andersen RA (2002) Direct visuomotor transformations for reaching. *Nature* 416: 632-636.
- Carey DP, Hargreaves EL, Goodale MA (1996) Reaching to ipsilateral or contralateral targets: within-hemisphere visuomotor processing cannot explain hemispatial differences in motor control. *Exp Brain Res* 12:496-504.
- Casadio M, Sanguineti V, Solaro C, Morasso PG (2007) A Haptic Robot reveals the Adaptation Capability of Individuals with Multiple Sclerosis. *The International Journal of Robotics Research* 26;1225 DOI: 10.1177/0278364907084981.
- Chang SW, Papadimitriou C, Snyder LH (2009) Using a compound gain field to compute a reach plan. *Neuron* 64: 744-755.

- Chang SWC, Snyder LH (2010) Idiosyncratic and systematic aspects of spatial representations in the macaque parietal cortex. *Proceedings of the National Academy of Sciences* 107: 7951-7956.
- Christel MI, Billard A (2002) Comparison between macaques' and humans' kinematics of prehension: the role of morphological differences and control mechanisms. *Behav Brain Res* 131:169-184.
- Colby CL, Duhamel JR, Goldberg ME (1993) Ventral intraparietal area of the macaque: anatomic location and visual response properties. *J Neurophysiol* 69: 902-914.
- Colby CL, Gattass R, Olson CR, Gross CG (1988) Topographical organization of cortical afferents to extrastriate visual area PO in the macaque: a dual tracer study. *J Comp Neurol* 269:392-413.
- Crawford JD, Henriques DY, Medendorp WP (2011) Three-dimensional transformations for goal-directed action. *Annu Rev Neurosci* 34: 309-331.
- Cruse H, Brüwer H (1987) The human arm as a redundant manipulator: the control of path and joint angles. *Biological Cybernetics* 57:137-144.
- Cumming BG, DeAngelis GC (2001) The physiology of stereopsis. *Annu Rev Neurosci* 24:203-38
- Danckert J, Goldberg L, Broderick C (2009) Damage to superior parietal cortex impairs pointing in the sagittal plane. *Exp Brain Res* 195: 183-191.
- Desmurget M, Epstein CM, Turner RS, Prablanc C, Alexander GE, Grafton ST (1999) Role of the posterior parietal cortex in updating reaching movements to a visual target. *Nature neuroscience* 2:563-567.
- Eskandar EN, Assad JA (1999) Dissociation of visual, motor and predictive signals in parietal cortex during visual guidance. *Nat Neurosci* 2: 88-93.
- Fabbri S, Caramazza A, Lingnau A (2010) Tuning curves for movement direction in the human visuomotor system. *J Neurosci* 30:13488-13498.
- Fabbri S, Caramazza A, Lingnau A (2012) Distributed sensitivity for movement amplitude in directionally tuned neuronal populations. *J Neurophysiol* 107: 1845-1856.
- Fattori P, Breveglieri R, Amoroso K, Galletti C (2004) Evidence for both reaching and grasping activity in the medial parieto-occipital cortex of the macaque. *Eur J Neurosci* 20: 2457-2466.
- Fattori P, Gamberini M, Kutz DF, Galletti C (2001) 'Arm-reaching' neurons in the parietal area V6A of the macaque monkey. *Eur J Neurosci* 13: 2309-2313.

- Fattori P, Kutz DF, Breveglieri R, Marzocchi N, Galletti C (2005) Spatial tuning of reaching activity in the medial parieto-occipital cortex (area V6A) of macaque monkey. *Eur J Neurosci* 22: 956-972.
- Ferraina S, Brunamonti E, Giusti MA, Costa S, Genovesio A, Caminiti R (2009) Reaching in Depth: Hand Position Dominates over Binocular Eye Position in the Rostral Superior Parietal Lobule. *J Neurosci* 29: 11461-11470.
- Ferraina S, Garasto MR, Battaglia-Mayer A, Ferraresi P, Johnson PB, Lacquaniti F, Caminiti R (1997) Visual Control of Hand-reaching Movement: Activity in Parietal Area 7m. *European Journal of Neuroscience* 9: 1090-1095.
- Flanders M, Helms Tillery SI, Soechting JF (1992) Early stages in a sensorimotor transformation. *Behav Brain Sci* 15: 309-362.
- Fluet M-C, Baumann MA, Scherberger Hr (2010) Context-Specific Grasp Movement Representation in Macaque Ventral Premotor Cortex. *The Journal of Neuroscience* 30: 15175-15184.
- Fogassi L, Gallese V, Gentilucci M, Chieffi S, Rizzolatti G (1991) Studio cinematografico dei movimenti di raggiungimento e prensione nella scimmia. *Boll Soc Ital Biol Sper* 7:715-721.
- Foley JM (1980) Binocular distance perception. *Psychol Rev* 87: 411-434.
- Freedman EG, Sparks DL (1997) Eye-head coordination during head-unrestrained gaze shifts in rhesus monkeys. *J Neurophysiol* 77: 2328-2348.
- Fu Q-G, Flament D, Coltz JD, Ebner TJ (1995) Temporal encoding of movement kinematics in the discharge of primate primary motor and premotor neurons. *J Neurophysiol* 73: 836-854.
- Fu Q-G, Suarez JI, Ebner TJ (1993) Neuronal specification of direction and distance during reaching movements in the superior precentral premotor area and primary motor cortex of monkeys. *J Neurophysiol* 70: 2097-2116.
- Fu QG, Suarez JI, Ebner TJ (1993) Neuronal specification of direction and distance during reaching movements in the superior precentral premotor area and primary motor cortex of monkeys. *Journal of Neurophysiology* 70: 2097-2116.
- Galletti C, Battaglini PP, Fattori P (1993) Parietal neurons encoding spatial locations in craniotopic coordinates. *Exp Brain Res* 96: 221-229.
- Galletti C, Battaglini PP, Fattori P (1995) Eye position influence on the parieto-occipital area PO (V6) of the macaque monkey. *Eur J Neurosci* 7: 2486-2501.

- Galletti C, Fattori P, Kutz DF, Battaglini PP (1997) Arm movement-related neurons in the visual area V6A of the macaque superior parietal lobule. *Eur J Neurosci* 9:410-413.
- Galletti C, Fattori P, Gamberini M, Kutz DF (1999a) The cortical visual area V6: brain location and visual topography. *Eur J Neurosci* 11:3922-3936
- Galletti C, Fattori P, Kutz DF, Gamberini M (1999b) Brain location and visual topography of cortical area V6A in the macaque monkey. *Eur J Neurosci* 11:575-582
- Galletti C, Gamberini M, Kutz DF, Fattori P, Luppino G, Matelli M (2001) The cortical connections of area V6: an occipito-parietal network processing visual information. *Eur J Neurosci* 13:1572-1588.
- Galletti C, Breveglieri R, Lappe M, Bosco A, Ciavarro M, Fattori P (2010) Covert shift of attention modulates the ongoing neural activity in a reaching area of the macaque dorsomedial visual stream. *PLoS One* 5: e15078.
- Galletti C, Fattori P, Battaglini PP, Shipp S, Zeki S (1996) Functional demarcation of a border between areas V6 and V6A in the superior parietal gyrus of the macaque monkey. *Eur J Neurosci* 8: 30-52.
- Galletti C, Fattori P, Gamberini M, Kutz DF (1999) The cortical visual area V6: brain location and visual topography. *Eur J Neurosci* 11: 3922-3936.
- Galletti C, Fattori P, Kutz DF, Gamberini M (1999) Brain location and visual topography of cortical area V6A in the macaque monkey. *Eur J Neurosci* 11: 575-582.
- Galletti C, Kutz D, Gamberini M, Breveglieri R, Fattori P (2003) Role of the medial parieto-occipital cortex in the control of reaching and grasping movements. *Experimental Brain Research* 153: 158-170.
- Galletti C, Fattori P (2003) Neuronal mechanisms for detection of motion in the field of view. *Neuropsychologia* 41:1717-1727
- Gamberini M, Galletti C, Bosco A, Breveglieri R, Fattori P (2011) Is the Medial Posterior Parietal Area V6A a Single Functional Area? *The Journal of Neuroscience* 31: 5145-5157.
- Gamberini M, Passarelli L, Fattori P, Zucchelli M, Bakola S, Luppino G, Galletti C (2009) Cortical connections of the visuomotor parietooccipital area V6Ad of the macaque monkey. *J Comp Neurol* 513: 622-642.

- Genovesio A, Ferraina S (2004) Integration of Retinal Disparity and Fixation-Distance Related Signals Toward an Egocentric Coding of Distance in the Posterior Parietal Cortex of Primates. *J Neurophysiol* 91: 2670-2684.
- Georgopoulos AP, Kalaska JF, Massey JT (1981) Spatial trajectories and reaction times of aimed movements: effect of practice, uncertainty, and change in target location. *J Neurophysiol* 46:725-43.
- Georgopoulos AP, Massey JT (1988) Cognitive spatial-motor processes. 2. Information transmitted by the direction of two-dimensional arm movements and by neuronal populations in primate motor cortex and area 5. *Exp Brain Res* 69:315-326
- Gentilucci M, Castiello U, Corradini ML, Scarpa M, Umiltà C, Rizzolatti G (1991) Influence of different types of grasping on the transport component of prehension movements. *Neuropsychologia* 29:361-378.
- Gnadt JW, Mays LE (1995) Neurons in monkey parietal area LIP are tuned for eye-movement parameters in three-dimensional space. *J Neurophysiol* 73: 280-297.
- Gordon J, Ghilardi MF, Ghez C (1994a) Accuracy of planar reaching movements. I. Independence of direction and extent variability. *Exp Brain Res* 99: 97-111.
- Gordon J, Ghilardi MF, Cooper SE, Ghez C (1994b) Accuracy of planar reaching movements. II. Systematic extent errors resulting from inertial anisotropy. *Exp Brain Res* 99:112-130
- Hadjidimitrakis K, Breveglieri R, Placenti G, Bosco A, Sabatini SP, Fattori P (2011) Fix Your Eyes in the Space You Could Reach: Neurons in the Macaque Medial Parietal Cortex Prefer Gaze Positions in Peripersonal Space. *PLoS ONE* 6: e23335.
- Hadjidimitrakis K, Bertozzi F, Breveglieri R, Bosco A, Galletti C, Fattori P (2013) Common Neural Substrate for Processing Depth and Direction Signals for Reaching in Monkey Medial Posterior Parietal Cortex. *Cerebral Cortex* doi:10.1093/cercor/bht021
- Hayhoe MM, Shrivastava A, Mruczek R, Pelz JB (2003) Visual memory and motor planning in a natural task. *J Vis* 3: 49-63.
- Heider B, Karnik A, Ramalingam N, Siegel RM (2010) Neural Representation During Visually Guided Reaching in Macaque Posterior Parietal Cortex. *J Neurophysiol*: jn.01050.02009.
- Hoptman MJ, Davidson RJ (1994) How and why do the two cerebral hemispheres interact? *Psychol Bull* 116:195-219.

- Jeannerod M (1988) The neural and behavioural organization of goal-directed movements. Clarendon Press, Oxford.
- Jindrich DL, Courtine G, Liu JJ, McKay HL, Moseanko R, Bernot TJ, Roy RR, Zhong H, Tuszynski MH, Edgerton VR (2011) Unconstrained three-dimensional reaching in Rhesus monkeys. *Exp Brain Res* 209:35-50.
- Johnson PB, Ferraina S, Bianchi L, Caminiti R (1996) Cortical networks for visual reaching: physiological and anatomical organization of frontal and parietal lobe arm regions. *Cereb Cortex* 6: 102-119.
- Jones EG, Coulter JD, Hendry SHC (1978) Intracortical connectivity of architectonic fields in the somatic sensory, motor and parietal cortex of monkey. *J Comp Neurol* 181: 291-348.
- Kudoh N, Hattori M, Numata N, Maruyama K (1997) An analysis of spatiotemporal variability during prehension movements: effects of object size and distance. *Exp Brain Res* 117:457-464
- Kurata K (1993) Premotor cortex of monkeys: set- and movement-related activity reflecting amplitude and direction of wrist movements. *J Neurophysiol* 69: 187-200.
- Kutz DF, Fattori P, Gamberini M, Breveglieri R, Galletti C (2003) Early- and late-responding cells to saccadic eye movements in the cortical area V6A of macaque monkey. *Exp Brain Res* 149: 83-95.
- Kutz DF, Marzocchi N, Fattori P, Cavalcanti S, Galletti C (2005) Real-Time Supervisor System Based on Trinary Logic to Control Experiments With Behaving Animals and Humans. *J Neurophysiol* 93: 3674-3686.
- Lacquaniti F and Soechting JF (1982) Coordination of arm and wrist motion during a reaching task. *J Neurosci* 2: 399-408.
- Lacquaniti F (1997) Frame of reference in sensorimotor coordination. In Boller F and Grafman J (eds), *Handbook of Neuropsychology*, Vol 11 Elsevier, Amsterdam, pp. 27-64
- Lacquaniti F, Caminiti R (1998) Visuo-motor transformations for arm reaching. *The European Journal of Neuroscience* 10:195-203
- Land MF, Hayhoe M (2001) In what ways do eye movements contribute to everyday activities? *Vision Res* 41: 3559-3565.
- Luppino G, Ben Hamed S, Gamberini M, Matelli M, Galletti C (2005) Occipital (V6) and parietal (V6A) areas in the anterior wall of the parieto-occipital sulcus of the

- macaque: a cytoarchitectonic study. *European Journal of Neuroscience* 21: 3056-3076.
- Marzi CA, Bisiacchi R, Nicoletti R (1991) Is interhemispheric transfer of visuomotor information asymmetric? Evidence from a meta-analysis. *Neuropsychologia* 29:1163-1177.
- Marzocchi N, Breveglieri R, Galletti C, Fattori P (2008) Reaching activity in parietal area V6A of macaque: eye influence on arm activity or retinocentric coding of reaching movements? *Eur J Neurosci* 27: 775-789.
- Matelli M, Luppino G, Rizzolatti G (1991) Architecture of superior and mesial area 6 and the adjacent cingulate cortex in the macaque monkey. *J Comp Neurol* 311:445-462.
- Matelli M, Govoni P, Galletti C, Kutz DF, Luppino G (1998) Superior area 6 afferents from the superior parietal lobule in the macaque monkey. *J Comp Neurol* 402: 327-352.
- McGuire LM, Sabes PN (2011) Heterogeneous representations in the superior parietal lobule are common across reaches to visual and proprioceptive targets. *J Neurosci* 31: 6661-6673.
- McIntyre J, Stratta F, Lacquaniti F (1997) Viewer-Centered Frame of Reference for Pointing to Memorized Targets in Three-Dimensional Space. *J Neurophysiol* 78: 1601-1618.
- Messier J, Kalaska JF (1999) Comparison of variability of initial kinematics and endpoints of reaching movements. *Exp Brain Res* 125:139-152.
- Messier J, Kalaska JF (2000) Covariation of Primate Dorsal Premotor Cell Activity With Direction and Amplitude During a Memorized-Delay Reaching Task. *Journal of Neurophysiology* 84: 152-165.
- Monaco S, Kroliczak G, Quinlan DJ, Fattori P, Galletti C, Goodale MA, Culham JC (2010) Contribution of visual and proprioceptive information to the precision of reaching movements. *Exp Brain Res* 202: 15-32.
- Morasso P (1981) Spatial control of arm movements. *Exp Brain Res* 42:223-227.
- Nakamura K, Chung HH, Graziano MSA, Gross CG (1999) Dynamic representation of eye position in the parieto-occipital sulcus. *J Neurophysiol* 81: 2374-2385.
- Nakamura K, Colby CL (2000) Visual, saccade-related, and cognitive activation of single neurons in monkey extrastriate area V3A. *J Neurophysiol* 84: 677-692.

- Naselaris T, Merchant H, Amirikian B, Georgopoulos AP (2006) Large-Scale Organization of Preferred Directions in the Motor Cortex. I. Motor Cortical Hyperacuity for Forward Reaching. *Journal of Neurophysiology* 96: 3231-3236.
- Neggens SFW, Bekkering H (2001) Gaze Anchoring to a Pointing Target Is Present During the Entire Pointing Movement and Is Driven by a Non-Visual Signal. *Journal of Neurophysiology* 86: 961-970.
- Péllisson D, Prablanc C, Goodale MA, Jeannerod M (1986) Visual control of reaching movements without vision of the limb. II. Evidence of fast unconscious processes correcting the trajectory of the hand in the final position of a double-step stimulus. *Exp Brain Res* 62: 303-311.
- Perenin MT and Vighetto A (1988) Optic ataxia: A specific disruption in visuomotor mechanisms. I. Different aspects of the deficit in reaching for objects. *Brain* 111(Pt 3), 643-647.
- Pouget A, Sejnowski TJ (1994) A neural model of the cortical representation of egocentric distance. *Cereb Cortex* 4:314-329.
- Prado J, Clavagnier S, Otzenberger H, Scheiber C, Kennedy H, Perenin MT (2005) Two cortical systems for reaching in central and peripheral vision. *Neuron* 48:849-858.
- Rosenbaum DA (1980) Human movement initiation: specification of arm, direction and extent. *J Exp Psychol* 109:444-474.
- Roy AC, Paulignan Y, Farnè A, Joffrais C, Boussaoud D (2000) Hand kinematics during reaching and grasping in the macaque monkey. *Behavioural Brain Research* 117:75-85.
- Roy AC, Paulignan Y, Meunier M, Boussaoud D (2002) Prehension movements in the macaque monkey: effects of object size and location. *J Neurophysiol* 88:1491-1499
- Roy AC, Paulignan Y, Meunier M, Boussaoud D (2006) Prehension movements in the macaque monkey: effects of perturbation of object size and location. *Exp Brain Res* 169:182-193.
- Sainburg RL, Lateiner JE, Latash ML, Bagesteiro LB (2003) Effects of Altering Initial Position on Movement Direction and Extent. *Journal of Neurophysiology* 89: 401-415.
- Sakata H, Taira M (1994) Parietal control of hand action. *Curr Opin Neurobiol* 4:847-856.
- Sartori L, Ciani AC, Bulgheroni M, Castiello U (2012) Reaching and grasping behaviour in *Macaca fascicularis*: a kinematic study. *Exp Brain Res*

- Scott SH, Sergio LE, Kalaska JF (1997) Reaching movements with similar hand paths but different arm orientations. II. Activity of individual cells in dorsal premotor cortex and in parietal area 5. *J Neurophysiol* 78:2413-2426.
- Scott SH, Gribble PL, Graham KM, Cabel DW (2001) Dissociation between hand motion and population vectors from neural activity in motor cortex. *Nature* 413:161-165.
- Shen L, Alexander GE (1997) Preferential representation of instructed target location versus limb trajectory in dorsal premotor area. *J Neurophysiol* 77:1195-1212.
- Shipp S, Blanton M, Zeki S (1998) A visuo-somatomotor pathway through superior parietal cortex in the macaque monkey: cortical connections of areas V6 and V6A. *European Journal of Neuroscience* 10: 3171-3193.
- Snyder LH, Batista AP, Andersen RA (1997) Coding of intention in the posterior parietal cortex. *Nature* 386: 167-170.
- Strick PL, Kim CC (1978) Input to primate motor cortex from posterior parietal cortex (area 5). I. Demonstration by retrograde transport. *Brain Res* 157: 325-330.
- Tannè J, Boussaoud D, Boyer-Zeller N, Rouiller EM (1995) Direct visual pathways for reaching movements in the macaque monkey. *Neuroreport* 7:267-272.
- Tillery SI, Soechting JF, Ebner TJ (1996) Somatosensory cortical activity in relation to arm posture: nonuniform spatial tuning. *J Neurophysiol* 76: 2423-2438.
- Ungerleider L and Mishkin M (1982) Two cortical visual system. In: Ingle DJ, Goodale MA, Mansfield RWJ (eds) *Analysis of motor behaviour*. MIT Press, Cambridge, MA, pp 549-586
- van Beers RJ, Wolpert DM, Haggard P (2002) When feeling is more important than seeing in sensorimotor adaptation. *Curr Biol* 12: 834-837.
- Van Pelt S, Medendorp WP (2008) Updating Target Distance Across Eye Movements in Depth. *J Neurophysiol* 99: 2281-2290.
- Viguièr A, Clement G, Trotter Y (2001) Distance perception within near visual space. *Perception* 30:115-124.
- Vindras P, Desmurget M, Viviani P (2005) Error parsing in visuomotor pointing reveals independent processing of amplitude and direction. *J Neurophysiol* 94: 1212-1224.
- Von Hofsten (1977) Binocular convergence as a determinant of reaching behavior in infancy. *Perception* 6:139-144.
- Wenger KK, Musch KL, Mink JW (1999) Impaired reaching and grasping after focal inactivation of globus pallidus pars interna in the monkey. *J Neurophysiol* 82:2049-2060.

Zar J (1999) Biostatistical Analysis. Upper Saddle River, New Jersey: Prentice-Hall.